



University of Pennsylvania
ScholarlyCommons

Publicly Accessible Penn Dissertations


2012

The Role of TSC2 and Deptor in Fetal Cortical Development

Victoria Tsai

University of Pennsylvania, victoria.tsai1@gmail.com

Follow this and additional works at: <https://repository.upenn.edu/edissertations>

 Part of the [Developmental Biology Commons](#), and the [Neuroscience and Neurobiology Commons](#)

Recommended Citation

Tsai, Victoria, "The Role of TSC2 and Deptor in Fetal Cortical Development" (2012). *Publicly Accessible Penn Dissertations*. 714.

<https://repository.upenn.edu/edissertations/714>

This paper is posted at ScholarlyCommons. <https://repository.upenn.edu/edissertations/714>
For more information, please contact repository@pobox.upenn.edu.

The Role of TSC2 and Deptor in Fetal Cortical Development

Abstract

Tuberous Sclerosis Complex (TSC) is an autosomal dominant genetic disorder that results from mutations in the TSC1 or TSC2 genes. TSC is a multisystem hamartoma syndrome with manifestations in the brain, heart, lungs, kidney, skin and eyes. Neurologically, TSC patients may exhibit severe epilepsy, cognitive disabilities, and autism spectrum disorders. TSC1 and TSC2 proteins form a heterodimeric complex that serves to inhibit mammalian target of rapamycin (mTOR) signaling pathway. TSC1 and TSC2 receive activating or inhibitory signaling from multiple inputs including growth factors, insulin signaling, energy and amino acid levels, and proinflammatory pathways, and then integrate those signals to regulate the activity of mTOR. mTOR signaling plays a critical role in regulating cell growth, transcription, translation, and autophagy. Animal models have shed light on certain features of TSC, but failed to recapitulate the disease completely and currently further research is under way to better understand this devastating disorder. To date, mTOR signaling hyperactivation has been demonstrated in TSC tubers at postnatal time points, thus we set out to study the profile of mTOR activation in the fetal brain. We utilized both mouse neural progenitors in vitro and developing brain in vivo systems to understand the effects of Tsc1 and Tsc2 during brain development. Furthermore, after the identification of a new mTOR regulatory protein Deptor (DEPDC6 gene), which inhibits the mTORC1 and mTORC2 signaling pathways similar to TSC1-TSC protein complex, we examined its role in brain development. We found that Deptor shRNA knockdown results in mTORC1 and mTORC2 activation in vitro as well as abnormal migration in vivo. Our results show that mTOR signaling pathway could be the common pathway on which TSC1, TSC2, and DEPTOR converge and exert their effects on brain development. These results suggest mTOR signaling and its downstream effectors could be targets for therapeutic treatment during embryogenesis and could potentially prevent abnormal brain development.

Degree Type

Dissertation

Degree Name

Doctor of Philosophy (PhD)

Graduate Group

Neuroscience

First Advisor

Peter B. Crino

Keywords

brain development, deptor, epilepsy, mtor, tsc2, tuberous sclerosis complex

Subject Categories

Developmental Biology | Neuroscience and Neurobiology

This dissertation is available at ScholarlyCommons: <https://repository.upenn.edu/edissertations/714>

THE ROLE OF TSC2 and DEPTOR in FETAL CORTICAL DEVELOPMENT

Victoria Tsai

A DISSERTATION

in

Neuroscience

Presented to the Faculties of University of Pennsylvania

in

Partial Fulfillment of the Requirements for the

Degree of Doctor of Philosophy

2012

Supervisor of Dissertation

Signature _____

Peter B. Crino, M.D., Ph.D., Associate Professor of Neurology

Graduate Group Chairperson

Signature_____

Joshua I. Gold, Ph.D., Associate Professor of Neuroscience

Dissertation Committee

Tom Curran, Ph.D., FRS, Professor of Cell and Developmental Biology and Pathology and Laboratory Medicine

Michael Granato, Ph.D., Professor of Cell and Developmental Biology

Dennis L. Kolson, M.D., Ph.D., Associate Professor of Neurology

Zhaolan Joe Zhou, Ph.D., Chair, Assistant Professor of Genetics

Copyright Notice

THE ROLE OF TSC2 and DEPTOR in FETAL CORTICAL DEVELOPMENT

COPYRIGHT

2012

Victoria Tsai

This work is licensed under the Creative Commons Attribution-Non-Commercial-

ShareAlike 3.0 License

<http://creativecommons.org/licenses/by-ny-sa/2.0/>

Dedication

For Mom and Dad,

For Grandma and Grandpa,

For Ludmila.

ACKNOWLEDGEMENTS

First and foremost I want thank my mentor, Peter Crino, for his mentorship and support throughout my Ph.D. thesis work. I couldn't have done it without you.

I want to thank my wonderful family, Mom, Dad, Grandma, Grandpa, and Ludmila for their continuous love, support, and encouragement. Thank you for always being there for me and supporting me in all my endeavors.

I want to thank my Thesis Committee, Zhaolan Joe Zhou (chair), Tom Curran, Michael Granato, and Dennis Kolson for all their support and helpful advice throughout my Ph.D. thesis work.

I want to thank the entire Crino laboratory for all their help, especially Marianna, Ksenia, Whitney, Ben, Jackie B., Jackie E., Jelte, Kei, and Julie. Furthermore, I would like to thank the Kolson lab, especially Lorraine, Pat, Stephanie, Denise, and Alex.

I would like to thank the Neuroscience Graduate Group, especially Josh Gold, Mikey Nusbaum, Rita Balice-Gordon, and Jane Hoshi.

Finally, I want to thank my friends, both near and far, for your friendship and the support you've given me throughout the years.

ABSTRACT

THE ROLE OF TSC2 and DEPTOR in FETAL CORTICAL DEVELOPMENT

Victoria Tsai

Peter B. Crino

Tuberous Sclerosis Complex (TSC) is an autosomal dominant genetic disorder that results from mutations in the *TSC1* or *TSC2* genes. TSC is a multisystem hamartoma syndrome with manifestations in the brain, heart, lungs, kidney, skin and eyes. Neurologically, TSC patients may exhibit severe epilepsy, cognitive disabilities, and autism spectrum disorders. TSC1 and TSC2 proteins form a heterodimeric complex that serves to inhibit mammalian target of rapamycin (mTOR) signaling pathway. TSC1 and TSC2 receive activating or inhibitory signaling from multiple inputs including growth factors, insulin signaling, energy and amino acid levels, and proinflammatory pathways, and then integrate those signals to regulate the activity of mTOR. mTOR signaling plays a critical role in regulating cell growth, transcription, translation, and autophagy. Animal models have shed light on certain features of TSC, but failed to recapitulate the disease completely and currently further research is under way to better understand this devastating disorder. To date, mTOR signaling hyperactivation has been demonstrated in TSC tubers at postnatal time points, thus we set out to study the profile of mTOR activation in the fetal brain. We utilized both mouse neural progenitors *in vitro* and developing brain *in vivo* systems to understand the effects of Tsc1 and Tsc2 during brain development. Furthermore, after the identification of a new mTOR regulatory protein Deptor (*DEPDC6* gene), which inhibits the mTORC1 and mTORC2 signaling pathways similar to TSC1-TSC protein complex, we examined its role in brain development. We

found that Deptor shRNA knockdown results in mTORC1 and mTORC2 activation *in vitro* as well as abnormal migration *in vivo*. Our results show that mTOR signaling pathway could be the common pathway on which TSC1, TSC2, and DEPTOR converge and exert their effects on brain development. These results suggest mTOR signaling and its downstream effectors could be targets for therapeutic treatment during embryogenesis and could potentially prevent abnormal brain development.

TABLE OF CONTENTS

Dedication.....	iii
ACKNOWLEDGEMENTS	iv
ABSTRACT	v
LIST OF ILLUSTRATIONS	xii
LIST OF ABBREVIATIONS	xiv
CHAPTER 1. INTRODUCTION	1
CHAPTER 2. TUBEROUS SCLEROSIS COMPLEX: GENETIC BASIS AND CLINICAL MANAGEMENT STRATEGIES ¹	4
2.1. Tuberous Sclerosis Complex.....	5
2.2. Clinical Diagnostic Features	5
2.2a. Neurological Manifestations.....	5
Table 2-1. TSC Clinical Diagnostic Criteria	9
2.2b. Dermatological Features.....	10
2.2c. Renal Lesions	10
2.2d. Pulmonary Manifestations	11
2.2e. Cardiac Manifestations	12
2.2f. TSC and Cancer Predisposition	12
2.3. Genetics	13
Figure 2-1. TSC1-TSC2 Signaling Pathway.	15
2.4. Role of TSC1 and TSC2 Proteins in Cellular Function	16
2.5. Animal Models of Tuberous Sclerosis Complex	19

Table 2-2. TSC Mouse Models	24
2.6. Clinical Management Strategies for TSC	27
CHAPTER 3. FETAL BRAIN mTOR SIGNALING PATHWAY ACTIVATION IN TUBEROUS SCLEROSIS COMPLEX ²	29
3.1. Introduction	30
3.2. Materials and Methods.....	32
3.2a. Human TSC Fetal and Adult Tuber Specimens.....	32
3.2b. Cell Culture and Transfection	33
3.2c. In Utero Electroporation (IUE) and Rapamycin Administration.....	34
3.2d. Quantitative Analysis	35
3.3. Results	37
3.3a. Activation of mTOR Pathway in Human Fetal TSC Brain.....	37
Figure 3-1. mTORC1 and mTORC2 signaling pathway activation in fetal and adult TSC brains.....	39
3.3b. Depletion of Tsc2 and Activation of mTOR in mNPCs In Vitro	40
3.3c. Tsc2 Regulation of mNPC Size is Rapamycin-dependent.....	41
Figure 3-2. Tsc2 shRNA KD in mNPCs results in mTORC1 and mTORC2 pathway activation and increased cell size in vitro.....	43
3.3d. Tsc2 Depletion In Vivo Results in a Cortical Malformation	44
Figure 3-3. Focal Tsc2 shRNA KD results in a cortical malformation and cytomegaly in vivo.....	45
3.3e. Tsc2 Depletion Results in Increased Cell Volume In Vivo.....	46
3.3f. Tsc2 Knockdown In Vivo Results in Cell-Autonomous and Non-Cell- Autonomous Lamination Defects of Layer II-III.....	46

Figure 3-4. In vivo Tsc2 shRNA KD results in cell-autonomous and non-cell-autonomous lamination defect.	49
3.3g. Migratory Defect following Tsc2 Knockdown is Prevented with Rapamycin Treatment	51
3.3h. Rapamycin Treatment Rescues Cytomegaly and Non-Cell-Autonomous Effects due to Tsc2 Knockdown	52
Figure 3-5. Fetal rapamycin treatment rescues the lamination defect, cytomegaly and non-cell-autonomous lamination effects following Tsc2 shRNA knockdown in vivo.	54
Supplemental Figure 3-1.	56
Supplemental Figure 3-2.	57
Supplemental Figure 3-3.	58
Supplemental Figure 3-4.	59
Supplemental Figure 3-5.	60

CHAPTER 4: DEPTOR, A NOVEL mTOR-REGULATORY PROTEIN IS EXPRESSED IN THE BRAIN AND ITS LOSS RESULTS IN A CORTICAL MALFORMATION	61
4.1. Introduction	62
4.2. Materials and Methods.....	63
4.3. Results	66
4.3a. Deptor is Expressed in Human and Mouse Brain.....	66
Figure 4-1. Deptor is expressed in the human brain and murine neural cells.	67
4.3b. Deptor is Expressed in mNPCs, Neurons, and Astrocytes.....	68
Figure 4-2. Deptor is expressed is developmentally expressed in the mouse brain.	69

Figure 4-3. Deptor is present in cytoplasmic and nuclear compartments in mouse neural progenitor cells.	70
Figure 4-4. Deptor is more highly expressed in the astrocytes compared to neurons.	71
4.3c. Deptor shRNA KD in mNPCs Results in mTORC1 and mTORC2 Signaling Pathway Activation	72
Figure 4-5. Mouse neural progenitor cells with stable Deptor knockdown express SOX2 and Nestin, and show mTOR activation.	73
4.3d. Deptor KD in mNPCs Results in a Migration Defect In Vitro	75
Figure 4-6. Deptor knockdown results in impaired migration in vitro	76
4.3e. Deptor shRNA KD In Vivo During Embryogenesis by In Utero Electroporation Leads to a Cortical Malformation	79
Figure 4-7. Deptor depletion in vivo results in a cortical malformation.	80
CHAPTER 5. CONCLUSION, DISCUSSION AND FUTURE DIRECTIONS ²	81
5.1. Tsc2 Work Discussion	82
5.2. Deptor Work Discussion.....	86
5.3. Remaining Questions	87
5.3a. mTOR activation in Neural Progenitor Cells vs. Mature Neurons and Astrocytes	87
5.3b. Cell-Autonomous vs. Non-Cell-Autonomous Effects	87
5.3d. Is Deptor Associated with Any Neurological Diseases?	88
5.3c. TSC2 vs. DEPTOR	88
5.3e. Therapeutic Treatment Approaches	89
BIBLIOGRAPHY	91

LIST OF TABLES

Table 2-1. TSC Clinical Diagnostic Criteria

Table 2-2. TSC Mouse Models

LIST OF ILLUSTRATIONS

Figure 2-1. TSC1-TSC2 signaling pathway.

Figure 3-1. mTORC1 and mTORC2 signaling pathway activation in fetal and adult TSC brains.

Figure 3-2. Tsc2 shRNA KD in mNPCs results in mTORC1 and mTORC2 pathway activation and increased cell size *in vitro*.

Figure 3-3. Focal Tsc2 shRNA KD results in a cortical malformation and cytomegaly *in vivo*.

Figure 3-4. *In vivo* Tsc2 shRNA KD results in cell-autonomous and non-cell-autonomous lamination defect.

Figure 3-5. Fetal rapamycin treatment rescues the lamination defect, cytomegaly and non-cell-autonomous lamination effects following Tsc2 shRNA knockdown *in vivo*.

Supplemental Figure 3-1.

Supplemental Figure 3-2.

Supplemental Figure 3-3.

Supplemental Figure 3-4.

Supplemental Figure 3-5.

Figure 4-1. Deptor is expressed in the human brain and murine neural cells.

Figure 4-2. Deptor is expressed is developmentally expressed in the mouse brain.

Figure 4-3. Deptor is present in cytoplasmic and nuclear compartments in mouse neural progenitor cells.

Figure 4-4. Deptor is more highly expressed in the astrocytes compared to neurons.

Figure 4-5. Mouse neural progenitor cells with stable Deptor knockdown express SOX2 and Nestin, and show mTOR activation.

Figure 4-6. Deptor knockdown results in impaired migration *in vitro*.

Figure 4-7. Deptor depletion *in vivo* results in a cortical malformation.

LIST OF ABBREVIATIONS

- AML: angiomyolipomas
- cKO: conditional knockout
- CP: cortical plate
- DEPCD6*: gene that encodes DEPTOR protein
- GFP: green fluorescent protein
- IZ: intermediate zone
- KO: knockout
- LAM: lymphangiomyomatosis
- MRI: magnetic resonance imaging
- mNPCs: mouse neural progenitor cells
- mTOR: mammalian target of rapamycin
- mTORC1: mTOR complex 1
- mTORC2: mTOR complex 2
- Rheb: Ras homolog enriched in brain
- shRNA: short hairpin ribonucleic acid (RNA)
- SVZ: subventricular zone
- TBC1D7: TBC1 domain family, member 7
- TSC: Tuberous Sclerosis Complex
- TSC1*: Tuberous Sclerosis Complex gene 1
- TSC2*: Tuberous Sclerosis Complex gene 2
- VZ: ventricular zone

CHAPTER 1. INTRODUCTION

An estimated 1 million individuals are affected with Tuberous Sclerosis Complex (TSC) worldwide, involving all racial and ethnic groups. TSC is an autosomal dominant multi-system disorder with an incidence of 1 in 6000 live births (Crino et al., 2006). The majority of individuals with TSC exhibit neurological deficits, including cognitive disability, epilepsy, and autism spectrum disorders, that are directly linked to developmental malformations of the cerebral cortex known as cortical tubers. Histopathological studies revealed that tubers have loss of normal six-layered structure of cortex, and consist of abnormal dysmorphic neurons and cytomegalic 'giant' cells (GCs) which are immunoreactive for neuronal and glial cell markers and exhibit mTOR signaling pathway activation (Crino et al., 2006). TSC results from mutations in either *TSC1* or *TSC2* genes, and the proteins for which they encode, TSC1 and TSC2, form a functional heterodimeric complex that serves as an upstream regulator of mTOR pathway through inhibition of a GTPase-activating protein Ras homolog enriched in brain (Rheb). mTOR integrates signals from various inputs including growth factors, nutrients, energy, and stresses, to regulate multiple cellular processes such as growth, transcription, translation, and autophagy (Sarbasov et al., 2005; Chong-Kopera et al., 2006; Wullschleger et al., 2006). mTOR is found in two functionally distinct complexes which share some of the protein components, but raptor is specific to mTOR complex 1 (mTORC1) and rictor to mTORC2 (Cybulski and Hall, 2009). mTORC1 regulates ribosome biogenesis, transcription, translation and autophagy via phosphorylation of effector proteins S6K1, S6 and 4E-BP1 (Huang and Manning, 2008). Much less is known about mTORC2 signaling and function, but its effectors include Akt, serum and glucocorticoid-inducible kinase 1 (SGK1), PKC α and PKC δ (Guertin et al., 2006; Zhao et al., 2009). mTORC2 has been shown to regulate actin cytoskeletal organization, but through unknown mechanisms (Masri et al., 2007; Dada et al., 2008).

Rapamycin, an mTORC1 inhibitor, has been tested in clinical trials and shown to improve lung and renal manifestations of TSC, however significant effects on epilepsy, autism and cognitive disabilities have not been realized, suggesting non-mTORC1 signaling or negative feedback loop effects and the need for more targeted treatment approaches. To date, TSC animal models have only recapitulated certain aspects of tuber pathology, however the mechanisms governing loss of hexalaminar structure, ectopic cell positioning, cytomegaly and aberrant differentiation have not been elucidated.

Deptor is a newly discovered mTOR interacting and regulatory protein that directly binds to mTOR and antagonizes mTORC1 and mTORC2 signaling, and may thus be similar in function to TSC1-TSC2 (Peterson et al., 2009). Deptor overexpression in HEK293 and HeLa cells inhibits mTORC1 activity and leads to activation of PI3K/mTORC2/Akt pathway due to removal of inhibitory arm from S6K1, and has been shown to be mutated in multiple myeloma (Peterson et al., 2009). To date there have been no studies to identify the expression or function of Deptor in the brain.

**CHAPTER 2. TUBEROUS SCLEROSIS COMPLEX: GENETIC BASIS AND CLINICAL
MANAGEMENT STRATEGIES ¹**

¹ This work was originally published in *Advances in Genetics and Genomics* journal. Tsai V and Crino PB. 2012. Tuberous sclerosis: genetic basis and management strategies. Copyright © 2012 Dove Press.

2.1. Tuberous Sclerosis Complex

Tuberous Sclerosis Complex (TSC) is an autosomal dominant disorder with an incidence of 1 in 6000-10000 live births (Osborne et al., 1991; Devlin et al., 2006). Currently an estimated 1 million individuals are affected worldwide, involving all racial and ethnic groups. TSC is characterized by hamartomas, or benign tumor-like growths, in multiple organs including brain, lungs, heart, kidney, skin and eyes (Roach et al., 1992; Roach et al., 1998; Crino et al., 2006). TSC exhibits both variable penetrance, with individuals from the same family showing differential severity of specific features, and pleiotropy, in which individuals sharing similar genotypes have disparate clinical manifestations. TSC is diagnosed according to a group of major and minor diagnostic criteria (Table 2-1) that were revised at an NIH sponsored consensus conference (2004) (Roach et al., 1998). Genetic testing is valuable in confirming an early diagnosis but is not currently considered requisite for clinical diagnosis.

2.2. Clinical Diagnostic Features

2.2a. Neurological Manifestations

Neurological disorders are among the most common causes of morbidity in TSC patients. Individuals with TSC exhibit epilepsy, cognitive disabilities, and autism spectrum disorders (Crino et al., 2006). Nearly 90% of TSC patients develop epilepsy throughout their lifetime, which is often progressive, and intractable to medications. TSC is also the most common genetic cause of infantile spasms, a devastating epilepsy syndrome that affects 30-40% newborn infants. Approximately 50-60% of TSC patients

exhibit behavioral abnormalities, cognitive disabilities, and autism spectrum disorders. With increasing numbers of cases that are diagnosed prenatally or in early infancy, prior to seizure onset, questions regarding possible prophylactic anticonvulsant therapy to prevent development of epilepsy have emerged (Yates et al., 2011).

TSC brain lesions include developmental brain malformations known as cortical tubers, subependymal nodules (SENs), and subependymal giant cell astrocytomas (SEGAs). Cortical tubers are present in 80% of TSC patients and are characterized histopathologically by loss of normal six-layered structure of the cerebral cortex. Tubers are composed of abnormal dysmorphic neurons, cytomegalic 'giant' cells (GCs), and proliferative astrocytes, which have abnormal cellular morphology, cytomegaly, aberrant axonal projections and dendritic arbors (Richardson, 1991). Fetal tubers have been identified as early as 20 weeks gestation (Park et al., 1997) and it is currently believed that *TSC1* and *TSC2* mutations alter the normal development of neural precursors between 7 and 20 weeks (Crino, 2004). A recent study utilizing magnetic resonance imaging (MRI) has described distinct cortical tuber types based on signal intensity of subcortical white matter (Gallagher et al., 2010). Tubers Type A were isointense on volumetric T1 images and had subtle hyperintensity on T2 weighted and fluid-attenuated inversion recovery (FLAIR); Type B were hypointense on volumetric T1, but hyperintense on T2 weighted and FLAIR; and Type C were hypointense on volumetric T1 images, hyperintense on T2 weighted, and heterogeneous on FLAIR (Gallagher et al., 2010). Furthermore, this study compared and correlated TSC manifestations in patients with different tuber types: Type A patients had a milder phenotype, whereas patients with predominantly Type C tubers had other MRI abnormalities in addition to tubers, such as SEGAs, and a higher probability of having autism spectrum disorders, history of infantile spasms, and higher frequency of epileptic seizures, compared to patients with Type A and Type B tubers (Gallagher et al., 2010).

In the few reported neuropathological analyses of the post-mortem TSC brains, disruption of normal brain architecture distinct from tubers including small structural abnormalities including heterotopias, subcortical nodules, radial migration lines, areas of hypomyelination, and small cortical dysplasias have been described (Richardson, 1991; Scheithauer and Reagan, 1999). These lesions differ from tubers in that they are smaller, GCs are an infrequent finding, cortical lamination is only mildly altered, and they do not exhibit calcification. Recent MRI analyses in TSC patients have confirmed subtle structural abnormalities outside of tubers in the cortex and within subcortical structures such as the thalamus and basal ganglia (Ridler et al., 2001; Bolton et al., 2002) and suggest that these non-tuber brain lesions, in addition to tubers, may contribute to autism and cognitive disability in TSC.

SENs are nodular lesions typically less than 1 cm in size and are located on the surfaces of the lateral and third ventricles. SENs are present in about 80% of TSC patients and are believed to be asymptomatic i.e., not related to cognitive deficits or epilepsy. Typically, SENs are covered by a thin layer of ependyma, can exhibit extensive vascularization and extend into the periventricular white matter and the basal ganglia. These lesions develop early, in fetal life, and often degenerate or calcify later in life.

It is widely believed that SENs transition to form SEGAs, although the molecular mechanisms governing transformation from SEN to SEGA are unknown. SEGAs generally appear within the first twenty years of life. SEGAs generally exceed 1 cm in diameter but can grow greater than 10 cm in size. SEGAs extend into the lateral ventricle and often obstruct the flow of cerebrospinal fluid through the lateral ventricle and foramen of Monro, causing hydrocephalus, focal neurological deficits, and death. Thus in a select group of TSC patients, SEGAs require surgical removal. Overall, SEGAs are relatively rare and represent only about 1-2% of pediatric brain tumors. SEGAs can occur as sporadic tumors, however most of these likely represent somatic

mosaic TSC cases i.e., TSC gene mutation occurring within a restricted population of cells within a limited number of organ systems.

Table 2-1. TSC Clinical Diagnostic Criteria

(Roach et al., 1998)

	Major Features	Minor Features
Brain	Cortical tuber	Cerebral white-matter radial migration lines
	Subependymal nodule (SEN)	
	Subependymal giant cell astrocytoma (SEGA)	
Lungs	Lymphangiomyomatosis (LAM)	
Heart	Cardiac rhabdomyoma	
Kidney	Renal angiomyolipoma (AML)	Multiple renal cysts
Skin	Facial angiofibromas	“Confetti” skin lesions
	Ungual or periungual fibroma	
	Hypomelanotic macules (three or more)	
	Shagreen patch	
Eyes	Retinal nodular hamartomas	Retinal achromatic patch
Other		Multiple pits in dental enamel
		Hamartomatous rectal polyps
		Bone cysts
		Gingival fibromas

Definitive TSC:
Two major features
One major plus two minor features
Probable TSC:
One major plus one minor feature
Possible TSC:
One major feature
Two or more minor features

2.2b. Dermatological Features

Skin lesions are detected at all ages in more than 90% of patients and serve as an important clinical diagnostic features in both children and adults with TSC. For example, hypopigmented macules (“ash leaf spots”), are a major diagnostic feature of TSC generally detected in infancy or early childhood. Hypopigmented macules are generally a few millimeters to centimeters in size and can be found anywhere on the face, limbs, or trunk. The Shagreen patch is usually identified as a few centimeters in diameter area of roughened skin over the lumbosacral or flank region with increasing incidence after the age of 5 years. Ungual fibromas are fleshy growths near or beneath the nail that typically appear after puberty and may develop at any time in later adulthood. Facial angiofibromas (formerly referred to as adenoma sebaceum) may be detected at any age but are generally more common in late childhood or adolescence. They appear around the malar region of the face and the chin but can be found within the nose and external ear.

2.2c. Renal Lesions

Over 80% of TSC patients have renal manifestations, including angiomyolipomas (AMLs) and polycystic kidney disease. Renal AMLs are benign tumors comprised of abnormal blood vessels, smooth muscle cells, and adipocytes. While AMLs can occur sporadically in TSC patients, multiple AMLs are typically found in both kidneys (bilateral). It is estimated that AMLs can be detected in 55-75% of adult TSC patients. One study of 25 boys and 35 girls reported that 75% percent of children with TSC had renal AMLs by age 10.5 years (Ewalt et al., 1998). AMLs are detected by ultrasound, computed tomography, or MRI of the abdomen. Because AMLs contain

abnormal vasculature (which often contains aneurysms), spontaneous and potentially life-threatening hemorrhage is an important complication. Current treatment of AMLs includes embolization or systemic treatment with sirolimus (Davies et al., 2008; Davies et al., 2011). Rarely, surgery is indicated. In addition to AMLs, TSC patients may develop cysts, polycystic kidney disease and renal cell carcinomas (RCC; see below). Epithelial cysts, which can be multiple and are generally asymptomatic, may also be associated with hypertension and renal failure. Two to three percent of TSC patients carry a contiguous germline deletion, affecting both *TSC2* and *PKD1* genes on 16p13, resulting in polycystic kidney disease renal insufficiency.

2.2d. Pulmonary Manifestations

Lymphangiomyomatosis (also called lymphangiomyomatosis or LAM), affects women almost exclusively, and is characterized by widespread pulmonary proliferation of abnormal smooth muscle cells and cystic changes within the lung parenchyma (see review by Yu et al., 2010) (Yu et al., 2010). LAM often presents clinically with dyspnea or pneumothorax during early adulthood. While LAM can occur as a sporadic disorder, the incidence of radiographic evidence of LAM among women with TSC is 26-39%. Many women with radiographic evidence of LAM are clinically asymptomatic.

Recent studies have focused on understanding whether LAM results as a consequence of metastasis of benign tumors from other parts of the body. Approximately 60% of women who have sporadic LAM also present with renal AMLs. Genetic analyses and fluorescent *in situ* hybridization studies of recurrent LAM following lung transplantation provide support for benign tumor metastasis, since cells with the same gene mutation were found in the transplanted allograft (Karbowiczek et al., 2003).

2.2e. Cardiac Manifestations

Cardiac rhabdomyomas develop in approximately 50% of the TSC patients and may result in ventricular obstruction, arrhythmias, or congestive heart failure. However, in most TSC patients rhabdomyomas regress spontaneously with time and many disappear by the first year of life. As a rule, new rhabdomyomas do not appear in later life. In TSC patients with cardiac rhabdomyomas, medications are prescribed to treat arrhythmias and congestive heart failure, and some undergo surgery to relieve ventricular obstruction.

2.2f. TSC and Cancer Predisposition

TSC is not classically defined as a cancer predisposition syndrome and few epidemiological studies have accurately assessed the cumulative risk of developing, for example, RCC, in TSC. RCC occurs in TSC in perhaps 1-3% of patients and likely clinically presents at an earlier age than the general population. Conversely, mutations in *TSC1* or *TSC2* have been reported in several sporadic cancers such as transitional cell cancer of the bladder (van Tilborg et al., 2001; Adachi et al., 2003; Knowles et al., 2003; Pymar et al., 2008), urothelial carcinoma (Mhaweck-Fauceglia et al., 2008; Sjobahl et al., 2011), and neuroendocrine tumors (Larson et al., 2011). These tumors are not part of the diagnostic criteria for TSC, and thus their relation to the pathogenesis of TSC is unknown.

2.3. Genetics

TSC results from mutations in *TSC1* (9q34) or *TSC2* (16p13.3) gene (1993; van Slegtenhorst et al., 1997). *TSC1* is an 8.6 kb transcript, with a total genomic extent of 55 kb, consisting of 23 exons, and encoding an 1164 amino acid, 130 kD protein TSC1 (hamartin) (van Slegtenhorst et al., 1997). *TSC2* is a 5.5 kb transcript, with a total genomic extent of 40 kb, consisting of 41 exons, and encoding an 1807 amino acid, 180 kD protein TSC2 (tuberin). Approximately 20% of affected TSC individuals have an inherited *TSC1* or *TSC2* mutation, while in 80%, TSC results from a sporadic mutation. Over 1000 unique *TSC1* and *TSC2* allelic variants have been reported due to nonsense, missense, insertion and deletion mutations, involving nearly all exons of *TSC1* and *TSC2* (Jones et al., 1997; Jones et al., 1999; Niida et al., 1999; van Slegtenhorst et al., 1999; Dabora et al., 2001; Sancak et al., 2005; Napolioni et al., 2009). A study examining the differences between patients with *TSC1* versus *TSC2* mutations, found that individuals with sporadic *TSC1* mutations had an age range, average age, and median age that was similar to patients with sporadic *TSC2* mutations (Dabora et al., 2001). Furthermore, TSC patients with a sporadic *TSC1* gene mutation had on average milder disease manifestations, in particular neurological manifestations, than patients with *TSC2* mutations of similar age. Germline and somatic mutations were more common in *TSC2* gene than in *TSC1* (Dabora et al., 2001). A subset of patients that did not have any identifiable mutation in *TSC1* or *TSC2* gene. In another study, in a cohort of 362 patients, 276 had a definite clinical diagnosis of TSC and had a mutation detection rate of 85% (Sancak et al., 2005). However, approximately 15% had no identifiable mutation in either *TSC1* or *TSC2*, which could have been due to large deletions, somatic mosaicism or an unidentified locus. When examining the spectrum of TSC gene mutations, *TSC2* mutations were 3.4 times more common than *TSC1*

mutations (Sancak et al., 2005). In this study, *TSC1* mutations and familial *TSC2* mutations were associated with less severe phenotypes than sporadic *TSC2* mutations (Sancak et al., 2005). In a more recent study in 325 patients, mutations in either *TSC1* or *TSC2* genes were identified in 72% of *de novo* and 77% of familial cases, however, 29% of patients had no mutation identified (Au et al., 2007). Current estimate is that mutations in *TSC1* or *TSC2* genes have been identified in 70-90% of TSC patients, however 10-15% have no identified mutation (Qin et al., 2010b).

Aside from broad associations, there are few genotype-phenotype correlations. Prenatal molecular diagnosis using amniocentesis and chorionic villus sampling has been shown to be accurate in 48 out of 50 fetal cases at risk with TSC due to family history or fetal detection of cardiac rhabdomyoma on ultrasound, showing promise for early TSC diagnosis (Milunsky et al., 2009).

While loss of heterozygosity has been reported for hamartomas in almost all TSC lesions (Green et al., 1994a; Green et al., 1994b; Henske et al., 1996; Henske et al., 1997; Wolf et al., 1997; Niida et al., 2001; Chan et al., 2004; Cai et al., 2010), there is no consensus on the mechanism of cortical tuber formation in the brain. A recent report implementing single cell sequencing of *TSC1* and *TSC2* in phosphorylated ribosomal protein S6 (P-S6) immunolabeled GCs showed that tubers contain both germline and somatic mutations suggesting a mechanism of biallelic gene inactivation (Crino et al., 2010). In an animal model of TSC which is discussed in a subsequent section of this review, a second 'hit' was focally induced on a heterozygous background for a *Tsc1* mutation and resulted in cellular abnormalities reminiscent of tubers (Feliciano et al., 2011), providing support for biallelic gene inactivation in tuber formation. However another group reported that a second mutational 'hit' in *TSC1*, *TSC2*, or *KRAS* is a rare event in tubers (Qin et al., 2010a). Thus further investigation will need to be conducted to determine the molecular mechanism of cortical tuber formation in TSC.

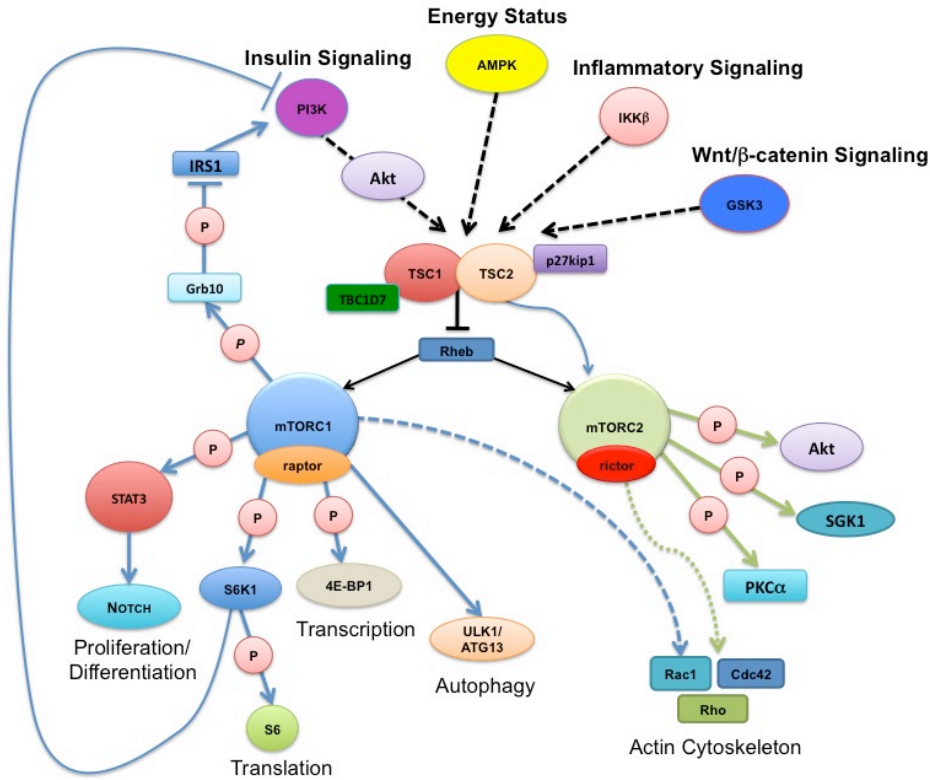


Figure 2-1. TSC1-TSC2 Signaling Pathway.

TSC1 and TSC2 proteins form a heterodimeric complex that serves as an inhibitor of mammalian target of rapamycin (mTOR) signaling pathway through GTPase Rheb. mTOR forms two distinct complexes with other proteins, among them raptor, specific to mTOR complex 1 (mTORC1) and rictor, specific to mTORC2, to regulate different aspects of cellular function, including transcription, translation, proliferation, differentiation, and autophagy. TSC1 and TSC2 integrate signals from various inputs upstream, among them insulin signaling, energy status, inflammatory, and Wnt/b-catenin signaling, and regulate mTOR pathway activity accordingly.

2.4. Role of TSC1 and TSC2 Proteins in Cellular Function

TSC1 and TSC2 proteins have been shown to regulate multiple cellular processes in both mTOR-dependent and mTOR-independent mechanisms. TSC1 and TSC2 proteins form a heterodimeric complex that serves as an upstream regulator of the mTOR pathway. TSC2 acts as a GTPase-activating protein towards Ras homolog enriched in brain (Rheb), which results in inhibition of mammalian target of rapamycin (mTOR) signaling (Fig. 1) (Tee et al., 2003). TSC1 protein stabilizes TSC2 by binding to it and prevents its ubiquitination (Benvenuto et al., 2000; Chong-Kopera et al., 2006). mTOR is an evolutionarily conserved serine/threonine kinase that integrates signals from various inputs including growth factors, nutrients, energy, and stresses, to regulate multiple cellular processes such as growth, transcription, translation, and autophagy (Fig. 1) (Sarbasov et al., 2005; Chong-Kopera et al., 2006; Wullschleger et al., 2006). mTOR is found in two functionally distinct complexes: mTOR complex 1 (mTORC1), which is comprised of mTOR, raptor (regulatory associated protein of mTOR) and PRAS40, and mTORC2, which is made up of mTOR, rictor (rapamycin insensitive component of mTOR), mSin1, and Protor1/2 (Cybulski and Hall, 2009).

mTORC1 regulates ribosome biogenesis, transcription, translation and autophagy (Wullschleger et al., 2006) via phosphorylation of several downstream effector proteins including S6K, S6 and 4E-BP1 (Huang and Manning, 2008). Loss of function mutations in *TSC1* or *TSC2* lead to aberrant activation of mTOR signaling, resulting in increased phosphorylation of S6K1, S6, and 4E-BP1. (Huang and Manning, 2008) Notch signaling is an important regulator of progenitor cell self-renewal, proliferation, differentiation, and survival (Lathia et al., 2008). Reduction in Notch1/Jagged1 signaling *in vivo* decreases the number of proliferating cells in postnatal

subventricular zone (SVZ) (Androutsellis-Theotokis et al., 2006). A recent study showed that mTOR regulates differentiation through STAT3-p63-Jagged1-Notch pathway in TSC fibroblast, LAM and mouse kidney tumor cells (Ma et al., 2010). A recent phosphoproteome analysis suggested that mTORC1 may actually modulate phosphorylation of several hundred proteins thus positing TSC1:TSC2:mTOR as a pivotal signaling node in many types of undifferentiated and differentiated cells (Hsu et al., 2011; Yu et al., 2011). Rapamycin is a macrolide antibiotic that is a highly specific mTORC1 inhibitor, functioning through FKBP12 (Sabers et al., 1995; Wiederrecht et al., 1995).

Much less is known about mTORC2 signaling and function, but its effectors include Akt, serum and glucocorticoid-inducible kinase 1 (SGK1), and PKC α . (Guertin et al., 2006; Zhao et al., 2009) mTORC2 has been shown to regulate actin cytoskeletal organization and hyperactivated mTORC2 signaling results in altered cell motility in endothelial cells and glioma cell lines (Masri et al., 2007; Dada et al., 2008), however through unknown mechanisms. mTORC2 is relatively insensitive to immediate direct inhibition by rapamycin (Sarbasov et al., 2005); although long-term treatment in mammalian cells can prevent *de novo* mTORC2 assembly (Sarbasov et al., 2006). Torin1 has been shown to inhibit both mTORC1 and mTORC2 signaling (Peterson et al., 2009). While TSC1-TSC2 complex serves an inhibitory role on mTORC1 signaling, some studies have reported opposite effects on mTORC2, and showed that TSC1-TSC2 is required for its proper activation. A study in renal AMLs and *Tsc2*^{+/-} mouse kidney tumors has reported that while mTORC1 biomarkers are increased in TSC tissues, mTORC2 effectors are attenuated (Yang et al., 2006; Huang et al., 2008; Huang et al., 2009). However further investigation needs to be conducted to understand mTORC2 signaling dysregulation in TSC.

Tsc1 protein has been found to interact with ezrin-radixin-moesin family of actin-binding proteins (Lamb et al., 2000). Another binding partner of TSC1, known as TBC1 domain family, member 7 (TBC1D7), may play pivotal roles in regulating the GAP activity effects exerted on Rheb. TSC1 stabilizes TBC1D7, and overexpression of TSC1 results in increased levels of TBC1D7 and its knockdown in reduced levels of TBC1D7 (Sato et al., 2010). Knockdown of TBC1D7 using siRNA resulted in inhibition of cell growth in lung cancer cells, whereas transplantation of COS-7 cells overexpressing TBC1D7 into BALB/cAJcl-*nu/nu* mice resulted in tumor development (Sato et al., 2010). Thus future investigation needs to be conducted into the role of TBC1D7 in regulation of mTOR pathway and TSC pathogenesis. Tsc2 has been shown to directly bind to p27kip1 and regulates its cellular localization and stability by preventing degradation by SCF-type E3 ubiquitin ligase complex (Soucek et al., 1997; Soucek et al., 1998; Miloloza et al., 2000; Rosner et al., 2003; Rosner and Hengstschlager, 2004; Rosner et al., 2007). p27kip1 is a cyclin-dependent kinase inhibitor of G₁ cell cycle progression and regulates proliferation. Akt phosphorylates Tsc2 on Ser939 and Thr1462, and thus controls its nuclear and cytoplasmic localization (Rosner et al., 2007). In G₀ arrested cells, Akt is downregulated and majority of Tsc2 is localized to the nucleus, however when the cells re-enter cell cycle, Akt is upregulated, Tsc2 is phosphorylated, and in turn is primarily found in the cytoplasm. (Rosner et al., 2007) Interestingly, p70S6K1 is found in both nucleus in the cytoplasmic compartments, however when it is phosphorylated (Thr389) by mTORC1, it becomes predominantly localized to the nucleus (Rosner and Hengstschlager, 2011).

Tsc1 knockout (KO) or *Tsc2* shRNA knockdown in hippocampal pyramidal neurons results in enlarged cell somas and altered dendritic spine morphology which were dependent on cofilin Ser3 phosphorylation (Tavazoie et al., 2005). These findings implicated regulation of actin cytoskeletal dynamics as the underlying molecular

mechanism for aberrant neuronal structural changes following loss of either *Tsc1* or *Tsc2* (Tavazoie et al., 2005). A recent study utilizing scratch-induced polarization “wound healing” assay in *Tsc2*^{-/-} fibroblasts demonstrated that *Tsc2* has a critical role in cell spreading, polarity and migration by regulating Cdc42 and Rac1 GTPase activation (Larson et al., 2010). Rapamycin treatment rescued the cell polarization defect in *Tsc2*^{-/-} fibroblasts and increased the activation of Cdc42 and Rac1, thus demonstrating mTORC1-dependence (Larson et al., 2010). mTORC2 has been shown to regulate the actin cytoskeleton and its deactivation by rictor shRNA knockdown leads to stress fiber formation and delocalized paxillin (an adapter protein present at the junction between actin cytoskeleton and plasma membrane) staining, which is phenotypically similar to *Tsc2*^{-/-} HeLa cells (Jacinto et al., 2004). Further studies will need to be conducted in order to determine whether regulation of cell migration by *Tsc1*-*Tsc2* is through mTORC1 or mTORC2 signaling pathways.

2.5. Animal Models of Tuberous Sclerosis Complex

Animal models have provided invaluable insight into TSC disease pathogenesis and cellular pathophysiology. Early studies in *Drosophila* showed that inactivating mutations in *dTsc1* and *dTsc2* cause indistinguishable phenotypes with deregulation of various processes, including increased cell size and enhanced cell proliferation (Ito and Rubin, 1999; Gao and Pan, 2001; Potter et al., 2001; Tapon et al., 2001). These findings led to identification of the link between *dTsc1*, *dTsc2*, and insulin growth factor signaling, and ultimately to the role of mTOR in TSC. Since then, the Eker rat, which has a spontaneous mutation in the *Tsc2* gene (an insertion which results in production of

abnormal larger protein), has been described as an autosomal dominant hereditary TSC animal model with predispositions to renal adenoma and carcinoma (Eker, 1954; Yeung et al., 1994). Eker rats develop kidney cystadenoma lesions by 4 months, and pituitary adenomas, uterine leiomyomas, and leiomyosarcomas, and splenic hemangiosarcomas between 14 months to 2 years (Everitt et al., 1992; Hino et al., 1993). Loss of heterozygosity is seen in majority of these tumors and established *Tsc2* as a tumor suppressor gene.

More recently, transgenic strategies in mice have resulted in the generation of several different *Tsc1* and *Tsc2* KO models (see Table 2-2 for details). *Tsc1* or *Tsc2* KO (*Tsc1*^{-/-}, *Tsc2*^{-/-}) results in embryonic lethality. Specifically, *Tsc1*^{-/-} mice die at E9.5-13.5 and have developmental delay, liver hypoplasia, neural tube closure defects, and poor abdominal organ development (Kobayashi et al., 2001; Kwiatkowski et al., 2002; Wilson et al., 2005). *Tsc2*^{-/-} mice die earlier than *Tsc1*^{-/-} (between E9.5-12.5) and also have developmental delay, neural tube closure defects, exencephaly, liver hypoplasia, poor development of abdominal organs, and thickened myocardia (Kobayashi et al., 1999; Onda et al., 1999; Hernandez et al., 2007; Pollizzi et al., 2009b).

Heterozygote *Tsc1*^{+/-} and *Tsc2*^{+/-} mice develop bilateral renal cystadenomas, liver hemangiomas, lung adenomas and extremity angiosarcomas by 15 months of age and lesion development is milder in *Tsc1*^{+/-} mice compared to *Tsc2*^{+/-} mice (Kobayashi et al., 1999; Onda et al., 1999; Kobayashi et al., 2001; Kwiatkowski et al., 2002; Wilson et al., 2005; Hernandez et al., 2007; Pollizzi et al., 2009b) (see Table 2-2; for detailed review see Kwiatkowski D. J., 2010 (Kwiatkowski, 2010)). Rapamycin and other related mTORC1 inhibitors have been shown to be effective in blocking tumor development in *Tsc1*^{+/-} and *Tsc2*^{+/-} mouse models, similar to the results seen in Eker rat model (Kenerson et al., 2005; Lee et al., 2005; Pollizzi et al., 2009a). Furthermore, rapamycin treatment resulted in a decrease in size of renal and pituitary tumors and improved

survival, however, evidence of drug resistance was reported in a small percentage of lesions after long-term therapy (Kenerson et al., 2005).

Several conditional knockout (cKO) TSC mouse models have been generated subsequently. Neuronal *Tsc1* cKO in mice (*Tsc1^{fl/fl}; Synapsin1-Cre*) results in spontaneous seizures in 10% of mice, ectopic, enlarged, and aberrant neurons, reduced myelination (Meikle et al., 2007), hyperexcitability and tonic spasms leading to premature death. (Wang et al., 2007) Mice with *Tsc1* cKO in astrocytes (*Tsc1^{fl/fl}; GFAP-Cre*) have megalencephaly, epilepsy, increased astrocytic proliferation, aberrant hippocampal organization, and die prematurely (Uhlmann et al., 2002b). *Tsc1* cKO in the forebrain (*Tsc1^{fl/fl}; Emx1-Cre*) results in enlarged brain size and cytomegalic cells within the cerebral cortex, and the mice die by postnatal day 25 (Carson et al., 2011). Recently, a new model of focal *Tsc1* KO in a subpopulation of progenitor cells on a heterozygous *Tsc1* background was described and the mice show aberrant lamination of the cerebral cortex, cytomegalic multinucleated neurons in the intermediate zone (similar to subcortical white matter in humans), and lower seizure threshold, providing support for biallelic gene inactivation in the brain (Feliciano et al., 2011).

Radial glia-specific *Tsc2* cKO mice (*Tsc2^{fl/ko}; hGFAP-Cre*) have many of the TSC features, including megalencephaly, cellular cytomegaly, and cortical lamination defects (Way et al., 2009). *Tsc2* cKO in astrocytes (*Tsc2^{fl/fl}; GFAP-Cre*) results in a more severe epilepsy phenotype than *Tsc1* cKO (*Tsc1^{fl/fl}; GFAP-Cre*), with an earlier onset and higher seizure frequency which were correlated with higher mTORC1 activation (Zeng et al., 2011). These findings support that mutations in *Tsc2* gene result in a more severe phenotype than mutations in *Tsc1*. Another *Tsc2* animal model which expresses a dominant negative *Tsc2* transgene shows mild but statistically significant impairments in social behavior and rotarod motor learning, recapitulating some of the behavioral abnormalities observed in TSC patients (Chevere-Torres et al., 2011). The dominant

negative Tsc2 is able to bind Tsc1, but the mutation affects its GAP domain and rabaptin-5 binding motif (Chevere-Torres et al., 2011).

Tsc1^{+/-} neurons with a single deleted copy of *Tsc1* exhibit morphological changes characteristic of *Tsc1*- and *Tsc2*-deficient neurons, suggesting that haploinsufficiency rather than complete lack of either *Tsc* gene could contribute to certain aspects of TSC neuropathogenesis (Tavazoie et al., 2005). While heterozygote *Tsc1*^{+/-} and *Tsc2*^{+/-} mice do not exhibit gross brain abnormalities, they have cognitive and social behavior deficits and impaired hippocampus-dependent learning (Goorden et al., 2007; Ehninger et al., 2008; Chevere-Torres et al., 2011). *Tsc2*^{+/-} mice have also been shown to have aberrant retinogeniculate projections with EphA receptor-dependent axon guidance in the visual system (Nie et al., 2010). This suggests that while there may be no gross apparent brain architectural changes due to *Tsc1* or *Tsc2* haploinsufficiency, there could be alterations in network circuitry.

Rapamycin treatment has been shown to be effective in brain abnormalities in TSC mouse models. Rapamycin treatment started prior to onset of seizures prevented the development of epilepsy in *Tsc1* cKO mice (*Tsc1*^{fl/fl}; *GFAP-Cre*) and improved survival, however if the treatment was stopped, the neurologic phenotype subsequently developed with a delay of several weeks, including the histopathologic abnormalities and epilepsy (Zeng et al., 2008). When treatment was started after epilepsy onset, rapamycin reduced the seizure frequency, thus supporting mTOR's role in early and late epileptogenesis, however its effects were not as robust as when rapamycin was began early (Zeng et al., 2008). Rapamycin treatment in heterozygous *Tsc2*^{+/-} mice reversed the learning abnormalities, thus demonstrating its potential in treatment of cognitive deficits in TSC (Ehninger et al., 2008).

Recently, in a model of *Tsc1* cKO in postnatal SVZ using a tamoxifen-inducible *Nestin-CreER*^{T2} mouse line, tamoxifen was administered at postnatal day 7 or 1 month,

resulting in enlarged brains at 3 and 6-7 months, however had no body weight differences (Zhou et al., 2011). Furthermore, *Tsc1-Nestin* cKO mice had hydrocephalus, an enlarged hippocampus, and small nodular structures and tumors were present near the interventricular foramen, reminiscent of SENs and SEGAs seen in TSC patients (Zhou et al., 2011). Most cells in these tumors had enlarged somas and stained positive for mature neuronal markers MAP2 and NeuN or astrocytic markers S100b and GFAP, but were low in Ki67 and did not exhibit multinucleation (Zhou et al., 2011). Another model of *Tsc1 Nestin-Cre* cKO exhibited normal body weight and organ development, but an enlarged head and the mice died within 24 hours after birth with lethality being most likely due to malnutrition, hypoglycemia, and hypothermia (Anderl et al., 2011b). The mutant brains grossly showed normal brain architecture, but the cerebral cortex was especially enlarged (Anderl et al., 2011b). Single rapamycin dose (1 mg/kg) was administered subcutaneously to the pregnant dam between embryonic days E15-17, and significantly increased the survival of the mutant mice up to postnatal day 20 (Anderl et al., 2011b). This study strengthens the potential of early rapamycin therapy in TSC.

In summary, TSC animal models have taught us a lot about TSC pathophysiology in certain organ systems. However the existing TSC animal models have failed to recapitulate all lesions seen in TSC human patients. For example, cortical tubers and LAM lesions have not been completely modeled in animal models. Further investigation and better TSC animal models will be pivotal in understanding of the disease mechanisms leading to TSC pathogenesis.

Table 2-2. TSC Mouse Models

Gene	Knockout Condition	Phenotype
Tsc1	Neo insertion and deletion of exons 6-8 (Kobayashi et al., 2001)	KO: embryonic lethal (E10.5-11.5) due to neural tube closure defects, exencephaly, abnormal morphology of myocardial cells, developmental delay, liver hypoplasia
		HET: kidney cysts and cystadenomas, liver hemangiomas, tail hemangioma, uterine leiomyoma/leiomyosarcoma
	Deletion of exons 17-18 (Kwiatkowski et al., 2002)	KO: embryonic lethal (E9-13.5) due to liver hypoplasia; developmental delay of approximately 1 embryonic day compared to littermates, poor development of abdominal organs, enlarged heart which was shifted inferiorly, pericardial effusions, circulatory failure due to anemia
		HET: bilateral kidney cystadenomas, liver hemangiomas (females: higher % affected, higher average grade; compared to males), forepaw angiosarcoma; premature death (higher in females than in males)
	Neo cassette insertion and deletion of exons 6-8 (Wilson et al., 2005; Goorden et al., 2007)	KO: embryonic lethal (E10.5-12.5), developmental delay, exencephaly, abnormal vacuolation of myocardial cells
		HET: kidney lesions (cysts, cystadenomas, solid carcinomas), metastatic renal cell carcinomas, liver hemangiomas, premature death; severity of phenotype was dependent on genetic background; impaired hippocampal-dependent learning and impaired social behavior
	Conditional <i>GFAP-Cre</i> (target: astrocytes), exons 17-18 (Uhlmann et al., 2002b)	cKO: megalencephaly, epilepsy, astrocytic proliferation, aberrant hippocampal neuronal organization, premature death
	Conditional <i>Synapsin1-Cre</i> (target: neurons), exons 17-18 (Meikle et al., 2007)	cKO: spontaneous seizures (10%), neuropathological abnormalities (ectopic, enlarged, aberrant neurons), reduced myelination, delayed developmental beginning

	Conditional <i>Synapsin1-Cre</i> (target: neurons), exons 17-18 (<i>Wang et al., 2007</i>)	cKO: bicuculline-induced epileptiform discharges, hyperexcitability, tonic spasms leading to death
	Conditional <i>Nestin-Cre</i> (target: neural progenitors), exons 17-18 (<i>Zhou et al., 2011</i>)	cKO: structural abnormalities resembling features of SENs and SEGAs in the lateral ventricle
	Conditional <i>Nestin-Cre</i> (target: neural progenitors), exons 17-18 (<i>Anderl et al., 2011b</i>)	cKO: enlarged brains, early lethality due to hypoglycemia, poor mother-pup interaction
	Conditional <i>Emx1-Cre</i> (target: neural progenitors of the forebrain), exons 17-18 (<i>Carson et al., 2011</i>)	cKO: enlarged brain size, enlarged cells, decreased myelination, premature death
	Focal deletion of exons 17-18 in brain on background of <i>Tsc1^{fl/mut}</i> (<i>Feliciano et al., 2011</i>)	Focal brain KO: ectopic cytomegalic and multinucleated neurons, lower seizure threshold
Tsc2	Eker rat; spontaneous insertion mutation (<i>Eker, 1954; Eker et al., 1981; Everitt et al., 1992; Hino et al., 1993; Yeung et al., 1994; Yeung et al., 1997; Mizuguchi et al., 2000</i>) (d)	Predisposition to kidney cystadenomas and renal cell carcinomas, pituitary adenoma, uterine leiomyomas, leiomyosarcomas, splenic hemangiosarcomas, some brain lesions
	Neo cassette insertion into exon 2 (<i>Onda et al., 1999</i>) (d)	KO: embryonic lethal (E9.5-12.5) due to liver hypoplasia; exencephaly, developmental delay of 1-2 embryonic days compared to littermate, poor development of abdominal organs, heart shifted inferiorly, pericardial effusions, circulatory failure due to anemia HET: kidney tumors (renal cysts and adenomas), renal cell carcinoma, liver hemangiomas, lung adenomas, and foot, tail, lip angiosarcomas; deficits in hippocampal-dependent learning
	Neo cassette insertion into exon 2 and deletion of exons 2-5 (<i>Kobayashi et al., 1999</i>) (d)	KO: embryonic lethal (E9-12.5) due to neural tube closure defects, exencephaly, abnormal thickened myocardia HET: multiple renal cell carcinomas, liver hemangiomas
	Neo cassette insertion into exon 1, deletion of exons 2-4 (<i>Hernandez et al., 2007</i>) (d)	KO: embryonic lethal (E9.5-17); neural tube closure defects, developmental delay HET: kidney cysts and tumors

	Deletion of exon 3 (hypomorphic allele, <i>de/3</i>) (Pollizzi et al., 2009b)	KO: embryonic lethal (E9.5-13.5; longer survival compared to previous <i>Tsc2</i> KO models(Kobayashi et al., 1999; Onda et al., 1999)), developmental delay, liver hypoplasia, poor/deficient hematopoiesis, hemorrhage in multiple sites (heart, liver)
		HET: kidney cysts and cystadenomas; phenotype less severe than that of previous <i>Tsc2</i> KO models(Kobayashi et al., 1999; Onda et al., 1999)
	Conditional <i>Insulin2-Cre</i> (target: pancreatic b-cells), exons 3-4 (Shigeyama et al., 2008)	cKO: hypoglycemia and hyperinsulinemia (age 4-28 weeks); hyperglycemia and hypoinsulinemia (after age 40 weeks)
	Conditional <i>hGFAP-Cre</i> (target: radial glial progenitor cells), exons 2-4 (Hernandez et al., 2007; Way et al., 2009)	cKO: megalencephaly, cellular cytomegaly, cortical and hippocampal lamination defects, astrocytosis, abnormal myelination, premature death
	Conditional <i>GFAP-Cre</i> (target: astrocytes), exons 2-4 (Zeng et al., 2011)	cKO: megalencephaly, hippocampal neuronal disorganization, astrocytic proliferation, premature death (phenotype more severe than <i>Tsc1 GFAP-Cre</i> cKO(Uhlmann et al., 2002a))
	Dominant negative transgene (delta RG) (Govindarajan et al., 2005; Chevere-Torres et al., 2011)	fibrovascular collagenoma in dermis, subpial external granule cells in cerebellum; deficits in social behavior and rotarod learning

2.6. Clinical Management Strategies for TSC

Up until 2007, treatment of TSC was largely symptomatic and not specific for the cell signaling pathways activated in TSC. Thus, anti-epileptic drugs and epilepsy surgery remain the mainstays of epilepsy therapy. Embolization or surgery is used for renal lesions, and oxygen supplementation can provide symptomatic relief for LAM. However, an initial clinical trial assessed the efficacy of sirolimus in reducing the volume of renal AMLs and showed improving pulmonary function tests in LAM (Bissler et al., 2008). A pivotal finding of this trial was that while AMLs did in fact show diminished volume after 12 months of rapamycin treatment, in the ensuing 12 months during which rapamycin was discontinued, there was re-growth of AMLs in many patients (Bissler et al., 2008). Phase 2 clinical trials with sirolimus showed that patients treated for 52 weeks had regression of kidney AMLs, SEGAs, and liver AMLs (Dabora et al., 2011). Most recently, the mTOR inhibitor everolimus showed efficacy in reducing SEGA volume after 6 months of treatment (Krueger et al., 2010). Furthermore, there was modest reduction in seizure frequency in 9 out of 16 TSC patients with seizures, however seizure frequency did not change in 6 individuals, and worsened in 1 patient (Krueger et al., 2010). These studies provided clear evidence that modulation of the mTOR pathway in TSC could benefit some patients and thus opened the conceptual door for syndrome specific therapy in TSC. Everolimus is the first mTOR inhibitor that has been FDA approved for treatment of SEGAs associated with TSC (Franz, 2011). Recently, there has also been a case report of regression of cardiac rhabdomyoma in a TSC patient 13 months after everolimus treatment (Tiberio et al., 2011). While cardiac rhabdomyomas have been shown to regress naturally, the time course in this specific patient who was diagnosed *in utero* and had no significant changes for the next 5 years, suggests that everolimus

might have played a role in the regression and near resolution of the rhabdomyoma (Tiberio et al., 2011). These results support the role of mTOR involvement in TSC pathogenesis and demonstrate potential of mTOR inhibitors as therapeutic treatments. However, a clear and overarching clinical challenge associated with the use of mTOR inhibitors is the need for continued therapy to prevent recurrence of lesion growth. The modest or non-effect of everolimus on epilepsy necessitates further investigation into the role of mTOR in epileptogenesis in TSC.

**CHAPTER 3. FETAL BRAIN mTOR SIGNALING PATHWAY ACTIVATION IN
TUBEROUS SCLEROSIS COMPLEX ²**

² This work was originally published in *Cerebral Cortex* journal. Tsai V, Parker WE, Orlova KA, Baybis M, Chi AWS, Berg BD, Birnbaum JF, Estevez J, Okochi K, Sarnat HB, Flores-Sarnat L, Aronica E, Crino PB. 2012. Fetal Brain mTOR Signaling Pathway Activation in Tuberous Sclerosis Complex. Copyright © 2012 Oxford University Press.

3.1. Introduction

Tuberous Sclerosis Complex (TSC) is an autosomal dominant disorder resulting from mutations in either *TSC1* or *TSC2* genes, characterized neurologically by intractable epilepsy, cognitive disability, and autism spectrum disorders. Cortical tubers are malformations of the cerebral cortex, which are detected as early as 20 weeks gestation (Park et al., 1997) and identified in over 80% of TSC brain specimens (Sparagana and Roach, 2000; DiMario, 2004; Crino et al., 2006). Tubers exhibit severely disorganized lamination and contain cells with abnormal cellular morphology, specifically enhanced cell size (cytomegaly). While tubers are believed to be closely linked to epileptogenesis in TSC, there is debate as to whether there is a relationship between tuber number or “tuber burden” and severity of neurocognitive deficits in TSC patients (Jambaque et al., 1991; Marcotte and Crino, 2006; Zaroff et al., 2006; Ess and Roach, 2012; Tillema et al., 2012).

The encoded *TSC1* and *TSC2* proteins form a functional heterodimeric complex that inhibits the mammalian target of rapamycin (mTOR) signaling pathway (Wullschleger et al., 2006; Huang and Manning, 2008). Loss of function mutations in *TSC1* or *TSC2* in neuroglial progenitor cells lead to constitutive activation of the mTOR cascade as evidenced by phosphorylation of p70 S6 kinase 1 (P-p70S6K1; T389) and ribosomal protein S6 (P-S6; S235/236) in pediatric and adult human tuber specimens and TSC animal models (Huang and Manning, 2008). Extant transgenic mouse strains lacking either *Tsc1* or *Tsc2* under conditional cell-specific promoters (e.g. hGFAP, Synapsin1) exhibit variable morphological and functional changes including astrocytosis, laminar disorganization, cytomegaly, spontaneous seizures, and decreased survival (Uhlmann et al., 2002b; Wang et al., 2007). Conditional *Tsc2* deletion in mouse radial

glial cells ($Tsc2^{hGFAP}Cre$) produces megalencephaly and cortical lamination defects (Way et al., 2009). $Tsc2^{hGFAP}Cre$ knockout mice have been shown to have a more severe seizure phenotype than $Tsc1^{hGFAP}Cre$ knockout mice (Zeng et al., 2011). In most $Tsc1$ or $Tsc2$ mouse mutants, transgene expression occurs across much of the developing telencephalon as opposed to within focal brain regions similar to tubers in TSC. Recently, a murine model was reported in which biallelic $Tsc1$ mutations engineered in neuroglial progenitor cells caused focal brain malformations (Feliciano et al., 2011). Generating focal malformations on a background of morphologically intact cortex provides an attractive strategy to test the new pharmacotherapies on lesion formation, as well as the surrounding cortex.

Since hyperactivation of mTOR signaling has thus far been demonstrated in tubers only at postnatal time points and since to date, no studies have evaluated mTOR complex 2 (mTORC2) signaling in TSC brain, we examined the phosphorylation status of mTORC1 substrates P-p70S6K1, P-S6, and c-myc and mTORC2 complex substrates P-PKC α (S657), P-Akt (Ser473), P-SGK1 (S422) and P-NDRG1 (Thr346) in human fetal tubers to determine the activation state of mTORC1 and mTORC2 during fetal development. Because recent human and animal genotype-phenotype analyses have demonstrated that $TSC2$ gene mutations are associated with a more severe clinical phenotype than $TSC1$, and because many of the existing conditional knockout mouse strains target $Tsc1$, we then focused our *in vitro* and *in vivo* studies in mouse neuroglial progenitor cells on $Tsc2$. First, we show that shRNA-mediated KD of $Tsc2$ *in vitro* in mouse neural progenitor cells (mNPCs) leads to mTORC1 and mTORC2 activation, thus modeling human fetal brain tissue, and enhanced cell size that is prevented with the mTORC1 inhibitor rapamycin. We then show that $Tsc2$ shRNA KD in fetal mouse brains *in vivo* using *in utero* electroporation causes aberrant cortical lamination that can be prevented with *in utero* rapamycin treatment. Our goal was to generate focal KD of $Tsc2$

to study the effects of Tsc2 loss on neural progenitor cells as well as on surrounding cells in the developing cortex.

3.2. Materials and Methods

3.2a. Human TSC Fetal and Adult Tuber Specimens

Human fetal tuber specimens were obtained post-mortem following fetal demise (n=4; a twin pair, ages 23 weeks gestations, and single specimens at 34 and 38 weeks gestation) and the detection of tubers and subependymal nodule or cardiac rhabdomyoma (major diagnostic criteria for TSC) confirmed the diagnosis of TSC. The genotype of the 23-week twin pair was an identified *TSC2* mutation (2713C-T; R905W; mutation data was not available for the other human specimens). Control fetal brain specimens with normal cytoarchitecture (n=2; age: 28, 33 weeks gestation) were analyzed. Control adult brains were obtained post-mortem. Adult TSC tuber specimens were obtained following surgical resection from 2 female TSC patients. For Western analysis, control specimen was obtained post-mortem (male; age: 28 years) and TSC tuber following surgical resection (male; age: 2 years).

Fixed, paraffin-embedded specimens, 5 sections per case, were probed with a panel of antibodies including P-p70S6K1 (T389; Cell Signaling), P-S6 (S235/236; Cell Signaling), c-myc (Abcam), P-PKC α (S657; Santa Cruz Biotechnology), P-SGK1 (S422; Santa Cruz Biotechnology), P-Akt (S473; Cell Signaling), P-NDRG1 (T346; Cell Signaling), and PKC α (Cell Signaling) overnight at 4°C. Immunolabeling was visualized with avidin-biotin complex (Vectastain ABC Kit; Vector Labs) and 3,3'-diaminobenzidine (Sigma-Aldrich).

3.2b. Cell Culture and Transfection

mNPCs derived from the subventricular zone (SVZ) of postnatal day 1 C57BL/6 mice, were cultured on poly-D-lysine (PDL) coated plates in Dulbecco's modified Eagle medium: nutrient mixture F-12 (DMEM/F12) supplemented with 1% fetal bovine serum (FBS), 1% N2 supplement, fibroblast growth factor, and heparin (Orlova et al., 2010a). mNPCs express protein markers of a neuroglial progenitor state (SOX2, Nestin), and retain full differentiation capacity into neurons or astrocytes (Magnitsky et al., 2008; Orlova et al., 2010a).

mNPCs were transfected with shRNA plasmids containing a green fluorescent protein (GFP) reporter under the control of a cytomegalovirus (CMV) promoter (shRNA-GFP; SA Biosciences) targeting mouse *Tsc2* or scrambled sequence (control) using Lipofectamine LTX/Plus Reagents (Invitrogen). shRNA constructs were commercially confirmed for absence of interferon response. In keeping with existing standards for shRNA experimentation *in vitro* and *in vivo* (Samuel-Abraham and Leonard, 2010), multiple shRNA constructs to *Tsc2* and scrambled sequence were tested. GFP-positive mNPCs were sorted using fluorescence-activated cell sorting (FACS) with a FACS Aria flow cytometer (BD Biosciences) at 2-5 days post transfection (DPT), plated and grown for 3-5 days, and used to generate protein lysates for Western analysis. Rapamycin (100nM; Cell Signaling) was added directly to cell culture media and administered for 24 hours or daily for 5-7 days.

mNPCs lysates (radioimmunoprecipitation [RIPA] lysis buffer 50 mM Tris HCl, pH 8.0; 150 mM NaCl; 1% NP-40; 0.5% sodium deoxycholate, 0.1% SDS, with protease and phosphatase inhibitors) separated on a 4-15% SDS-PAGE gel (Bio-Rad), transferred onto PVDF membranes and probed with *Tsc2* (Abcam), phosphorylated 4E-

BP1 (P-4E-BP1; T37/46; Cell Signaling), 4E-BP1 (Cell Signaling), P-S6 (S235/236; Cell Signaling), S6 (Cell Signaling), P-PKC α (S657; Santa Cruz Biotechnology), PKC α (Cell Signaling), P-Akt (S473; Cell Signaling), Akt (Cell Signaling), P-NDRG1 (T346; Cell Signaling), NDRG1 (Abcam) antibodies overnight at 4°C and HRP-conjugated secondary antibodies (GE Healthcare) for 1 hour at room temperature, and visualized with ECL or ECL Plus (GE Healthcare). Membranes were probed with antibody to glyceraldehyde-3-phosphate dehydrogenase (GAPDH; Cell Signaling) to ensure equal protein loading.

3.2c. In Utero Electroporation (IUE) and Rapamycin Administration

Animal experiments were approved by the Institutional Animal Care and Use Committee of the University of Pennsylvania.

Time-pregnant C57BL/6J mice at embryonic day 14 (E14) were placed under isoflurane-induced anesthesia and the uterine horns were surgically exteriorized. shRNA-GFP plasmids targeting mouse Tsc2 or control scrambled sequence (3-8 mg/ml) diluted in TE Buffer (Qiagen) and Fast Green dye (0.3 mg/ml; Sigma-Aldrich), were microinjected through the uterine wall into one lateral ventricle of each embryo. Tsc2 shRNA clone #4 was used for IUE experiments. Five electrical pulses (40 V, 50 ms duration, 1000 ms intervals) (Saito, 2006) were delivered across the embryonic head using CUY21 Edit Square Wave Electroporator (Nepagene). Uterine horns were returned to the pelvic cavity and the abdominal wall was closed by suture. Females were returned to the cage and embryos were sacrificed 5 days later at E19.

BrdU (50 mg/kg body weight) was intraperitoneally injected at E14. Rapamycin (0.5, 2.5, or 5.0 mg/kg body weight) diluted in vehicle solution (5% PEG 400, 5% Tween

80, 0.9% NaCl/H₂O) was intraperitoneally injected daily for 4 days (E15-E18) or 5 days (E14-E18).

Fixed, cryoprotected embryonic mouse brains were cryostat sectioned at 20 μ m thickness. Sections were probed with antibodies to P-S6 (S235/236; Cell Signaling; Bethyl Laboratories), Cux1 (Santa Cruz Biotechnology), Ctip2, Tbr1, MAP2 (Abcam), and BrdU (Millipore). Sections were subsequently stained with Texas Red (Vector Labs), Cy3, Cy5 (Jackson ImmunoResearch), AlexaFluor647 (Invitrogen) secondary antibodies and Hoechst33342 (0.0001mg/ml; Invitrogen) to visualize cell nuclei and define the zones of the embryonic brain based on cellular density. Fluoromount-G (SouthernBiotech) mounting media was used to mount the sections.

3.2d. Quantitative Analysis

Cell size was compared by FACS sorting mNPCs transfected with scrambled or Tsc2 shRNA-GFP plasmids for GFP. The scrambled and Tsc2 shRNA transfected mNPCs were sorted using the same parameters and consecutively during one run. Forward scatter area (FSC-A) and side scatter area (SSC-A) histograms for scrambled and Tsc2 GFP-positive cell populations were compared. Mean and standard deviation were computed for FSC-A and SSC-A measurements and compared using one-way ANOVA ($p < 0.05$).

Total cell area of mNPCs was quantified in digital images (Leica DMI6000B microscope and Leica DFC360FX camera) by outlining the cell circumference of GFP-positive cells and utilizing the ImagePro Plus software (Media Cybernetics) area measurement function. Cell area measurements were compared between control, scrambled shRNA-, and Tsc2 shRNA-transfected mNPCs in untreated, vehicle (DMSO),

and rapamycin (100nM) treated conditions (one-way ANOVA, Tukey-Kramer post hoc analysis for multiple comparisons; $p < 0.05$).

The laminar position of shRNA-transfected cells *in vivo* was assessed at E19 in homologous cortical regions (n=5 embryos per condition; 3-8 rostral to caudal sections per embryo were analyzed). GFP-positive cells were identified in a focal region in frontal cortex anterior to the rostral hippocampus. The zones of the developing embryonic brain: ventricular zone (VZ)/SVZ, intermediate zone (IZ), and cortical plate (CP), were defined by the density of Hoechst-positive nuclei. The CP region was split into 3 equal segments: lower CP (LW_CP), middle CP (MID_CP), and upper CP (UP_CP), for further quantification. A region of interest (ROI) spanning these zones was delineated by a rectangle extending from the pial surface to the lateral ventricle that circumscribed the transfected region. The total number of transfected GFP-positive cells quantified was approximately equal for each experimental group. The number of GFP-positive cells within each zone and in the ROI was counted in a blinded fashion in 3-8 sections spanning rostral to caudal regions for each animal. The data were expressed as the percentage of total GFP-positive cells in a given ROI located in each defined zone \pm standard error of the mean (SEM; GraphPad Prism software, one-way ANOVA, Dunnett's post hoc analysis for multiple comparisons $p < 0.05$) (Nguyen et al., 2006).

Quantification of Cux1-positive cells surrounding the area of GFP-positive cells was conducted by calculating the density of Cux1-positive cells in each individual section (# of cells/ ROI area). ROI encompassed the area of GFP-positive cells spanning IZ, LW_CP and MID_CP regions. The average ROI area was 235,550 μm^2 . The density was then multiplied by the average ROI area and the numbers were statistically compared across different conditions. The data were expressed as total number of Cux1-positive cells in normalized ROI \pm SEM (GraphPad Prism software, one-way ANOVA and Tukey's post hoc analysis for multiple comparisons, $p < 0.05$).

3.3. Results

3.3a. Activation of mTOR Pathway in Human Fetal TSC Brain

Histological analysis of fetal TSC tissue (n=4) revealed isolated regions of cell clusters exhibiting disorganized lamination and multiple enlarged cells reminiscent of pathology in surgically resected tubers in pediatric and adult patients. Indeed, the detection of altered cortical lamination and enlarged cells supported a pathological diagnosis of tubers similar to the one described previously in a 20-week gestation TSC fetus (Park et al., 1997). Fetal TSC tuber tissue exhibited robust P-p70S6K1 (T389) and P-S6 (S235/236) expression, especially in enlarged cells, which correlated with the expression pattern in adult TSC tubers (Fig. 3-1). While quantitative comparison of mTOR substrates in each fetal specimen and the adult specimens was limited by our sample size, overall it appeared qualitatively that phospho-protein expression was more robust in adult tubers compared with early fetal (23 week) tissue but differences between fetal specimens could not be appreciated. In the monozygotic twins specimens, the extent of mTOR activation did not differ within specimens. In one fetal case, a subependymal nodule was available for analysis and exhibited P-p70S6K1 (T389) and P-S6 (S235/236) immunoreactivity (Fig. 3-1A). We have previously demonstrated that c-myc, a downstream transcriptional activator of mTORC1, is expressed in surgically resected cortical tubers (Orlova et al., 2010b). C-myc was detected in fetal TSC tuber specimens in a pattern similar to P-p70S6K1 and P-S6 (Fig. 3-1B). Analysis of mTOR activation in control fetal brain specimens (n=2) did not reveal immunoreactivity for P-

p70S6K1 (T389) P-S6 (S235/236), or c-myc. Furthermore, fetal and adult TSC tuber tissue was evaluated for mTORC2 immunoreactivity. P-PKC α (S657), P-SGK1 (S422), and P-Akt (S473) have been established as biomarkers for mTORC2 signaling pathway activation (Guertin and Sabatini, 2007). Phosphorylation of SGK1 at S422 results in activation of SGK1 and phosphorylation of its effector NDRG1 (T346) (Garcia-Martinez and Alessi, 2008). Robust immunoreactivity for P-PKC α (S657), P-SGK1 (S422), and P-Akt (473) was detected in fetal TSC tuber specimens, and immunoreactivity for P-PKC α (S657), P-SGK1 (S422), P-Akt (S473), and SGK1 substrate, P-NDRG1 (T346), was detected in adult TSC tuber cases (Fig. 3-1 B-D). P-PKC α (S657), P-SGK1 (S422), P-Akt (S473), and P-NDRG1 (T346) immunohistochemical staining was virtually absent in control specimens (Fig. 3-1B,C). Expression of the native PKC α isoform was the same in adult TSC and control brain tissue (Supplemental Fig. 3-1). These findings demonstrate for the first time there is mTORC1 activation in fetal tubers and that in addition to mTORC1 activation, there is also mTORC2 activation in fetal and adult TSC brains. As in adult TSC brains (Marcotte et al., 2012), specimens of perituberal cortex with normal cytoarchitecture in fetal cases do not demonstrate evidence of mTOR hyperactivation (see cortex surrounding the fetal tubers, Fig. 3-1A).

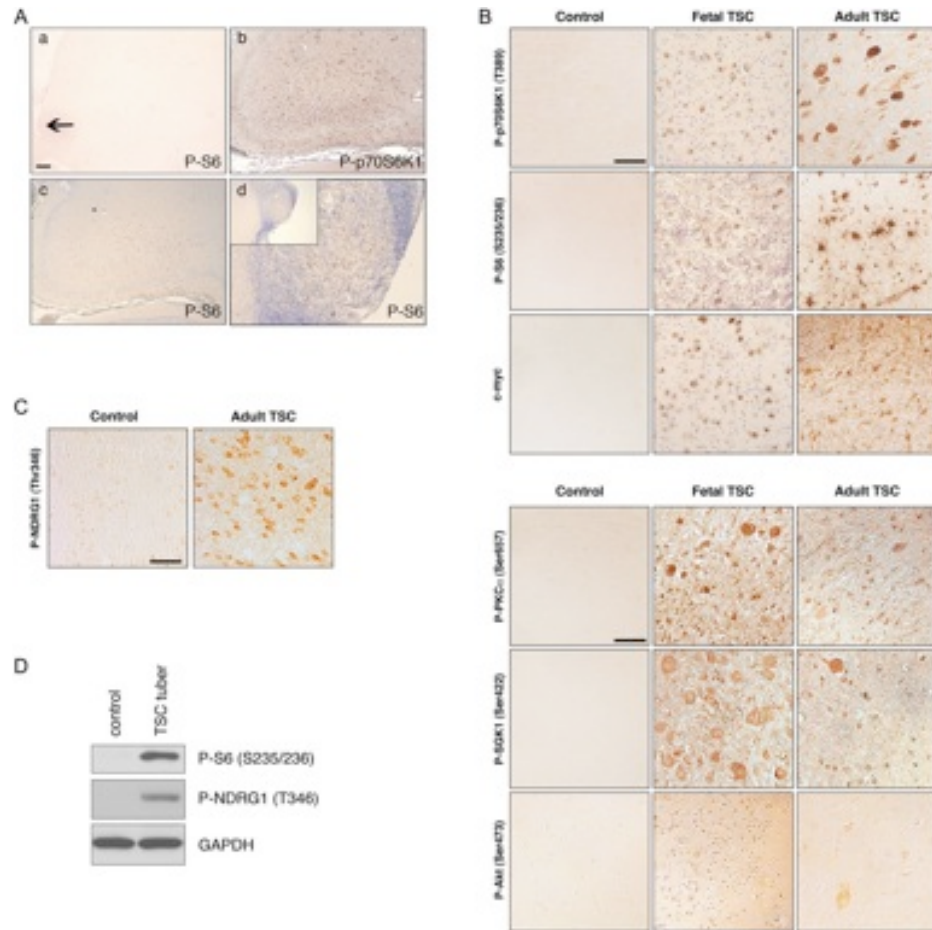


Figure 3-1. mTORC1 and mTORC2 signaling pathway activation in fetal and adult TSC brains.

(A) Control and fetal TSC tuber specimens. (a) Absence of P-S6 (S235/236) immunolabeling in control fetal brain (arrow depicts cortical surface). (b and c) Robust P-p70S6K1 (T389) and P-S6 (S235/236) in fetal TSC tuber. (d) P-S6 (S235/236) expression in fetal TSC subependymal nodule specimen. Inset, low magnification image. Scale bar: 200 μ m.

(B) mTORC1 signaling pathway activation in fetal and adult tubers, with robust immunoreactivity for P-p70S6K1 (T389), P-S6 (S235/236), and c-myc. mTORC2 signaling pathway activation in fetal and adult TSC tubers, with robust immunoreactivity for P-PKC α (S657), P-SGK1 (S422), and P-Akt (S473). Scale bar: 50 μ m.

(C) P-NDRG1 (T346) immunoreactivity was robust in adult TSC brain specimens compared with controls. Scale bar: 50 μ m.

(D) Western assay of human control and TSC tuber specimens. Increased levels of P-S6 (S235/236) and P-NDRG1 (T346) were observed in TSC tuber case compared with control brain. glyceraldehyde-3-phosphate dehydrogenase (GAPDH) was used as a loading control.

3.3b. Depletion of *Tsc2* and Activation of *mTOR* in *mNPCs In Vitro*

It is speculated by many investigators that tubers form because of the effects of loss of *TSC1* or *TSC2* on neural progenitors in the fetal human cortex. Thus, to investigate the effects of *Tsc2* loss in neural progenitor cells, *mNPCs* were transfected with 3 different shRNA constructs targeting disparate regions of *Tsc2* mRNA or a scrambled sequence not recognizing any known mouse mRNA as a control (Supplemental Fig. 3-1).

At 4-10 DPT, *Tsc2* shRNA-GFP clone#1 (5'-GCATGCAGTTCTCACCTTATT-3'), clone#3 (5'-AGAGCTGTCCAATGCCCTTAT-3') and clone#4 (5'-GAAGGATTTTCGTCCCTTATAT-3') resulted in reproducible *Tsc2* KD (Supplemental Fig. 3-1). Semi-quantitative densitometric analysis estimated *Tsc2* KD at approximately 40-70% for all 3 shRNAs. *Tsc2* shRNA clone #1 and #4 were chosen for subsequent *in vitro* *mNPC* experiments. *Tsc2* shRNA clone #1 and #4 showed enhanced *mTORC1* signaling in *mNPCs* as evidenced by increased levels of P-S6 (S235/236) and P-4E-BP1 (T37/46); native levels of these proteins did not change (Fig. 3-2A and Supplemental Fig. 3-1). Furthermore, *Tsc2* shRNA KD resulted in *mTORC2* signaling pathway activation as evidenced by increase in levels of P-Akt (S473) and P-NDRG1 (T346) compared to scrambled shRNA-transfected controls (Fig. 3-2A). Total (nonphosphorylated isoforms) for Akt and NDRG1 did not change, however, PKC α levels following KD were decreased compared to controls.

Previous studies have demonstrated that *mTORC2* activation is diminished in mouse embryonic fibroblasts (*mEFs*) lacking *Tsc2* (Huang et al., 2008). In keeping with these results, we also found decreased *mTORC2* activity in *Tsc2* null (*Tsc2*^{-/-}) *mEFs*, as evidenced by decreased levels of P-PKC α (S657), P-Akt (S473), P-NDRG1 (T346) compared to *Tsc2*^{+/+} controls (Fig. 3-2A; courtesy of Dr. Elizabeth Henske, Dana Farber

Cancer Center, Boston, MA). Thus, our results in fetal brain tissue and mNPCs showing enhanced mTORC2 activation suggests a specific signaling effect in neural progenitor cells distinct from other cell types.

3.3c. Tsc2 Regulation of mNPC Size is Rapamycin-dependent

At 4-10 DPT, Tsc2-depleted mNPCs were FACS sorted and showed increased forward scatter area (FSC-A), which is a measurement reflective of cell size (Fingar et al., 2002). The mean FSC-A of Tsc2 shRNA-transfected mNPCs (n=7379) was significantly greater than mean FSC-A of scrambled shRNA-transfected mNPCs (n=4681; $p<0.05$; Supplemental Fig. 3-1). Since the FSC-A is a relative measure between different experimental groups, fluorescent images were acquired of individual cells and the cell area, defined by the GFP fluorescence, was compared for scrambled shRNA control and Tsc2 shRNA-transfected mNPCs (Fig. 3-2B). Tsc2-depleted mNPCs (n=20) had cell area twice the size of scrambled shRNA control mNPCs (n=17; $p<0.01$). No change in cell area was found following administration of transfection reagents alone, as previously reported (Orlova et al., 2010a).

To determine whether increased cell size was mTORC1-dependent, control scrambled shRNA and Tsc2-depleted mNPCs were treated with the mTORC1 inhibitor rapamycin. Rapamycin (100nM) application for 24 hours had no significant effect on the cell size of wild-type or scrambled shRNA-GFP-transfected mNPCs, as has been previously reported (Orlova et al., 2010a). However, rapamycin treatment prevented cell size enlargement in Tsc2-depleted cells and mean FSC-A of rapamycin-treated Tsc2 shRNA KD cells (n=7353) was similar to control scrambled shRNA cells (Supplemental Fig. 3-1). Rapamycin prevented cell area increase of Tsc2 shRNA-transfected mNPCs (n=21; $p<0.05$), and the rapamycin-treated Tsc2 KD mNPCs had approximately the

same cell area as scrambled shRNA mNPCs (Fig. 3-2B). Thus, Tsc2 depletion in mNPCs results in enhanced cell size that is preventable by treatment with rapamycin, suggesting an mTORC1-dependent mechanism.

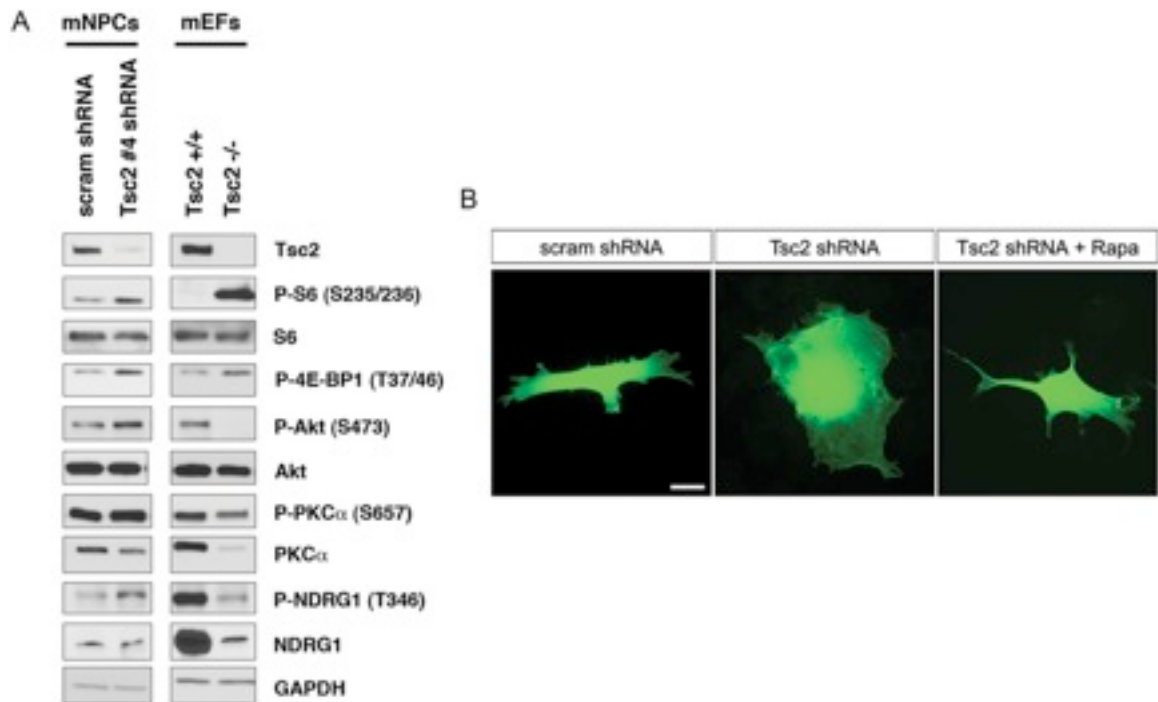


Figure 3-2. *Tsc2* shRNA KD in mNPCs results in mTORC1 and mTORC2 pathway activation and increased cell size in vitro.

(A) Western blot depicting reduced Tsc2 protein levels following Tsc2 shRNA KD in mNPCs with Tsc2 shRNA-GFP clone #4 at 4-10 DPT. Tsc2 shRNA-GFP clone #4 resulted in the highest level of Tsc2 KD and semiquantitative densitometric analysis estimated it at 40–70%. Tsc2 shRNA KD in mNPCs leads to increased P-S6 (S235/236) and P-4E-BP1 (T37/46) levels as a consequence of mTORC1 pathway activation compared with scrambled shRNA-GFP control. Total S6 and 4E-BP1 levels were unchanged (in addition see Supplementary Fig. 3-1). Similar results were observed in *Tsc2*^{-/-} mEFs, with increased P-S6 (S235/236) and P-4EBP1 (T37/46), compared with *Tsc2*^{+/+} mEFs. KD of Tsc2 shRNA in mNPCs also resulted in increased levels of P-Akt (S473), P-PKC α (S657), and P-NDRG1 (T346), which are biomarkers of mTORC2 signaling activation. These results were opposite of the pattern observed in *Tsc2*^{+/+} and *Tsc2*^{-/-} mEFs, as *Tsc2*^{-/-} mEFs show decreased mTORC2 signaling (decreased levels of P-Akt (S473), P-PKC α (S657), and P-NDRG1 (T346)), compared *Tsc2*^{+/+} mEFs. GAPDH was used as a loading control.

(B) mNPCs transfected with Tsc2 shRNA-GFP clone #4 (n=20) exhibit a 1.9-fold increase in total cell area compared with scrambled shRNA-GFP transfected control cells (n=17; $p < 0.01$). Rapamycin (100 nM) treatment rescued cell size enhancement with cell area being approximately the same size as vehicle-treated and untreated scrambled shRNA-GFP transfected control mNPCs (n=21; $p < 0.05$). Scale bar: 25 μ m.

3.3d. *Tsc2* Depletion *In Vivo* Results in a Cortical Malformation

To investigate the effects of TSC2 *in vivo* on cortical development, we transfected Tsc2 shRNA-GFP into embryonic mouse brains by *in utero* electroporation (IUE) at embryonic day 14 (E14) (Saito, 2006) and assessed the effects on migration and lamination at E19 (Fig. 3-3A). Scrambled shRNA-GFP plasmids were electroporated in a parallel set of experiments as controls for IUE and shRNA transfection.

By E19, GFP-positive cells transfected with control scrambled shRNA-GFP plasmid were primarily localized in the upper portion of the CP (UP_CP 67.3±1.3%) and a small number of transfected progenitors remained in VZ/SVZ (18.6±1.9%; Fig. 3-3B). In contrast, following transfection with Tsc2 shRNA-GFP, there were significantly fewer GFP-positive cells that reached the upper CP region (Tsc2 shRNA-GFP UP_CP 19.1±3.4%; $p < 0.05$ compared to scrambled shRNA-GFP controls) and there was an increase in the number of GFP-positive cells found in the VZ/SVZ region (37.6±1.9%; $p < 0.05$, compared to scrambled shRNA-GFP controls). Furthermore, very few scrambled shRNA-GFP cells were found in the IZ (4.6±1.0%), lower (LW_CP; 3.8±0.8%), or middle (MID_CP; 5.8±1.3%) cortical plate, whereas significantly more Tsc2-depleted GFP-positive cells were found in those regions (IZ 16.8±2.37%, LW_CP 12.1±2.8 %, MID_CP 14.3 ± 1.0%). Tsc2 shRNA KD led to a focal cortical malformation with fewer cells reaching their appropriate cortical laminar destination (UP_CP, layer II-III) and the majority of cells found in the VZ/SVZ, IZ, LW_CP and MID_CP (Fig. 3-3B). Immunohistochemical staining with MAP2 showed that cells which leave the VZ/SVZ in Tsc2 shRNA condition and express MAP2 appear to take on a neuronal phenotype (Fig. 3-3C).

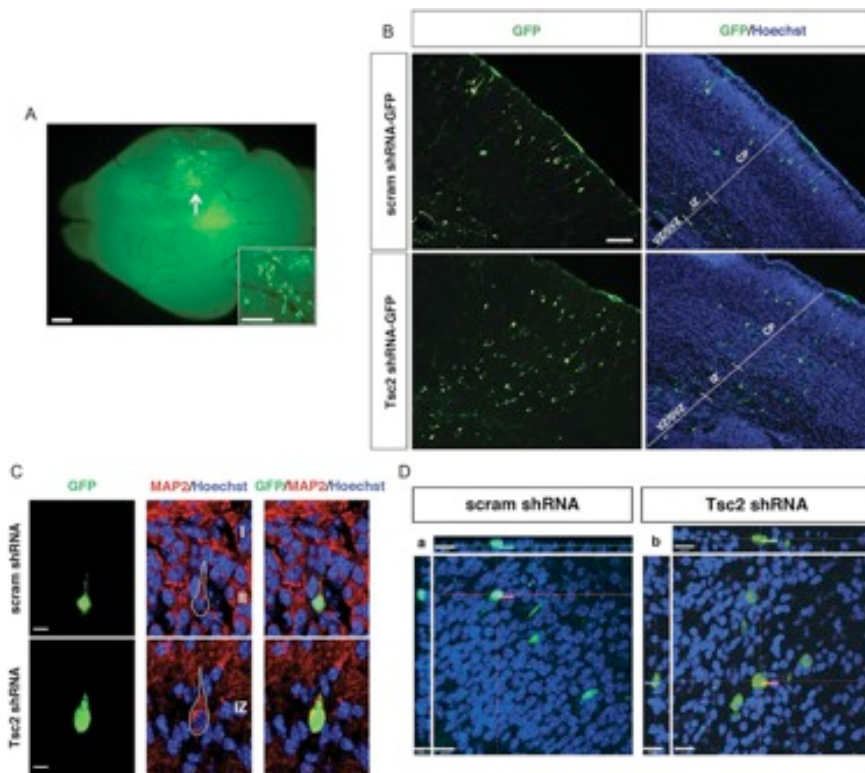


Figure 3-3. Focal *Tsc2* shRNA KD results in a cortical malformation and cytomegaly in vivo.

(A) Whole brain green fluorescent protein (GFP) fluorescence image demonstrating focal area of cell transfection (arrow) following *in utero* electroporation with *Tsc2* shRNA-GFP plasmid. Inset is a higher power magnification image showing GFP-expressing cells. Scale bar: 500 μm ; Inset scale bar: 100 μm .

(B) (Top) E19 brain transfected with control scrambled shRNA-GFP at E14, with the majority of GFP-positive cells reaching their appropriate destination in the upper region of cortical plate (layers II–III). (Bottom) E19 brain transfected with *Tsc2* shRNA-GFP at E14. *In vivo* *Tsc2* shRNA KD resulted in a focal lamination defect with the majority of cells localized in the VZ and IZ, and few reaching their appropriate destination in the upper region of cortical plate (layers II–III). For quantification, see text and Figure 5. Scale bar: 100 μm .

(C) MAP2 immunostaining of IUE E14–19 scrambled shRNA-GFP and *Tsc2* shRNA-GFP brains. (Top) Control scrambled shRNA GFP-positive cells in layers II–III express neuronal marker MAP2. (Bottom) *Tsc2* shRNA GFP-positive cells that leave VZ/SVZ, but do not reach their layers II–III cortical destination, also express MAP2 (image shown of cell located in the IZ). Hoechst33342 was used to visualize cell nuclei. Scale bar: 7 μm .

(D) Confocal images of IUE E14–19 (a) scrambled shRNA-GFP and (b) *Tsc2* shRNA-GFP transfected cells in layers II–III and IZ, respectively. *Tsc2* shRNA KD results in cell volume increase (cytomegaly), compared with scrambled shRNA-GFP control cells. For quantification, see text and Figure 5. Scale bar: 14 μm .

3.3e. Tsc2 Depletion Results in Increased Cell Volume In Vivo

To investigate whether Tsc2 depletion results in cytomegaly *in vivo*, we acquired z-stack images of GFP-positive cells using confocal microscopy. Cell volume was measured by defining the volume encompassed by the GFP fluorescence signal. Quantitative analysis revealed that GFP-positive Tsc2 shRNA cells in the IZ had approximately twice the volume ($408.4 \mu\text{m}^3$) of scrambled shRNA control cells in the UP_CP ($267.7 \mu\text{m}^3$) and some exhibited the morphology reminiscent of giant cells, with a laterally displaced nucleus as seen in human TSC tuber specimens (Fig. 3-3D, also see supplemental videos in Supplemental Figs. 3-2 and 3-3).

3.3f. Tsc2 Knockdown In Vivo Results in Cell-Autonomous and Non-Cell-Autonomous Lamination Defects of Layer II-III

To confirm the laminar destination of electroporated cells, sections were stained with homeobox transcription factor Cux1 which labels cells in superficial cortical layers II-III born on approximately E14-15 (Fig. 3-4A) (Nieto et al., 2004). Cux1-immunolabeling in scrambled shRNA condition revealed a band of cells primarily confined to the superficial part of the CP (layer II-III), thus IUE or plasmid transfection conditions alone did not alter normal cortical development or affect migration of cells destined for layer II-III of the cortex (Fig. 3-4A,B). Scrambled shRNA GFP-positive cells co-localized with Cux1-labeled cells in layer II-III at E19 and expressed Cux1 (100%; n=16) (Fig. 3-4A). Conversely, only 21% of GFP-positive cells following IUE with Tsc2 shRNA were Cux1-positive, while the majority (79%) were Cux1-negative (n=14) (Fig. 3-4A). Interestingly, while most Tsc2 shRNA GFP-positive cells were Cux1-negative, we noticed that there

was an increase in Cux1-labeling surrounding GFP-positive cells in IZ and lower CP regions below layer II-III (Fig. 3-4B). To verify that this was not a result of IUE, we compared the density of Cux1-labeled cells in the ROI surrounding the GFP-positive in scrambled shRNA condition, to density in similar location on the contralateral non-electroporated hemisphere (Supplemental Fig. 3-4). There was no statistical significance between the counts on the electroporated GFP-positive hemisphere and non-electroporated hemisphere in scrambled shRNA condition (Supplemental Fig. 3-4). To compare the counts in the scrambled shRNA and Tsc2 shRNA conditions, density in ROI of equal size was normalized to non-electroporated hemisphere as an internal control. The ratios were further normalized to scrambled shRNA counts and revealed that there was a 2-fold increase in the number of non-transfected Cux1-labeled cells surrounding the GFP-positive cells in IZ, LW_CP, and MID_CP in Tsc2 shRNA condition compared to scrambled shRNA controls (Fig. 3-4B; $p < 0.05$). These results suggest both cell-autonomous effects of Tsc2 KD on migration, as well as non-cell-autonomous lamination effects on the surrounding neighboring cells.

To test the effects of Tsc2 KD on neighboring cells in other cortical layers, we immunohistochemically labeled for Ctip2 and Tbr1, which are layer V and layer VI markers (Hevner et al., 2001; Arlotta et al., 2005; Chen et al., 2005; Molyneaux et al., 2005). In the scrambled shRNA-GFP control condition, virtually all cells that migrated into the CP reached layer II-III, above the line of Tbr1- and Ctip2-labeled cells (Fig. 3-4C). On the other hand, in the Tsc2 shRNA KD condition, majority of GFP-positive cells were localized to the VZ/SVZ, IZ and lower regions of the CP (LW_CP, MID_CP). As mentioned previously, only 21% of GFP-positive Tsc2 shRNA-transfected cells were Cux1-positive and thus we wanted to evaluate whether these cells that do not appropriately migrate do so because of expression of other layer-specific markers, such as Tbr1 and Ctip2. E19 sections were imaged by confocal microscopy and revealed that

the Tsc2 shRNA GFP-positive cells in the IZ were Ctip2- and Tbr1-negative (Fig. 3-4C). To further investigate whether the Tsc2 shRNA GFP-positive cells that migrated into the CP, but did not reach layers II-III, assume the identity of a different cortical layer (e.g. layer V or VI), we looked at their Ctip2 and Tbr1 expression pattern. Tsc2 shRNA GFP-positive cells in the LW_CP and MID_CP were MAP2-positive, and Ctip2- and Tbr1-negative, indicating that at least at E19, they do not express layers V and VI markers Tbr1 and Ctip2 and thus, likely do not acquire layer V or VI identity (Fig. 3-4C).

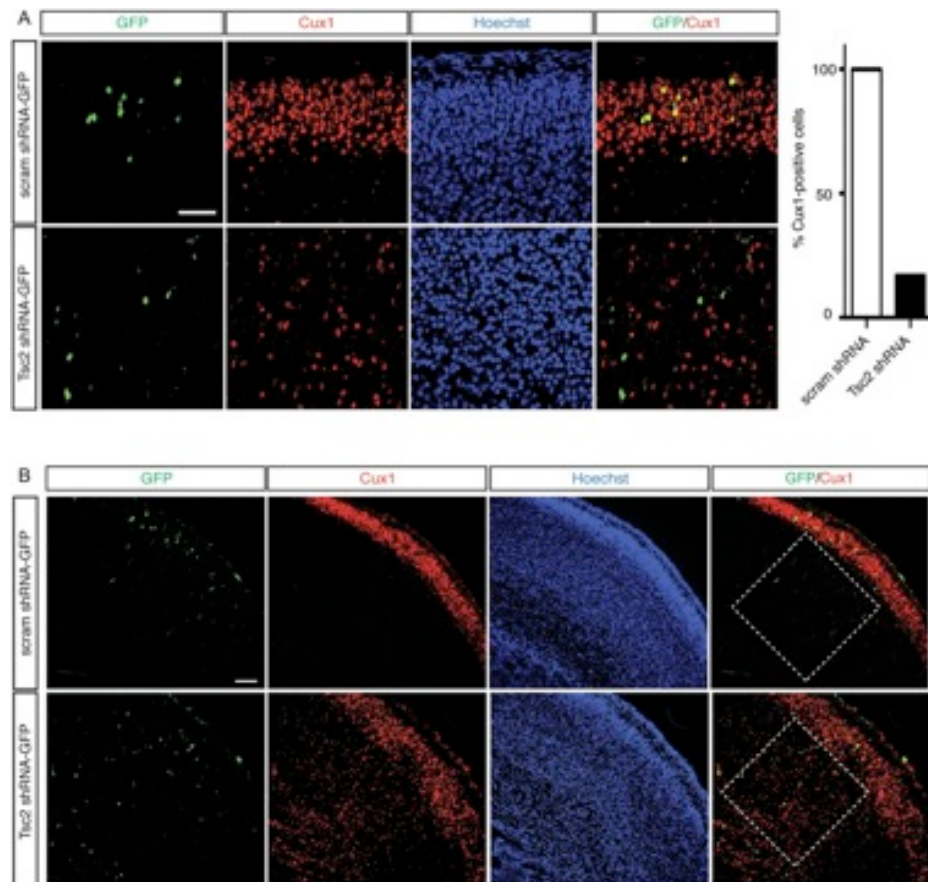


Figure 3-4. In vivo Tsc2 shRNA KD results in cell-autonomous and non-cell-autonomous lamination defect.

(A) IUE E14-19 scrambled shRNA-GFP and Tsc2 shRNA-GFP brains immunostained with a layer II–III marker Cux1. Scrambled shRNA GFP-positive cells co-localize with Cux1-immunoreactive cells in layers II–III at E19, and are Cux1-positive. In contrast, majority of Tsc2 shRNA KD GFP-positive cells, which did not reach their appropriate cortical destination (layers II–III), are Cux1-negative (79%). Quantification graph of GFP-positive cells analyzed by confocal microscopy in scrambled shRNA and Tsc2 shRNA brains, showing that 100% of cells in scrambled shRNA-GFP condition in layers II–III expressed Cux1, however only 21% of GFP-positive cells in Tsc2 shRNA KD condition were Cux1-positive. (scrambled shRNA-GFP n=16 cells, Tsc2 shRNA-GFP n=14 cells; 3 embryonic brains per condition were analyzed). Scale bar: 50 μ m.

(B) Non-cell-autonomous effects of Tsc2 shRNA KD on surrounding Cux1-positive cells. In the scrambled shRNA condition, there was a tight band of Cux1-positive cells (layers II–III) in the superficial region of the cortical plate. Very few Cux1-positive cells were noted in the ROI spanning the IZ, LW_CP, and MID_CP (white box). However, in the ROI surrounding the GFP-positive cells in Tsc2 shRNA KD condition, there was a significant increase in Cux1-positive cells. For quantification, see text and Figure 5. Scale bar: 100 μ m.

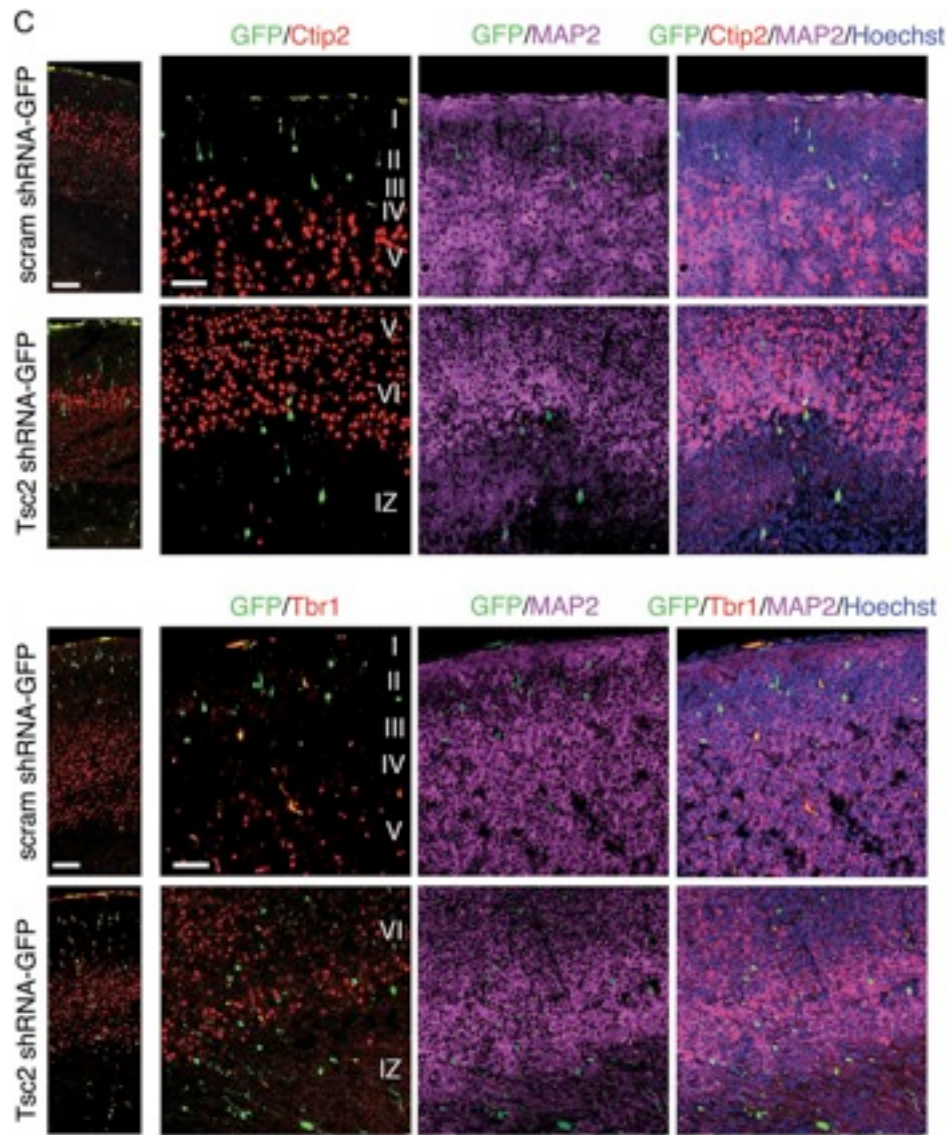


Figure 3-4. *In vivo* Tsc2 shRNA KD results in cell-autonomous and non-cell-autonomous lamination defect. (continued)

(C) Confocal images of IUE E14-19 scrambled shRNA-GFP and Tsc2 shRNA-GFP brains immunostained with deep layers V and VI, markers Ctip2 and Tbr1, and neuronal marker MAP2. Hoechst33342 was used to visualize cell nuclei. Tsc2 shRNA KD cells, which do not reach their appropriate cortical layer II–III destination, do not acquire identity of other cortical layers (e.g., V and VI). Scale bar: 100 and 50 μ m (left to right).

3.3g. Migratory Defect following Tsc2 Knockdown is Prevented with Rapamycin

Treatment

Enhanced P-S6 levels in cells transfected with Tsc2 suggested that the induced cortical lamination defect could be dependent on the hyperactive mTORC1 signaling. Mean P-S6 labeling intensity was measured, normalized to background, and demonstrated a 2-fold increase in P-S6 in Tsc2 shRNA-transfected cells compared with scrambled shRNA-transfected controls ($n=20$, $p<0.05$; Fig. 3-5B). To test this hypothesis, we administered rapamycin daily to the pregnant dam between E15-E18. Rapamycin treatment (2.5, 5.0 mg/kg body weight) led to near complete inhibition of mTOR signaling in liver (absent P-S6 levels) compared to vehicle or low dose (0.5 mg/kg) rapamycin at E19 (see Supplemental Fig. 3-5). In the brain, rapamycin (5.0 mg/kg) prevented the migratory defect of GFP-positive cells transfected with Tsc2 shRNA. Rapamycin treatment resulted in a 2-fold increase in the number of GFP-positive Tsc2 shRNA-transfected cells reaching the upper CP layers (UP_CP $46.5\pm4.8\%$; $p<0.05$ compared to untreated Tsc2 shRNA condition) and approximately a 2-fold decrease of transfected cells remaining within VZ/SVZ ($21.0\pm1.5\%$; $p<0.05$ compared to untreated Tsc2 shRNA condition) compared to vehicle treated animals (UP_CP $19.1\pm3.4\%$, VZ/SVZ $37.6\pm1.9\%$; Fig. 3-5A). In addition, no change was noted in the lamination pattern of the surrounding cortex either ipsi- or contralateral to the induced malformation (data not shown). Consistent with these findings, confocal fluorescence microscopy and immunodensitometry demonstrated that rapamycin treatment reduced P-S6 levels in the Tsc2 shRNA-GFP-transfected cells to near baseline ($p>0.05$ compared to control scrambled shRNA-GFP; Fig. 3-5B).

To test whether rapamycin alone altered normal cortical migration, we injected BrdU at E14 and administered rapamycin (5.0 mg/kg) for 5 days (E14-E18). At E19, the percentage of BrdU-labeled cells reaching CP in rapamycin-treated animals (CP 75.3±0.3%, IZ 10.3±0.7%, VZ/SVZ 14.4±0.5%; n=3) did not significantly differ from untreated animals (CP 78.8±2.0%, IZ 7.8±0.7%, VZ/SVZ 13.4±1.4%; n=4; $p>0.05$ for each region; Supplemental Fig. 3-5). However, incidental note was made of reduced brain weight and reduced body size following fetal rapamycin therapy (Supplemental Fig. 3-5).

3.3h. Rapamycin Treatment Rescues Cytomegaly and Non-Cell-Autonomous Effects due to Tsc2 Knockdown

Rapamycin treatment prevented cytomegaly (cell volume increase) in Tsc2 shRNA-transfected animals (162.8 μm^3 vs. untreated 408.4 μm^3 ; $p<0.05$; Fig. 3-5C). Cell volume in rapamycin-treated Tsc2 shRNA animals was smaller than scrambled shRNA control cells (267.7 μm^3), however it was not statistically significant ($p>0.05$). Furthermore, treatment with rapamycin prevented the increase in the number of Cux1-positive cells surrounding GFP-positive cells in animals transfected with Tsc2 shRNA (Fig. 3-5D). Quantitative measurements were taken in the ROI surrounding the region of transfected GFP-positive cells and were quantified. Quantitative analysis revealed that the 2-fold increase in Cux1-positive cells in the ROI spanning IZ, LW_CP, MID_CP regions was prevented with rapamycin treatment and there was no significant difference between the number of Cux1-positive cells in ROI in rapamycin-treated Tsc2 shRNA animals compared to scrambled shRNA animals (Fig. 3-5D). These results suggest that mTORC1 inhibition during fetal development may prevent cell non-autonomous effects as well as cell autonomous effects of Tsc2 loss.

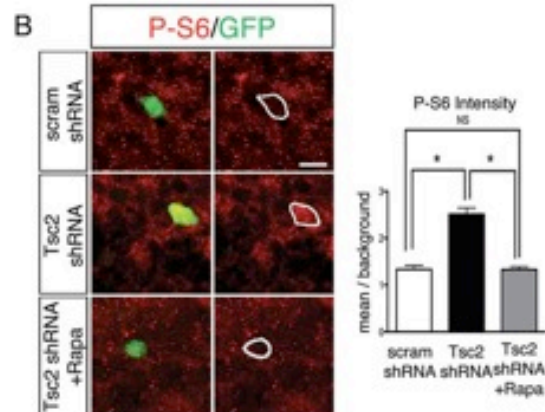
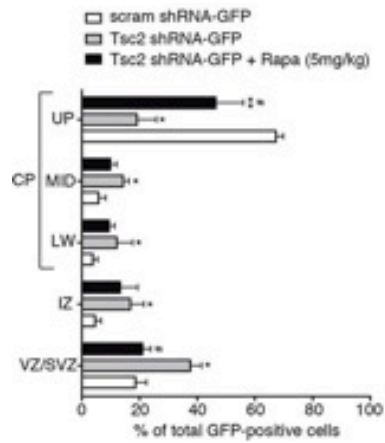
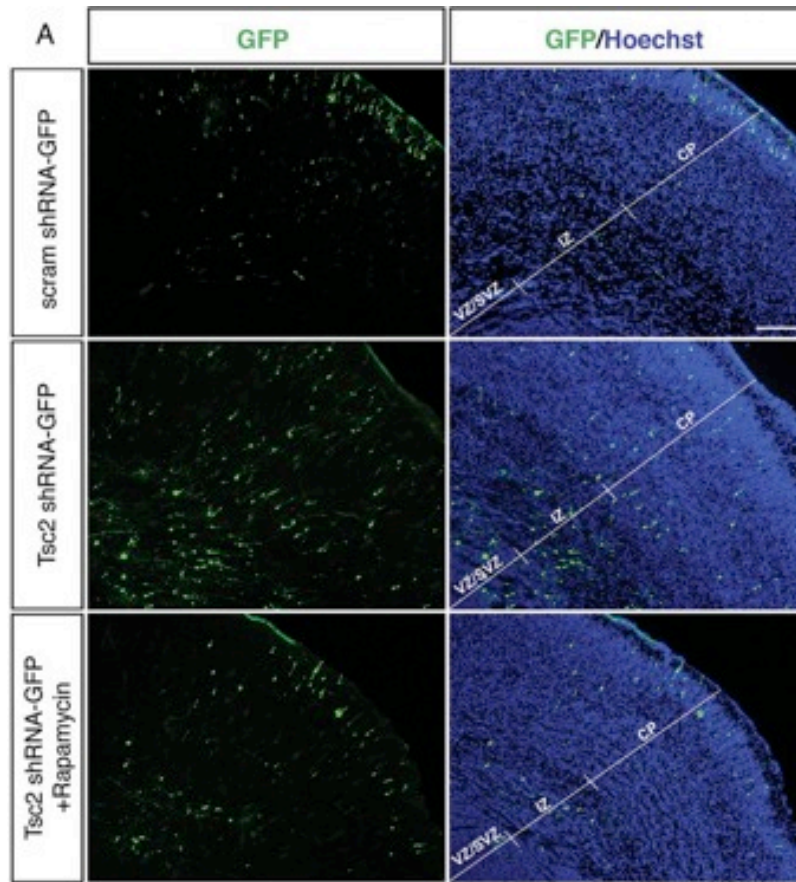


Figure 3-5. Fetal rapamycin treatment rescues the lamination defect, cytomegaly and non-cell-autonomous lamination effects following Tsc2 shRNA knockdown *in vivo*.

(A) (Top) Scrambled shRNA-GFP transfected cells at E14 laminate layers II-III of the cortex at E19 (UP_CP 67.3±1.3%, MID_CP 5.8±1.3%, LW_CP 3.8±0.8%, IZ 4.6±1.0%, VZ/SVZ 18.6±1.9%). (Middle) Tsc2 shRNA-GFP KD at E14 leads to a lamination defect with cells abnormally retained in the VZ/SVZ, IZ, and LW_CP at E19 as compared to scrambled shRNA-GFP controls (UP_CP 19.1±3.4%, MID_CP 14.3±1.0%, LW_CP 12.1±2.8%, IZ 16.8±2.4%, VZ/SVZ 37.6±1.9%; $p<0.05$). (Bottom) With daily rapamycin treatment (5.0 mg/kg body weight) for 4 days (E15-E18), a significantly greater number of Tsc2 shRNA-GFP KD cells reach their appropriate destination layer II-III of the cortex (UP_CP 46.4±4.8%; $p<0.05$) and fewer are retained in the VZ/SVZ (21.0±1.5%; $p<0.05$). (MID_CP 9.9±1.1%, LW_CP 9.4±1.0%, IZ 13.3±3.0%,). Graphic representation of the percentage of GFP-positive cells in each region: VZ/SVZ, IZ, LW_CP, MID_CP, and UP_CP of the total GFP-positive cells in scrambled shRNA-GFP, Tsc2 shRNA-GFP, and rapamycin-treated Tsc2 shRNA-GFP conditions. *Tsc2 shRNA-GFP vs. scram shRNA GFP ($p<0.05$); ** rapamycin-treated (5.0 mg/kg body weight; E15-E18) Tsc2 shRNA-GFP vs. scram shRNA GFP ($p<0.05$); # rapamycin-treated (5.0 mg/kg body weight; E15-E18) Tsc2 shRNA-GFP vs. Tsc2 shRNA-GFP ($p<0.05$). Scale bar: 100 μ m.

(B) Tsc2 shRNA KD *in vivo* results in mTORC1 hyperactivation that is rescued with rapamycin treatment. (Top) P-S6 (S235/236) immunolabeling in scrambled shRNA-GFP-transfected cells. (Middle) Following Tsc2 shRNA KD there was a marked two-fold increase in P-S6 intensity compared to scrambled shRNA controls. (Bottom) Daily treatment with rapamycin (E15-E18) prevented mTORC1 hyperactivation following Tsc2 shRNA KD as evidenced by decreased P-S6 intensity compared to untreated Tsc2 shRNA KD condition. Cells in rapamycin-treated Tsc2 shRNA-GFP animals exhibited P-S6 immunolabeling that was not different from that in scrambled shRNA controls. Quantification of P-S6 (S235/236) immunolabeling in scrambled shRNA-GFP, Tsc2 shRNA-GFP, and rapamycin-treated Tsc2 shRNA-GFP conditions represented as the mean intensity within the cell normalized to background intensity. * $p<0.05$. n=5 embryonic brains for scrambled and Tsc2 shRNA conditions, and n=4 embryonic brains for Tsc2+Rapamycin condition were analyzed. Scale bar: 10 μ m.

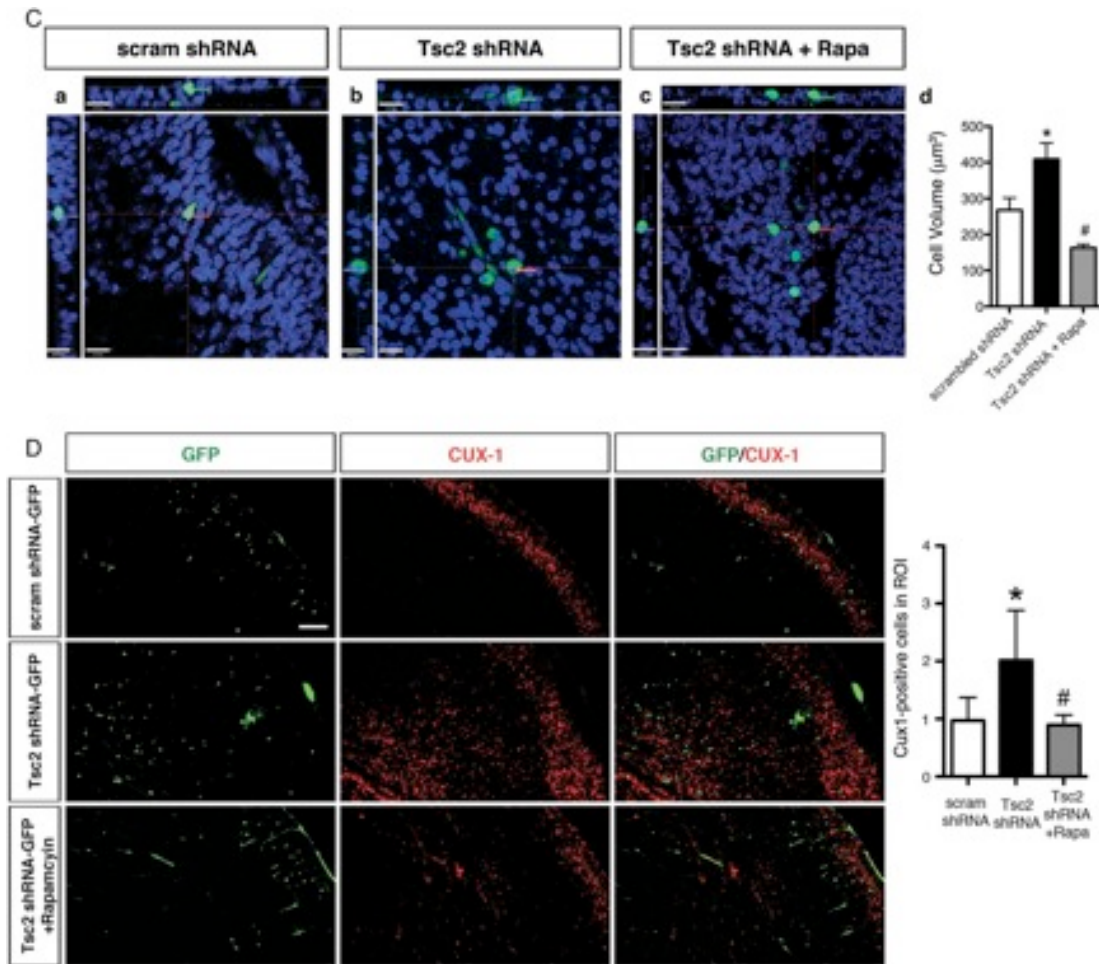
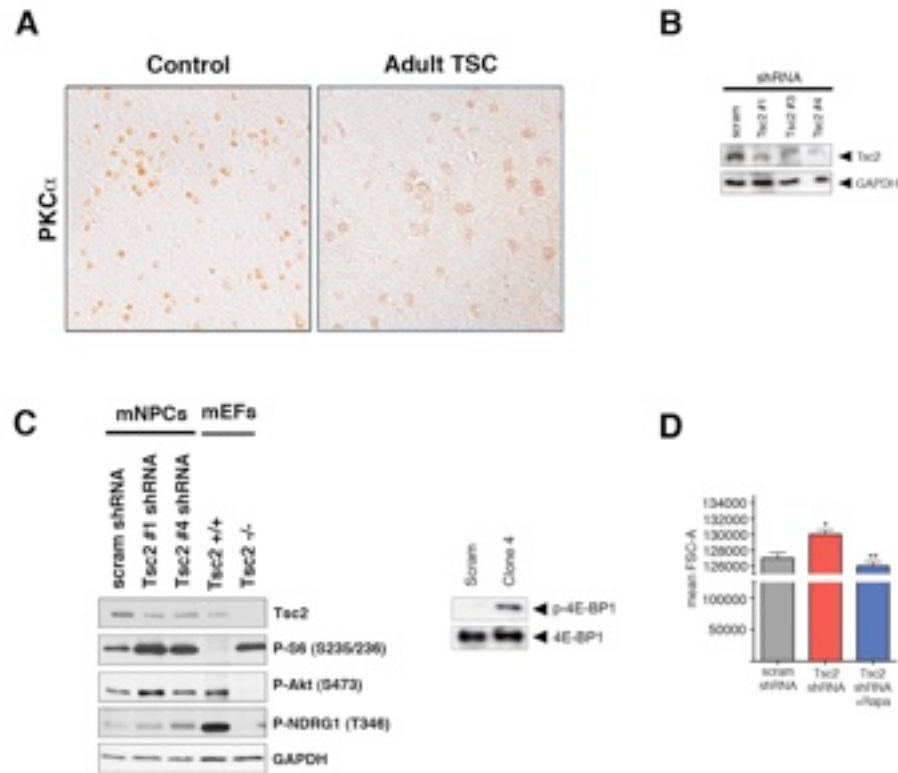


Figure 3-5. Fetal rapamycin treatment rescues the lamination defect, cytomegaly and non-cell-autonomous lamination effects following Tsc2 shRNA knockdown in vivo.

(continued)

(C) Daily rapamycin treatment (5.0 mg/kg; E15-18) prevents increase in cell volume (cytomegaly) following Tsc2 shRNA KD. Scrambled shRNA $268 \mu\text{m}^3$ (n=7), Tsc2 shRNA $408 \mu\text{m}^3$ (n=9), rapamycin-treated Tsc2 shRNA $163 \mu\text{m}^3$ (n=8). * scrambled shRNA vs. Tsc2 shRNA, $p < 0.05$; # Tsc2 shRNA vs. Tsc2 shRNA + Rapamycin, $p < 0.05$. Scale bar: $14 \mu\text{m}$.

(D) Rapamycin treatment prevented non cell-autonomous effects following Tsc2 shRNA KD. Tsc2 shRNA KD results in a 2-fold increase in Cux1-positive cell in ROI surrounding GFP-positive cells (n=3 embryonic brains) compared to scrambled shRNA control (n=4 embryonic brains). Daily rapamycin treatment results in a significant decrease in the number of Cux1-positive cells surrounding the GFP-positive Tsc2 shRNA KD cells (n=3 embryonic brains) compared to untreated Tsc2 shRNA condition. Quantification of Cux1-positive cells in ROI spanning IZ, LW_CP, MID_CP. * scrambled shRNA vs. Tsc2 shRNA, $p < 0.05$. # Tsc2 shRNA vs. Tsc2 shRNA + Rapamycin, $p < 0.05$. Scale bar: $100 \mu\text{m}$.



Supplemental Figure 3-1.

(A). PKC α immunostaining in control and adult TSC brains.

(B). Tsc2 shRNA KD with clones #1, #3, and #4. GAPDH was used as a loading control.

(C). mTORC1 activation (P-S6) and mTORC2 activation (P-Akt (S473) and P-NDRG1 (T348)) following KD with Tsc2 shRNA clones #1 and #4. Total 4E-BP1 levels are unchanged following Tsc2 shRNA KD. In Tsc2^{-/-} mEFs mTORC1 is activated, but mTORC2 signaling is diminished compared to Tsc2^{+/+} mEFs. GAPDH was used as a loading control.

(D) Forward scatter area (FSC-A) histograms of scrambled and Tsc2 shRNA-GFP transfected mNPCs following FACS sort for GFP-positive cells. Tsc2 shRNA-GFP transfected mNPCs histogram (red) is shifted to the right compared to scrambled shRNA-GFP control histogram (gray), indicating that FSC-A signal, which correlates with size of individual cells, is increased following Tsc2 KD. Treatment with rapamycin (100nM) following Tsc2 shRNA KD rescues the cell size phenotype and the histogram (blue) is shifted to the left compared to untreated Tsc2 shRNA transfected mNPCs. Quantification of FSC-A histogram means shows that Tsc2 shRNA KD (n=7379) results in significant FSC-A signal increase compared to scrambled shRNA transfected control cells (n=4681), and is rescued with rapamycin (100nM) treatment (n=7353). * $p < 0.05$, ** $p < 0.05$.

The video can be found on *Cerebral Cortex* journal website.

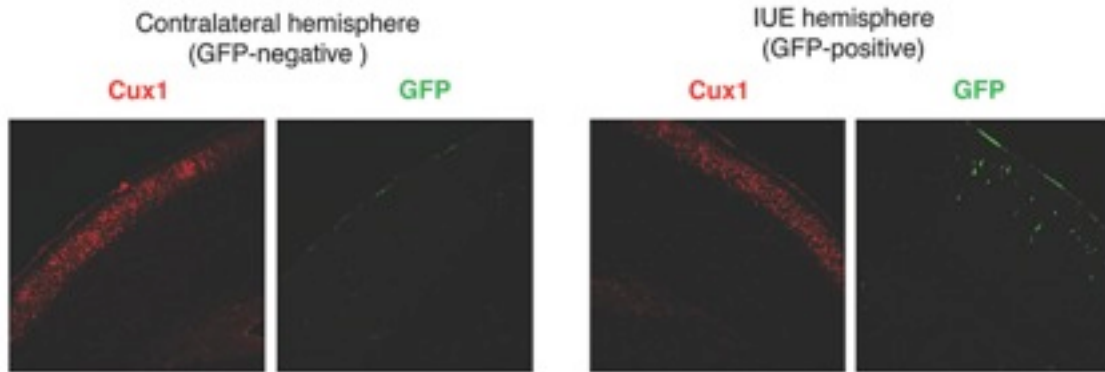
Supplemental Figure 3-2.

3-D confocal microscopy video of IUE E14-19 scrambled shRNA GFP-positive cells in UP_CP (layer II/III).

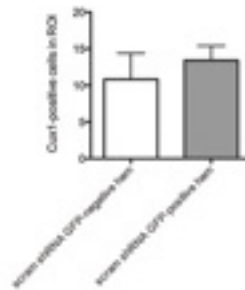
The video can be found on *Cerebral Cortex* journal website.

Supplemental Figure 3-3.

3-D confocal microscopy video of IUE E14-19 Tsc2 shRNA GFP-positive cells in IZ. The cells have increased volume ($408 \mu\text{m}^3$) compared to IUE E14-19 scrambled shRNA GFP-positive cells in UP_CP ($268 \mu\text{m}^3$; $p < 0.05$, see text).

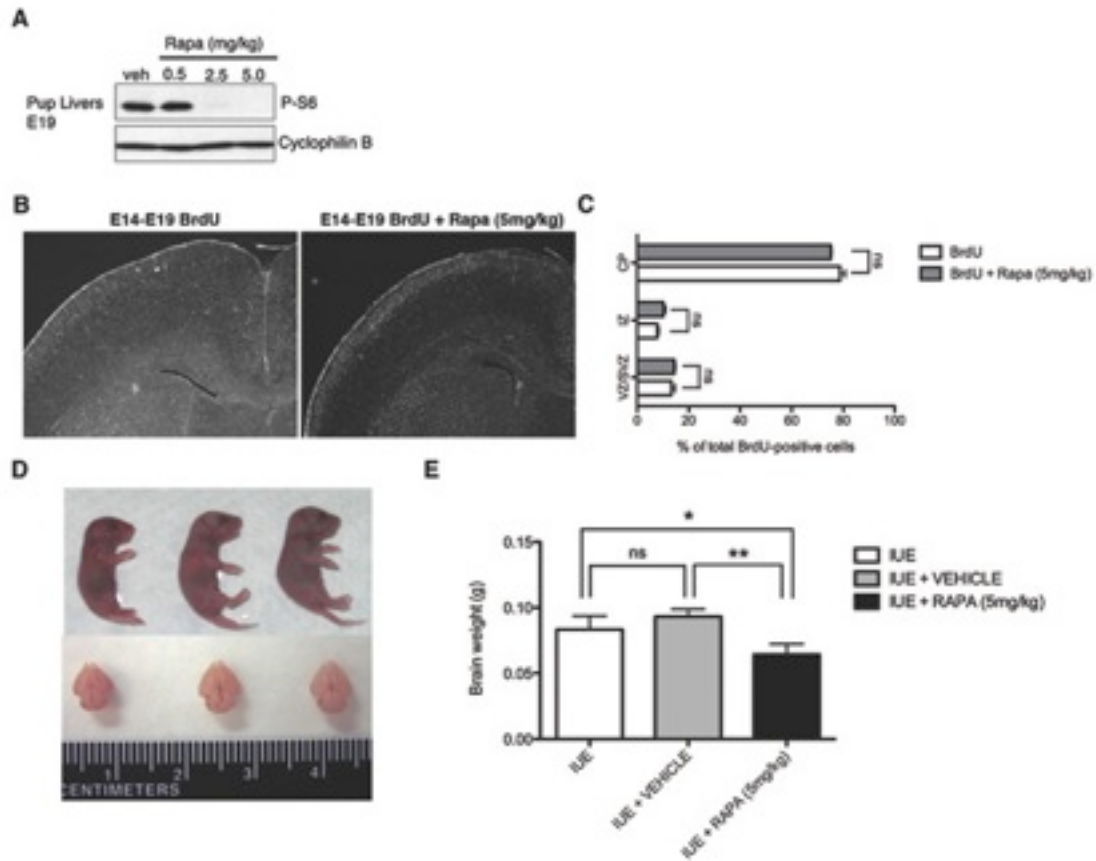


IUE E14-19 Scrambled shRNA-GFP
GFP-Negative vs. GFP-Positive Hemisphere



Supplemental Figure 3-4.

Quantification of Cux1-positive cells in an ROI in scrambled shRNA GFP-negative and GFP-positive hemispheres. There was no significant difference between the counts in the hemisphere containing GFP-positive cells and non-transfected GFP-negative hemisphere.



Supplemental Figure 3-5.

(A) E19 pup livers. Rapamycin (2.5 mg/kg and 5.0 mg/kg body weight doses) causes a dramatic reduction in mTOR signaling when administered daily (E14-E18) compared to vehicle-treated and low-dose rapamycin-treated animals (0.5 mg/kg body weight).

(B, C) BrdU-labeled cells at E14 are mostly in the CP at E19 (CP $78.8 \pm 2.0\%$, IZ $7.8 \pm 0.7\%$, VZ/SVZ $13.4 \pm 1.4\%$; $n=4$) and daily rapamycin treatment (5.0 mg/kg body weight; E14-E18) does not significantly alter cortical lamination pattern (CP $75.3 \pm 0.3\%$, IZ $10.3 \pm 0.7\%$, VZ/SVZ $14.4 \pm 0.5\%$; $n=3$; $p > 0.05$ for each region).

(D) Graphical representation comparing percentage of cells in each region between BrdU and rapamycin-treated (5.0 mg/kg body weight; E14-E18) BrdU conditions.

(E, from left to right) Whole-body and brain images of mouse pups at E19 in rapamycin-treated, vehicle-treated, and untreated BrdU-injected conditions.

(F) Graphical representation comparing brain weight (in grams) following *in utero* electroporation (IUE) procedure at E14 analysis at E19, untreated, vehicle-treated, and rapamycin-treated (5.0 mg/kg body weight; E15-E18) IUE. * $p < 0.05$, ** $p < 0.05$.

**CHAPTER 4: DEPTOR, A NOVEL mTOR-REGULATORY PROTEIN IS EXPRESSED
IN THE BRAIN AND ITS LOSS RESULTS IN A CORTICAL MALFORMATION**

4.1. Introduction

DEPTOR is a recently described mTOR-interacting protein that was found to be overexpressed in multiple myeloma cells and contributed to their survival (Peterson et al., 2009). DEPTOR is highly overexpressed in a subset of multiple myelomas harboring cyclin D1/D3 or c-MAF/MAFB translocations (Peterson et al., 2009). High DEPTOR expression was necessary to maintain the PI3K and Akt pathway activation and a reduction in DEPTOR levels resulted in apoptosis (Peterson et al., 2009). DEPTOR overexpression suppressed S6K1 signaling (mTORC1 signaling) but by relieving inhibition from mTORC1 to PI3K pathway, activates Akt signaling (mTORC2 signaling pathway) (Peterson et al., 2009). Several mTOR regulatory proteins have been shown to be involved in brain development, such as TSC1, TSC2, PTEN and STRAD α (Kwon et al., 2003; Way et al., 2009; Orlova et al., 2010a; Zhu et al., 2012). Thus we wanted to investigate whether the novel mTOR-interacting protein Deptor plays a role in brain development. First, we tested whether Deptor is expressed in the human and mouse brain. Then we examined the expression in mouse neural progenitor cells (mNPCs) and mixed neuronal and astrocytic cell cultures. We then generated a stable Deptor shRNA knockdown (KD) mNPCs cell line to study the effects of Deptor loss *in vitro*. Utilizing the *in vitro* scratch migration assay, we found that stable Deptor KD mNPCs had a defect in migration. To investigate the role of Deptor during brain development, we utilized the *in utero* electroporation strategy to knock down Deptor during embryogenesis. Deptor KD *in vivo* at embryonic day 14 (E14) led to a cortical migration defect at E19. These results show that Deptor may play a critical role in the brain and have an important function in brain development.

4.2. Materials and Methods

Human Brain Tissue

Adult brain specimens were obtained post-mortem.

Cell Culture

mNPCs were a generous gift from Dr. J. Wolfe (Children's Hospital of Philadelphia, PA) and derived from the subventricular zone of C57BL/6 postnatal day 1 mice. mNPCs were cultured on poly-D-lysine (PDL) coated plates in DMEM/F12, supplemented with 1% fetal bovine serum, 1% N-2 supplement, 1% penicillin/streptomycin, fibroblast growth factor, and heparin. mNPCs express neuroglial progenitor state markers SOX2 and Nestin and retain full capacity to differentiate into neurons and astrocytes (Magnitsky et al., 2008; Orlova et al., 2010a).

mNPCs were transfected with shRNA plasmids containing a GFP reporter and puromycin resistance gene (Origene) targeting mouse Deptor or scrambled (control) sequence using Lipofectamine LTX/ Plus Reagents (Invitrogen). shRNA constructs were commercially confirmed for absence of interferon response. In keeping with existing standards for shRNA experimentation *in vitro* and *in vivo* (Samuel-Abraham S and JN Leonard 2010), multiple shRNA constructs to Deptor and scrambled sequence were tested.

Stable Deptor shRNA KD mNPC cell lines were generated by selection puromycin (8 ug/uL), picking single transfected GFP-positive cells (for clonal cell populations) and growing them in the presence of puromycin (8 ug/uL). Stable cell line

clones were chosen for subsequent experiments based on highest level of Deftor KD (by Western analysis).

Rat and Mouse Cortical and Hippocampal Cultures

Primary rat cerebrocortical and hippocampal cultures were generated from embryonic day 17 (E17) Sprague-Dawley rat pups as previously described (Wilcox et al., 1994; Brewer, 1995). Cells were plated on cell culture dishes pre-coated with poly-L-lysine (Peptides International, Louisville, KY) and maintained in Neurobasal media supplemented with B27 (Invitrogen) at 37°C, 5% CO₂ incubator. Half of the media was replaced every 2-3 days, and cell cultures were used for experiments between 7 and 14 days *in vitro* (DIV).

Western Analysis

mNPCs were lysed in RIPA lysis buffer (50mM Tris HCl pH 8.0; 150 mM NaCl; 1% NP-40; 0.5% sodium deoxycholate, 0.1% SDS, protease and phosphatase inhibitors). Protein was separated on 4-15% SDS-PAGE Tris-Glycine gel (Bio-Rad), transferred onto PVDF membranes and probed with: Deftor (Millipore), mTORC1 markers P-S6 (S235/236; Cell Signaling), P-4E-BP1 (T37/46; Cell Signaling) and mTORC2 marker P-Akt (S473; Cell Signaling) antibodies overnight at 4°C and HRP-conjugated secondary antibodies (GE Healthcare) for 1 hour at room temperature, and visualized with ECL or ECL Plus (GE Healthcare). Membranes were probed with antibodies to GAPDH (Cell Signaling) to ensure equal protein loading.

Scratch Migration Assay

mNPCs were grown to confluency in a 6-well plate, pre-coated with PDL. A scratch was made across the middle of each well with a 1000 μ L pipette tip. In treatment conditions, rapamycin (100nM) and/or Torin1 (50nM) was applied at the time of the scratch. Cells were imaged at 0, 15, 20 hours (h) or 0, 16, 21 h. Five images were obtained for each scratch. Ten length measurements were made for each image (part of scratch). Fifty measurements were obtained for each scratch and averaged. Distance migrated at each time point was calculated by subtracting the length at time of image from the length of scratch at time 0 h. Paired t-test and one-way ANOVA were used for statistical comparison across different conditions.

In Utero Electroporation (IUE)

Animal experiments were approved by the Institutional Animal Care and Use Committee of the University of Pennsylvania.

Time-pregnant C57BL/6J mice at embryonic day 14 (E14) were placed under isoflurane-induced anesthesia and the uterine horns were surgically exteriorized. shRNA-GFP plasmids targeting mouse Deptor or control scrambled sequence diluted in TE Buffer (3-7 μ g/ml; Qiagen) and Fast Green dye (0.3 μ g/ml; Sigma-Aldrich), were microinjected through the uterine wall into one lateral ventricle of each embryo. Deptor shRNA clone #4 was used for IUE experiments. Five electrical pulses (40 V, 50 ms duration, 1000 ms intervals) (Saito T 2006) were delivered across the embryonic head using CUY21 Edit Square Wave Electroporator (Nepagene). Uterine horns were returned to the pelvic cavity and the abdominal wall was closed by suture. Females were returned to the cage and embryos were sacrificed five days later at E19.

4.3. Results

4.3a. *Deptor is Expressed in Human and Mouse Brain*

In order to investigate whether *Deptor* has a role in the brain, we first immunostained human brains to evaluate the presence of *Deptor*. Immunohistochemical staining with several *Deptor* antibodies revealed that *Deptor* is expressed in the human brain (Fig. 4-1). Furthermore, *Deptor* was expressed in the mouse brain at both embryonic and adult time points, as well as other organ systems including the heart, kidney, liver, skin by Western detection method (Fig. 4-1).

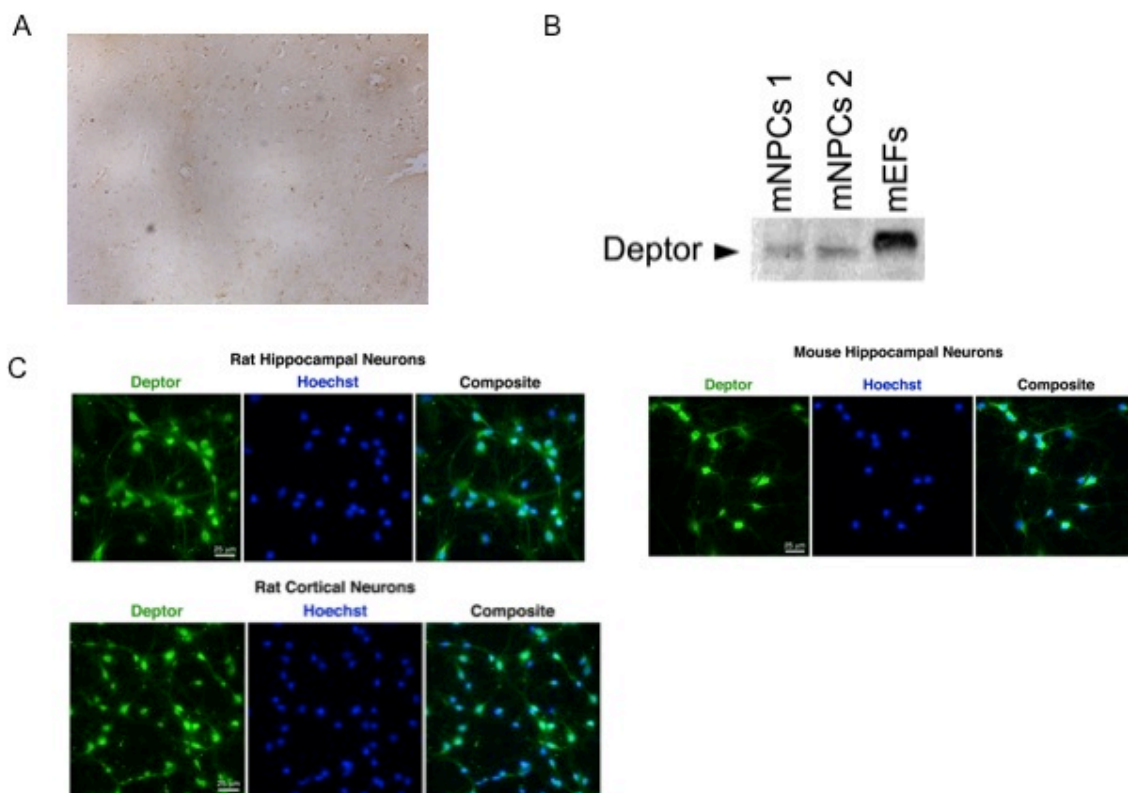


Figure 4-1. *Deptor* is expressed in the human brain and murine neural cells.

A. *Deptor* is expressed in the human brain.

B. *Deptor* is expressed in mouse neural progenitor cells (mNPCs).

C. *Deptor* is expressed in mouse and rat neurons and astrocytes.

4.3b. Deptor is Expressed in mNPCs, Neurons, and Astrocytes

Immunocytochemistry revealed that Deptor is expressed in mNPCs, as well as rat and mouse neurons (Fig. 4-1, 4-2). Cytoplasmic and nuclear fractions of mNPCs revealed that Deptor protein is present in both the cytoplasmic and nuclear compartments, similar to its binding partner mTOR (Fig. 4-3) (Peterson et al., 2009). Furthermore, when comparing rat mixed, neuronal, or astrocytic cell cultures, Deptor protein expression was found highest in the astrocytes (Fig. 4-4).

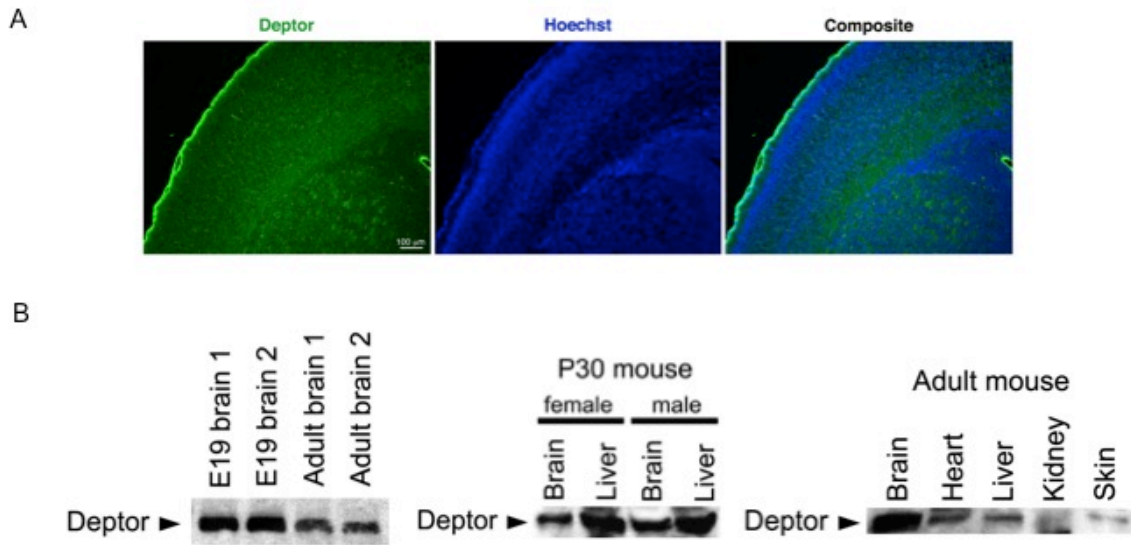


Figure 4-2. Deptor is expressed is developmentally expressed in the mouse brain.

A. Deptor is expressed in the mouse embryonic brain. Immunohistochemical staining with Deptor of mouse brain at embryonic day 19 (E19). Hoechst33342 was used to visualize the nuclelei

B. Deptor is developmentally expressed in the mouse brain at 19, postnatal day (P) 7, P30, and adult time.

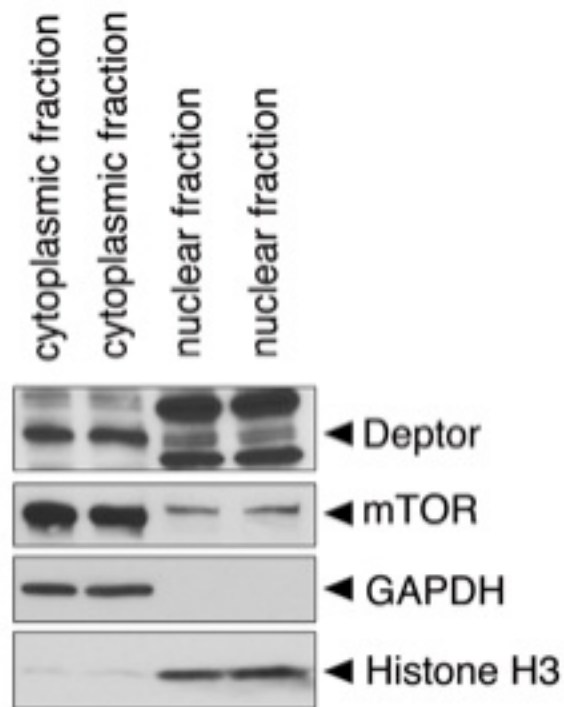


Figure 4-3. Deptor is present in cytoplasmic and nuclear compartments in mouse neural progenitor cells.

Western analysis of mNPCs cytoplasmic and nuclear compartments reveals presence of Deptor protein in both compartments, similar to its binding partner mTOR. GAPDH is specifically localized to the cytoplasm and Histone H3 to the nucleus.

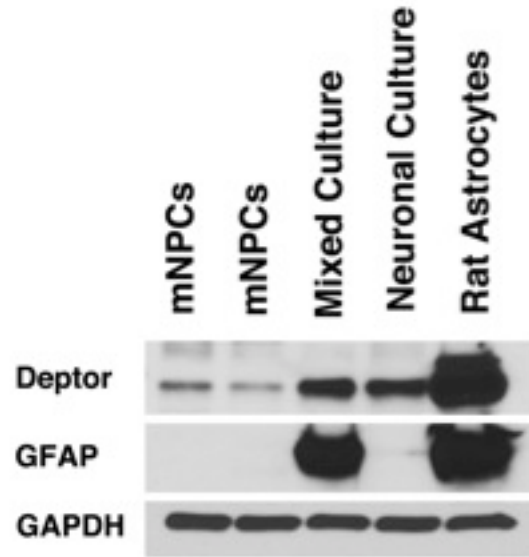


Figure 4-4. Deptor is more highly expressed in the astrocytes compared to neurons.

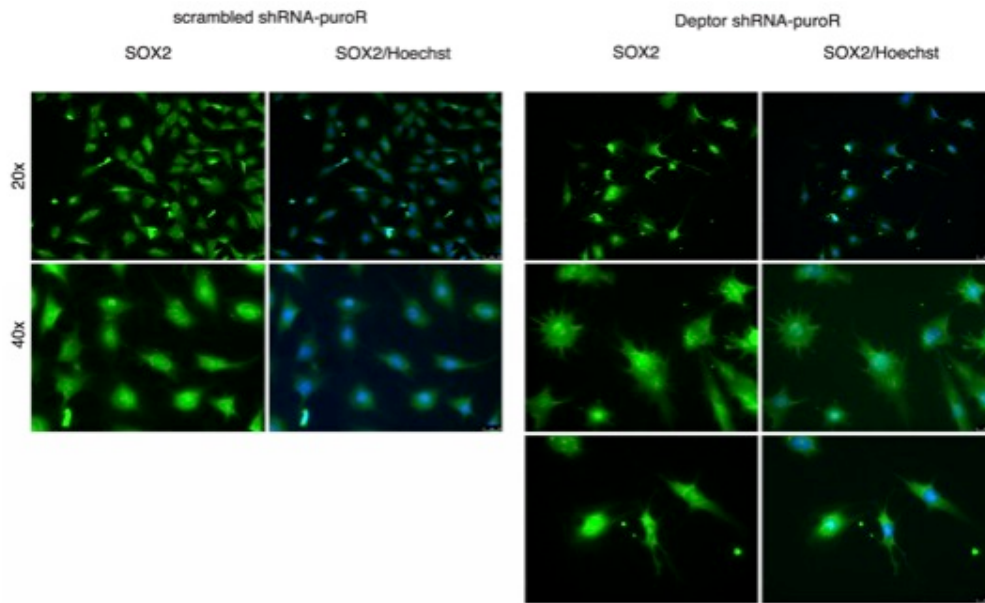
Comparing rat mixed, neuronal, and astrocytic cultures show that Deptor is most highly expressed by astrocytes. GFAP is an astrocyte specific marker. GAPDH was used as a loading control.

4.3c. Deptor shRNA KD in mNPCs Results in mTORC1 and mTORC2 Signaling

Pathway Activation

Stable cell lines were generated with puromycin-resistant shRNA against Deptor and a scrambled sequence was transfected as a control. Deptor depletion in mNPCs resulted in activation of mTORC1 (P-S6 (S235/236), P-4E-BP1 (T37/46)) and mTORC2 (P-Akt (S473)) signaling pathways (Fig. 4-5 and preliminary data). Furthermore, Deptor shRNA KD cells expressed progenitor cell markers SOX2 and Nestin, and appear not to have undergone differentiation (Fig. 4-5). However, the Deptor KD cells appeared to have abnormal morphology, with the possibility of increased focal adhesions (Fig. 4-5).

A.



B.

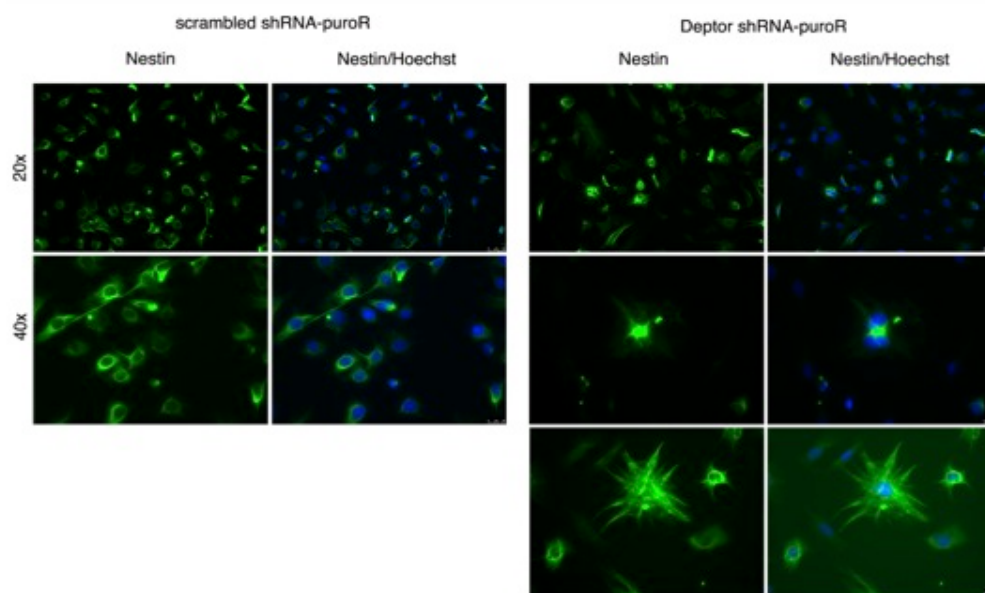


Figure 4-5. Mouse neural progenitor cells with stable *Deptor* knockdown express *SOX2* and *Nestin*, and show *mTOR* activation.

A. Stabled *Deptor* KD mNPCs express progenitor marker *SOX2*.

B. Stabled *Deptor* KD mNPCs express progenitor marker *Nestin*.

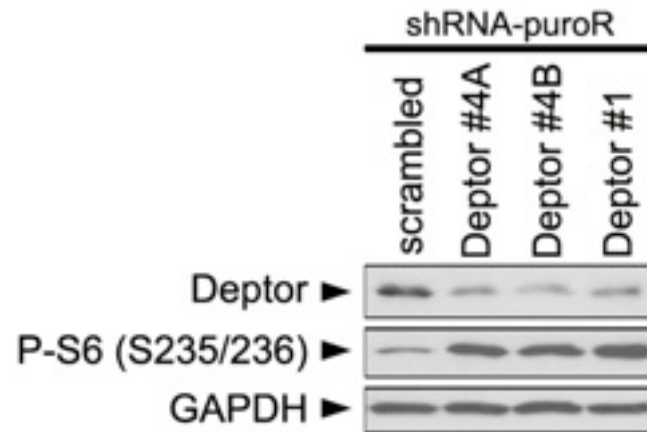


Figure 4-5. Mouse neural progenitor cells with stable *Deptor* knockdown express *SOX2* and *Nestin*, and show *mTOR* activation. (continued)

C. Stable *Deptor* KD in mNPCs results in *mTORC1* activation via increased levels of P-S6 (S235/236). *GAPDH* was used as a loading control.

4.3d. Deptor KD in mNPCs Results in a Migration Defect In Vitro

To investigate whether Deptor plays a role in migration, we utilized the wound-healing scratch assay and found that stable Deptor KD mNPCs close the wound significantly slower than the scrambled shRNA control or wild-type cells and have impaired migration (Fig. 4-6). Treatment with rapamycin, an mTORC1 inhibitor, or Torin1, mTORC1 and mTORC2 inhibitor, did not rescue the *in vitro* migration phenotype (Fig. 4-6, preliminary data).

A

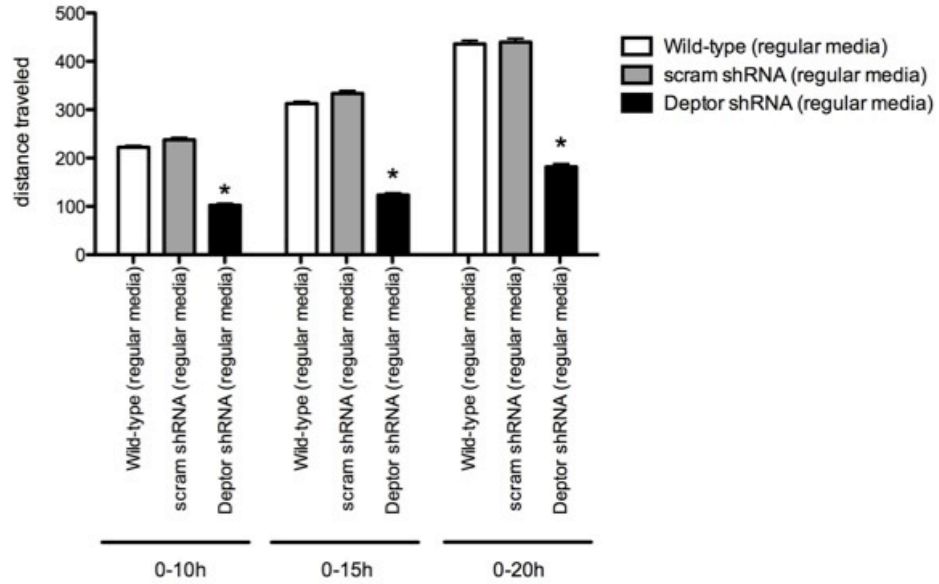


Figure 4-6. Deptor knockdown results in impaired migration *in vitro*

A. Scratch-induced wound healing assay in stable scrambled shRNA-puroR and Deptor shRNA-puroR cell lines. Deptor KD cells do not close the gap as compared to the scrambled shRNA control cells.

B

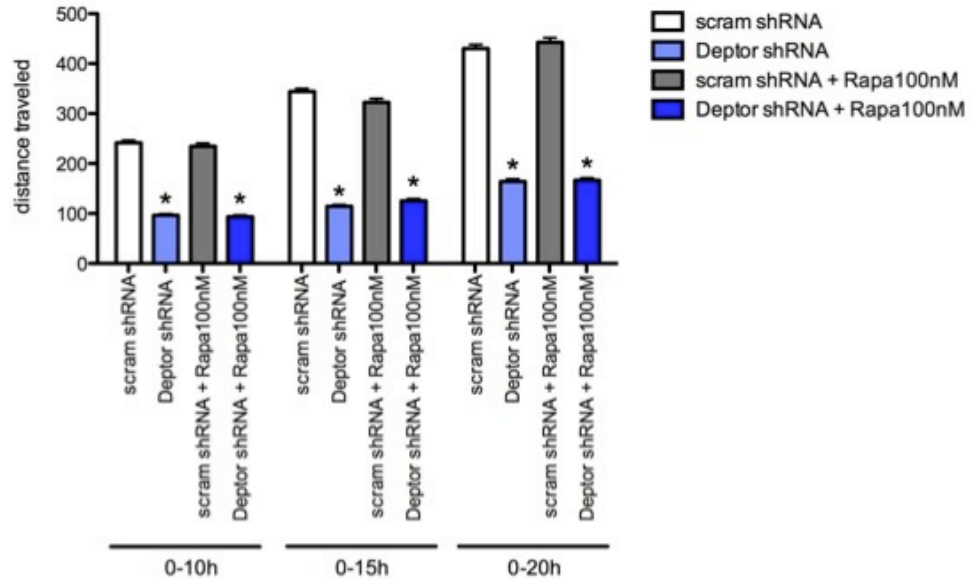


Figure 4-6. *Deptor* knockdown results in impaired migration *in vitro*. (continued)

B. Treatment with mTORC1 inhibitor rapamycin does not rescue the impaired migration *in vitro* following *Deptor* KD.

C

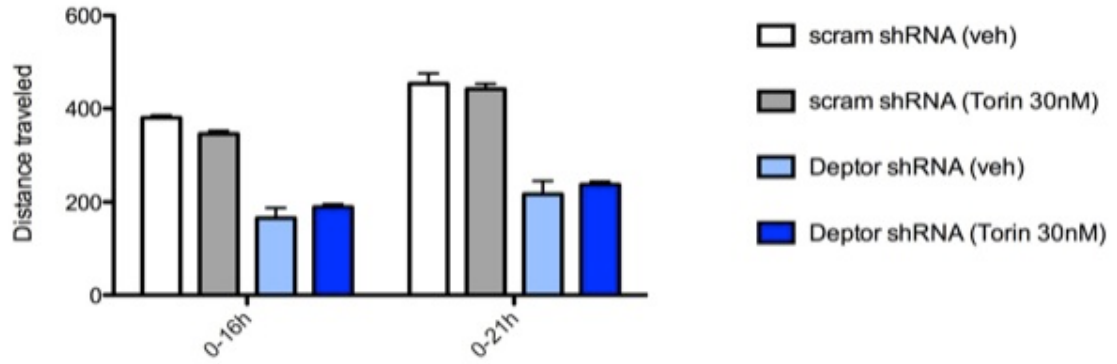


Figure 4-6. *Deptor* knockdown results in impaired migration *in vitro*. (continued)

C. Treatment with mTORC1 and mTORC2 inhibitor Torin1 does not rescue the impaired migration *in vitro* following *Deptor* KD.

4.3e. *Deptor shRNA KD In Vivo During Embryogenesis by In Utero Electroporation Leads to a Cortical Malformation*

To investigate the role of Deptor, a novel mTOR-regulatory protein, *in vivo* during embryonic brain development, we utilized the *in utero* electroporation strategy using shRNA targeting Deptor. IUE was performed at embryonic day 14 (E14) with GFP-tagged shRNA targeting mouse Deptor mRNA. Five days (E19) post introduction of Deptor shRNA plasmid into progenitor cells in the ventricular zone (VZ), GFP-positive cells were found to be primarily localized to the VZ/SVZ and IZ zones, and failed to reach layer II-III, like scrambled shRNA control cells (Fig. 4-7). Intraperitoneal rapamycin treatment (5 mg/ kg of body weight) resulted in a partial rescue, with more cells exiting the VZ/SVZ (preliminary data).

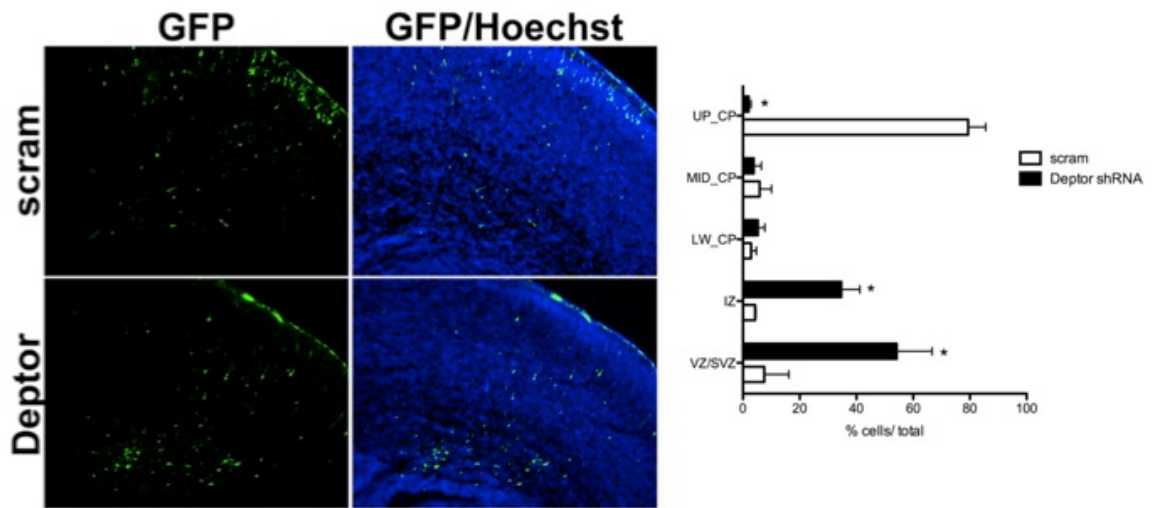


Figure 4-7. *Deptor* depletion *in vivo* results in a cortical malformation.

Deptor shRNA KD *in vivo* by *in utero* electroporation at E14 leads to a cortical malformation at E19. (Right) Quantification of GFP-positive cells in VZ/SVZ, IZ, LW_CP, MID_CP, UP_CP in scrambled shRNA-GFP and *Deptor* shRNA-GFP conditions.

CHAPTER 5. CONCLUSION, DISCUSSION AND FUTURE DIRECTIONS ²

² Part of Chapter 5: TSC work discussion, was originally published in *Cerebral Cortex* journal. Tsai V, Parker WE, Orlova KA, Baybis M, Chi AWS, Berg BD, Birnbaum JF, Estevez J, Okochi K, Sarnat HB, Flores-Sarnat L, Aronica E, Crino PB. 2012. Fetal Brain mTOR Signaling Pathway Activation in Tuberous Sclerosis Complex. Copyright © 2012 Oxford University Press.

5.1. Tsc2 Work Discussion

We demonstrate for the first time the profile of mTORC1 and mTORC2 signaling cascade activation in human fetal tuber tissue. We provide data quantifying the significant cellular enlargement following Tsc2 KD in neural progenitor cells *in vitro* and *in vivo* and show that enhanced cell size can be prevented by rapamycin treatment. We demonstrate for the first time that focal KD of Tsc2 during fetal brain development leads to a focal cortical lamination defect characterized by both cell-autonomous and non-cell-autonomous effects that can be prevented by *in utero* rapamycin treatment. The effects of rapamycin on mTOR signaling have been studied in the postnatal rodent brain however little is known of the effects of rapamycin on mTOR signaling during fetal brain development, an epoch that coincides with the pathogenesis of TSC. Taken together, these data suggest that hyperactive mTORC1 and mTORC2 signaling in neural progenitor cells leads to cellular features of TSC and that these effects could in theory be targeted therapeutically during *in utero* development.

Our findings support the hypothesis that mTORC1 activation is an early finding in fetal TSC brain lesions and provide a new window to understand the cellular pathogenesis of TSC. Of course, we acknowledge that only 4 specimens were analyzed, however, given the rarity of fetal TSC brain specimens, we were fortunate to assess 4 high-quality tissue samples. As alterations in cortical lamination that likely reflect nascent tubers have been reported in the fetal period by autopsy and magnetic resonance imaging studies (Park et al., 1997; Levine et al., 1999; Chen et al., 2010), we propose that mTORC1 hyperactivation is an early event in the pathogenesis of embryonic tuber formation (Crino, 2010). The detection of P-p70S6K1, P-S6, and c-myc provides strong

evidence that enhanced mTORC1 signaling in a focal region of the developing brain is intimately linked to abnormal architecture characteristic of tubers.

mTORC2 signaling, evidenced by increased levels of P-PKC α , P-Akt, P-SGK1, and P-NDRG1 is activated in the TSC adult and fetal brain specimens. Our findings differ from previous reports in human renal angiomyolipomas, *Tsc2*^{+/-} mouse kidney angiomyolipomas, *Tsc2*^{-/-} mouse embryonic fibroblasts, and human embryonic kidney 293 (HEK293) cells (Yang et al., 2006; Huang et al., 2008; Huang et al., 2009), which show that mTORC2 signaling cascade is attenuated in the absence of *Tsc2*. The disparity between these data and our own may reflect differential effects of mTORC2 in fetal neurons, or the presence of other modulators that are activated in TSC brain such as EGFR (Parker et al., 2011) that activate mTORC2 (Tanaka et al., 2011). In the adult tubers specimens, a possible contribution to changes in mTORC2 signaling from recurrent seizures is also possible. Two studies (Goto et al., 2011; Carson et al., 2012) have investigated mTORC2 substrates in brain lysates following *Tsc1* conditional knockout. In the *Emx-Tsc1* conditional knockout mouse strain (Carson et al., 2012) there was a reduction in phospho-NDRG1 at P15 whereas in the inducible in *Tsc1cc Nestin-rtTA+ TetOp-cre+* strain (Goto et al., 2011) there was a reduction in P-PKC α at P30. Neither of these studies examined embryonic tissue or neural progenitor cells.

There have been few studies to date providing data quantifying the effects of *Tsc2* KD or mTOR hyperactivation on cell size in neural progenitor cells although conditional knockout of *Tsc2* in radial glial cells *in vivo* causes enhanced cell size (Way et al., 2009). KD of *Tsc2* in mNPCs resulted in a 2-fold increase in cell size associated with enhanced mTOR activation. The effect on cell size was preventable with rapamycin treatment suggesting that cytomegaly in TSC is an mTORC1-dependent process. Similar mechanistic effects on cell size have been demonstrated in the mouse for two other known mTORC1 inhibitory proteins, PTEN and STRAD α (Kwon et al., 2003;

Orlova et al., 2010a), suggesting that mTORC1 signaling plays a pivotal role in cell size in the brain. Thus, mTORC1 inhibition may provide a potentially attractive strategy to prevent cytomegaly in neural progenitor cells. Further studies to define the precise role or mTORC2 activation in fetal TSC brain tissue is clearly warranted.

KD of Tsc2 during embryonic brain development resulted in a focal cortical lamination with the majority of cells being localized in deeper regions of the cortex instead of superficial layers II-III. This could potentially suggest that Tsc2 plays a role in migration. It was interesting to find that only 21% of Tsc2 KD cells were Cux1-positive, while the other 79% were Cux1-negative. Homeobox Cux1 transcription factor has been shown to regulate dendrite branching, development of spines, and synapse formation of layer II/III neurons (Cubelos et al., 2010). Given that cells electroporated with Tsc2 shRNA do not migrate appropriately and in addition do not express Cux1 could potentially result in dysregulated neuronal development (spines, dendrite branching) and aberrant targeting and synapse formation. Furthermore, the Tsc2 KD cells that started on their migrational route but were localized in the IZ and lower CP regions (LW_CP, MID_CP), did not express transcription factors Ctip2 and Tbr1 that are specific to deeper cortical layers V and VI, indicating that at least at this stage in development, they have not taken on the cell identity of another layer which surrounds them.

The observation that Tsc2 KD leads to altered laminar destination of Cux1-positive nontransfected cells suggests that there may be non-cell-autonomous effects of loss of Tsc2 function in the developing brain. It has previously been reported that RNAi KD of doublecortin gene *DCX* during brain development results in non-cell-autonomous defect in migration of neighboring cells (Bai et al., 2003). It is possible that Tsc2 KD results in mTORC1 hyperactivation, which in turn results in expression and secretion of factors that disrupt lamination of neighboring Cux1-positive cells. For example, following Tsc2 KD, mTORC1 activation could result in release of secretable factors that influence

migration and lamination of surrounding progenitor cells. We have previously demonstrated robust expression of numerous growth factors including NT4, VEGF, HGF, and EGF in tubers and in the *Tsc1^{GFAP}Cre* conditional mouse strain (Kyin et al., 2001; Parker et al., 2011) that could alter laminar destinations of migrating neurons.

While the existing conditional TSC mouse models provide invaluable systems to study brain development in TSC, rapamycin only partially reverses the structural abnormalities in these strains. In the *Tsc1^{syn}Cre* mouse strain (Meikle et al., 2007), treatment with rapamycin or RAD001, another mTOR inhibitor, improves survival and reduces neuronal enlargement *in vivo* (Meikle et al., 2008), but disorganized neocortical architecture is not fully rescued possibly because rapamycin and RAD001 were begun at postnatal timepoints. Similarly, postnatal treatment with rapamycin in both *Tsc1^{GFAP}Cre* (Zeng et al., 2008) and *Tsc2^{GFAP}Cre* (Zeng et al., 2010) mice ameliorated the seizure phenotype but only partially rectified the histopathological abnormalities. Rapamycin has not been previously assayed as a preventative approach for Tsc2-induced lesions *in utero*, however, in a previous study, prenatal rapamycin improved survival of *Tsc1^{nestin}Cre* conditional knockout mice (Anderl et al., 2011a). Our results demonstrate for the first time that selective effects of Tsc2 KD on neural progenitor cells or during fetal brain development (e.g., cytomegaly, altered cortical lamination, enhanced mTOR signaling), can be prevented with rapamycin treatment. In concert with the discovery of mTOR cascade hyperactivation in fetal tuber specimens, we suggest the possibility that prenatal treatment with mTOR pathway inhibitors could prevent or reduce neurological disability in TSC. In 2 recent clinical trials (Bissler et al., 2008; Krueger et al., 2010), tuber size was not altered following treatment with the rapamycin analog everolimus and seizures were reduced in only 50% of patients (age range: 3-34) receiving the drug (Krueger et al., 2010). However, white matter abnormalities in TSC can be reversed with everolimus (Tillema et al., 2012). Postnatal treatment with mTOR inhibitors may miss a

critical period in the pathogenesis of tuber formation and thus have limited benefit for all neurological features of TSC. However we acknowledge that rapamycin has independent effects on development including reduction of body size and brain weight, alterations in gene expression, and cognitive function (Ruegg et al., 2007; Way et al., 2012) that require important consideration for further clinical studies.

5.2. Deptor Work Discussion

Our results demonstrate for the first time that DEPTOR is expressed in human and murine brain. We show that Deptor shRNA KD *in vitro* in neural progenitor cells causes mTORC1 and mTORC2 signaling pathway activation. Furthermore, *in vivo* KD of Deptor during embryonic brain development results in a focal cortical malformation. Treatment with mTORC1 inhibitor rapamycin and dual mTORC1 and mTORC2 inhibitor Torin1, did not rescue the *in vitro* migration phenotype. Limited improvement in cell migration was observed *in vivo* with fetal rapamycin treatment. Interestingly, this was different from the results we previously observed in our studies with Tsc2 (Tsai et al., 2012).

Several questions arise on the limited efficacy of rapamycin and Torin1 treatments. Given that DEPTOR directly interacts with mTOR, it is possible that DEPTOR protein is necessary for mTORC1 and mTORC2 complex function. While studies in other cell types (Peterson et al., 2009) and our results in mouse neural progenitor cells show that Deptor inhibits mTORC1 and mTORC2 signaling, it could have a secondary role in facilitating certain mTORC1 and mTORC2 functions. Lack of Deptor could also result in mTORC1 signaling activation and negative feedback loop

from S6 kinase, in which case rapamycin and Torin1 may not be the most effective inhibitors.

5.3. Remaining Questions

5.3a. *mTOR activation in Neural Progenitor Cells vs. Mature Neurons and Astrocytes*

mTOR signaling (mTORC1 and mTORC2) has various downstream effects on different cellular functions (e.g. transcription, translation, autophagy, actin cytoskeleton dynamics) and thus it would be important to evaluate whether there is differential activation in immature (neural stem and progenitor cells) vs. mature (neurons, astrocytes, glia) neural cells. Furthermore it would be critical to determine the role that the timing of mTOR signaling pathway activation or deactivation would play on subsequent phenotype effects (e.g. mTOR signaling dysregulation in very early stages of development vs. later stages).

5.3b. *Cell-Autonomous vs. Non-Cell-Autonomous Effects*

It would be interesting and important to investigate further what the cell-autonomous and non-cell-autonomous roles Tsc2 and Deptor play. Specifically, what effects do these mTOR-regulatory genes and proteins exert on the affected cell (cell harboring mutation, knockdown, or knockout). Furthermore, how does the affected cell influence the signaling of other surrounding unaffected cells. Given that we have observed an increase in cell size following Tsc2 KD in mNPCs, as well as non-cell-autonomous effects *in vivo*, it would potentially be very interesting to do the following experiment. First, culture Tsc2 KD and wild-type mNPCs for several days. Then, take

the media from the Tsc2 KD cells and replace the wild-type mNPC plates' media with this media and grow for several days. If the non-cell-autonomous effects are through a secreted factor, we should potentially observe an increase in cell size in wild-type mNPCs grown in media from Tsc2 KD cells, when comparing to wild-type mNPCs grown in regular media the whole time.

5.3d. Is Deptor Associated with Any Neurological Diseases?

DEPTOR-related research is still in its early stages. To date, no reports have been published describing DEPTOR's function in the brain. Given that approximately 10-15% of diagnosed TSC cases do not have either a *TSC1* or *TSC2* gene mutation identified, could *DEPTOR* be the *TSC3* gene? To answer this question, it would be important to screen individuals with a TSC clinical diagnosis for a *DEPTOR* (*DEPDC6*) gene mutation. However it is also possible that *DEPTOR* could be mutated in other neurological disorders characterized by cortical malformation and epilepsy, such as hemimegalencephaly. Given the domains within DEPTOR protein (2 DEP and 1 PDZ) it would be important to find its binding partners. Identification of DEPTOR's binding partners would provide insight into its potential function in neural cell physiology.

5.3c. TSC2 vs. DEPTOR

In light of the different effects of Tsc2 shRNA KD and Deptor shRNA KD *in vitro* and *in vivo* (Chapters 3 and 4), Deptor shRNA KD appears to be more severe than Tsc2 shRNA KD *in vivo*, and less responsive to mTORC1 inhibitor rapamycin, unlike in the Tsc2 shRNA KD condition. It would be important to investigate further the mechanisms for why different mTOR-regulatory proteins have different effects on cell function.

There could be several possibilities:

1. The mTOR-regulatory protein (e.g. *TSC2* or *DEPTOR*) has a different degree of regulation on mTOR signaling (mTORC1 and mTORC2).
2. The mTOR-regulatory protein has different degree of regulation on either mTORC1- or mTORC2-specific signaling. (For example, TSC1-TSC2 complex could have a greater effect on mTORC1-specific signaling, whereas DEPTOR could regulate both mTORC1 and mTORC2 signaling equally.)
3. One mTOR-regulatory protein (e.g. *TSC2*) has different binding partners from other regulatory mTOR proteins (e.g. *DEPTOR*) which results in the different phenotypes.

5.3e. Therapeutic Treatment Approaches

With genetic testing being available, it would be crucial for to understand for a disease like TSC the contribution of either *TSC1* or *TSC2* gene to the disease and how the different mutations in either gene produce their phenotypic effects. TSC individuals exhibit variable penetrance, or variable severity of disease manifestations. Thus it would be important to understand what accounts for the differences in disease severity.

Understanding the mechanistic differences between various mTOR-regulatory proteins would be crucial in designing new treatment approaches for individuals with different gene mutations (e.g. *TSC1* vs. *TSC2* vs. *DEPTOR*), since each gene and mutation could have different regulatory contributions on the mTOR pathways (e.g. mTORC1, mTORC2, or other downstream effectors). Specifically, given the complicated nature of mTOR signaling, with multiple regulatory proteins, as well as positive and negative feedback loops, it would be important to consider how the gene and protein of

interest regulate that pathway. Furthermore, should the therapies target mTORC1 only, mTORC2 only, both mTORC1 and mTORC2, or combination treatments targeting both mTORC1 and/or mTORC2 and the Akt and/or S6 kinase signaling (e.g., to account for the negative feedback loop in the mTOR pathway).

Another important consideration is when to begin therapy. It has previously been shown in various TSC animal models that mTOR inhibition with rapamycin improves seizures and learning more effectively when administered early. In our Tsc2 study in a developmental mouse model system, we were able to rescue the cell migration phenotype by fetal rapamycin treatment. However the decrease in body and brain weight brings up important considerations for treatment with mTOR inhibitors during embryonic development. While fetal rapamycin treatment did not disrupt the normal cell migration in the brain, the effects on other processes such as synapse formation and dendrite branching, as well as on different cell types (e.g., neurons vs. astrocytes vs. glia) would have to be carefully considered. Future studies and insights into the mechanism of mTOR dysregulation downstream of mTORC1 and mTORC2 signaling would provide the possibility of designing more targeted therapeutic approaches which could potentially be safer for administration during fetal development.

BIBLIOGRAPHY

(1993) Identification and characterization of the tuberous sclerosis gene on chromosome 16. *Cell* 75:1305-1315.

Adachi H, Igawa M, Shiina H, Urakami S, Shigeno K, Hino O (2003) Human bladder tumors with 2-hit mutations of tumor suppressor gene TSC1 and decreased expression of p27. *J Urol* 170:601-604.

Anderl S, Freeland M, Kwiatkowski DJ, Goto J (2011a) Therapeutic value of prenatal rapamycin treatment in a mouse brain model of tuberous sclerosis complex. *Hum Mol Genet* 20:4597-4604.

Anderl S, Freeland M, Kwiatkowski DJ, Goto J (2011b) Therapeutic value of prenatal rapamycin treatment in a mouse brain model of Tuberous Sclerosis Complex. *Hum Mol Genet*.

Androutsellis-Theotokis A, Leker RR, Soldner F, Hoepfner DJ, Ravin R, Poser SW, Rueger MA, Bae SK, Kittappa R, McKay RD (2006) Notch signalling regulates stem cell numbers in vitro and in vivo. *Nature* 442:823-826.

Arlotta P, Molyneaux BJ, Chen J, Inoue J, Kominami R, Macklis JD (2005) Neuronal subtype-specific genes that control corticospinal motor neuron development in vivo. *Neuron* 45:207-221.

Au KS, Williams AT, Roach ES, Batchelor L, Sparagana SP, Delgado MR, Wheless JW, Baumgartner JE, Roa BB, Wilson CM, Smith-Knuppel TK, Cheung MY, Whittemore VH, King TM, Northrup H (2007) Genotype/phenotype correlation in 325 individuals referred for a diagnosis of tuberous sclerosis complex in the United States. *Genet Med* 9:88-100.

- Bai J, Ramos RL, Ackman JB, Thomas AM, Lee RV, LoTurco JJ (2003) RNAi reveals doublecortin is required for radial migration in rat neocortex. *Nat Neurosci* 6:1277-1283.
- Benvenuto G, Li S, Brown SJ, Braverman R, Vass WC, Cheadle JP, Halley DJ, Sampson JR, Wienecke R, DeClue JE (2000) The tuberous sclerosis-1 (TSC1) gene product hamartin suppresses cell growth and augments the expression of the TSC2 product tuberin by inhibiting its ubiquitination. *Oncogene* 19:6306-6316.
- Bissler JJ, McCormack FX, Young LR, Elwing JM, Chuck G, Leonard JM, Schmithorst VJ, Laor T, Brody AS, Bean J, Salisbury S, Franz DN (2008) Sirolimus for angiomyolipoma in tuberous sclerosis complex or lymphangiomyomatosis. *N Engl J Med* 358:140-151.
- Bolton PF, Park RJ, Higgins JN, Griffiths PD, Pickles A (2002) Neuro-epileptic determinants of autism spectrum disorders in tuberous sclerosis complex. *Brain* 125:1247-1255.
- Brewer GJ (1995) Serum-free B27/neurobasal medium supports differentiated growth of neurons from the striatum, substantia nigra, septum, cerebral cortex, cerebellum, and dentate gyrus. *J Neurosci Res* 42:674-683.
- Cai X, Pacheco-Rodriguez G, Fan QY, Haughey M, Samsel L, El-Chemaly S, Wu HP, McCoy JP, Steagall WK, Lin JP, Darling TN, Moss J (2010) Phenotypic characterization of disseminated cells with TSC2 loss of heterozygosity in patients with lymphangiomyomatosis. *Am J Respir Crit Care Med* 182:1410-1418.
- Carson RP, Van Nielen DL, Winzenburger PA, Ess KC (2011) Neuronal and glia abnormalities in Tsc1-deficient forebrain and partial rescue by rapamycin. *Neurobiol Dis.*

- Carson RP, Van Nielen DL, Winzenburger PA, Ess KC (2012) Neuronal and glia abnormalities in Tsc1-deficient forebrain and partial rescue by rapamycin. *Neurobiol Dis* 45:369-380.
- Chan JA, Zhang H, Roberts PS, Jozwiak S, Wieslawa G, Lewin-Kowalik J, Kotulska K, Kwiatkowski DJ (2004) Pathogenesis of tuberous sclerosis subependymal giant cell astrocytomas: biallelic inactivation of TSC1 or TSC2 leads to mTOR activation. *J Neuropathol Exp Neurol* 63:1236-1242.
- Chen B, Schaevitz LR, McConnell SK (2005) Fezl regulates the differentiation and axon targeting of layer 5 subcortical projection neurons in cerebral cortex. *Proc Natl Acad Sci U S A* 102:17184-17189.
- Chen CP, Su YN, Chang TY, Liu YP, Tsai FJ, Chen MR, Hwang JK, Chen TH, Wang W (2010) Prenatal diagnosis of rhabdomyomas and cerebral tuberous sclerosis by magnetic resonance imaging in one fetus of a dizygotic twin pregnancy associated with a frameshift mutation in the TSC2 gene. *Taiwan J Obstet Gynecol* 49:387-389.
- Chevere-Torres I, Maki JM, Santini E, Klann E (2011) Impaired social interactions and motor learning skills in tuberous sclerosis complex model mice expressing a dominant/negative form of tuberin. *Neurobiol Dis*.
- Chong-Kopera H, Inoki K, Li Y, Zhu T, Garcia-Gonzalo FR, Rosa JL, Guan KL (2006) TSC1 stabilizes TSC2 by inhibiting the interaction between TSC2 and the HERC1 ubiquitin ligase. *J Biol Chem* 281:8313-8316.
- Crino PB (2004) Molecular pathogenesis of tuber formation in tuberous sclerosis complex. *J Child Neurol* 19:716-725.
- Crino PB (2010) The pathophysiology of tuberous sclerosis complex. *Epilepsia* 51 Suppl 1:27-29.

- Crino PB, Nathanson KL, Henske EP (2006) The tuberous sclerosis complex. *N Engl J Med* 355:1345-1356.
- Crino PB, Aronica E, Baltuch G, Nathanson KL (2010) Biallelic TSC gene inactivation in tuberous sclerosis complex. *Neurology* 74:1716-1723.
- Cubelos B, Sebastian-Serrano A, Beccari L, Calcagnotto ME, Cisneros E, Kim S, Dopazo A, Alvarez-Dolado M, Redondo JM, Bovolenta P, Walsh CA, Nieto M (2010) Cux1 and Cux2 regulate dendritic branching, spine morphology, and synapses of the upper layer neurons of the cortex. *Neuron* 66:523-535.
- Cybulski N, Hall MN (2009) TOR complex 2: a signaling pathway of its own. *Trends Biochem Sci* 34:620-627.
- Dabora SL, Jozwiak S, Franz DN, Roberts PS, Nieto A, Chung J, Choy YS, Reeve MP, Thiele E, Egelhoff JC, Kasprzyk-Obara J, Domanska-Pakiela D, Kwiatkowski DJ (2001) Mutational analysis in a cohort of 224 tuberous sclerosis patients indicates increased severity of TSC2, compared with TSC1, disease in multiple organs. *Am J Hum Genet* 68:64-80.
- Dabora SL, Franz DN, Ashwal S, Sagalowsky A, Dimario FJ, Jr., Miles D, Cutler D, Krueger D, Uppot RN, Rabenou R, Camposano S, Paolini J, Fennessy F, Lee N, Woodrum C, Manola J, Garber J, Thiele EA (2011) Multicenter Phase 2 Trial of Sirolimus for Tuberous Sclerosis: Kidney Angiomyolipomas and Other Tumors Regress and VEGF- D Levels Decrease. *PLoS One* 6:e23379.
- Dada S, Demartines N, Dormond O (2008) mTORC2 regulates PGE2-mediated endothelial cell survival and migration. *Biochem Biophys Res Commun* 372:875-879.
- Davies DM, Johnson SR, Tattersfield AE, Kingswood JC, Cox JA, McCartney DL, Doyle T, Elmslie F, Saggart A, de Vries PJ, Sampson JR (2008) Sirolimus therapy in

tuberous sclerosis or sporadic lymphangioleiomyomatosis. *N Engl J Med* 358:200-203.

Davies DM, de Vries PJ, Johnson SR, McCartney DL, Cox JA, Serra AL, Watson PC, Howe CJ, Doyle T, Pointon K, Cross JJ, Tattersfield AE, Kingswood JC, Sampson JR (2011) Sirolimus therapy for angiomyolipoma in tuberous sclerosis and sporadic lymphangioleiomyomatosis: a phase 2 trial. *Clin Cancer Res* 17:4071-4081.

Devlin LA, Shepherd CH, Crawford H, Morrison PJ (2006) Tuberous sclerosis complex: clinical features, diagnosis, and prevalence within Northern Ireland. *Dev Med Child Neurol* 48:495-499.

DiMario FJ, Jr. (2004) Brain abnormalities in tuberous sclerosis complex. *J Child Neurol* 19:650-657.

Ehninger D, Han S, Shilyansky C, Zhou Y, Li W, Kwiatkowski DJ, Ramesh V, Silva AJ (2008) Reversal of learning deficits in a *Tsc2*^{+/-} mouse model of tuberous sclerosis. *Nat Med* 14:843-848.

Eker R (1954) Familial renal adenomas in Wistar rats; a preliminary report. *Acta Pathol Microbiol Scand* 34:554-562.

Eker R, Mossige J, Johannessen JV, Aars H (1981) Hereditary renal adenomas and adenocarcinomas in rats. *Diagn Histopathol* 4:99-110.

Ess KC, Roach ES (2012) New therapies for tuber-less sclerosis: white matter matters? *Neurology* 78:520-521.

Everitt JI, Goldsworthy TL, Wolf DC, Walker CL (1992) Hereditary renal cell carcinoma in the Eker rat: a rodent familial cancer syndrome. *J Urol* 148:1932-1936.

Ewalt DH, Sheffield E, Sparagana SP, Delgado MR, Roach ES (1998) Renal lesion growth in children with tuberous sclerosis complex. *J Urol* 160:141-145.

- Feliciano DM, Su T, Lopez J, Platel JC, Bordey A (2011) Single-cell Tsc1 knockout during corticogenesis generates tuber-like lesions and reduces seizure threshold in mice. *J Clin Invest*.
- Fingar DC, Salama S, Tsou C, Harlow E, Blenis J (2002) Mammalian cell size is controlled by mTOR and its downstream targets S6K1 and 4EBP1/eIF4E. *Genes Dev* 16:1472-1487.
- Franz DN (2011) Everolimus: an mTOR inhibitor for the treatment of tuberous sclerosis. *Expert Rev Anticancer Ther* 11:1181-1192.
- Gallagher A, Grant EP, Madan N, Jarrett DY, Lyczkowski DA, Thiele EA (2010) MRI findings reveal three different types of tubers in patients with tuberous sclerosis complex. *J Neurol* 257:1373-1381.
- Gao X, Pan D (2001) TSC1 and TSC2 tumor suppressors antagonize insulin signaling in cell growth. *Genes Dev* 15:1383-1392.
- Garcia-Martinez JM, Alessi DR (2008) mTOR complex 2 (mTORC2) controls hydrophobic motif phosphorylation and activation of serum- and glucocorticoid-induced protein kinase 1 (SGK1). *Biochem J* 416:375-385.
- Goorden SM, van Woerden GM, van der Weerd L, Cheadle JP, Elgersma Y (2007) Cognitive deficits in Tsc1^{+/-} mice in the absence of cerebral lesions and seizures. *Ann Neurol* 62:648-655.
- Goto J, Talos DM, Klein P, Qin W, Chekaluk YI, Anderl S, Malinowska IA, Di Nardo A, Bronson RT, Chan JA, Vinters HV, Kernie SG, Jensen FE, Sahin M, Kwiatkowski DJ (2011) Regulable neural progenitor-specific Tsc1 loss yields giant cells with organellar dysfunction in a model of tuberous sclerosis complex. *Proc Natl Acad Sci U S A* 108:E1070-1079.
- Govindarajan B, Brat DJ, Csete M, Martin WD, Murad E, Litani K, Cohen C, Cerimele F, Nunnelley M, Lefkove B, Yamamoto T, Lee C, Arbiser JL (2005) Transgenic

expression of dominant negative tuberin through a strong constitutive promoter results in a tissue-specific tuberous sclerosis phenotype in the skin and brain. *J Biol Chem* 280:5870-5874.

Green AJ, Johnson PH, Yates JR (1994a) The tuberous sclerosis gene on chromosome 9q34 acts as a growth suppressor. *Hum Mol Genet* 3:1833-1834.

Green AJ, Smith M, Yates JR (1994b) Loss of heterozygosity on chromosome 16p13.3 in hamartomas from tuberous sclerosis patients. *Nat Genet* 6:193-196.

Guertin DA, Sabatini DM (2007) Defining the role of mTOR in cancer. *Cancer Cell* 12:9-22.

Guertin DA, Stevens DM, Thoreen CC, Burds AA, Kalaany NY, Moffat J, Brown M, Fitzgerald KJ, Sabatini DM (2006) Ablation in mice of the mTORC components raptor, rictor, or mLST8 reveals that mTORC2 is required for signaling to Akt-FOXO and PKC α , but not S6K1. *Dev Cell* 11:859-871.

Henske EP, Scheithauer BW, Short MP, Wollmann R, Nahmias J, Hornigold N, van Sleightenhorst M, Welsh CT, Kwiatkowski DJ (1996) Allelic loss is frequent in tuberous sclerosis kidney lesions but rare in brain lesions. *Am J Hum Genet* 59:400-406.

Henske EP, Wessner LL, Golden J, Scheithauer BW, Vortmeyer AO, Zhuang Z, Klein-Szanto AJ, Kwiatkowski DJ, Yeung RS (1997) Loss of tuberin in both subependymal giant cell astrocytomas and angiomyolipomas supports a two-hit model for the pathogenesis of tuberous sclerosis tumors. *Am J Pathol* 151:1639-1647.

Hernandez O, Way S, McKenna J, 3rd, Gambello MJ (2007) Generation of a conditional disruption of the Tsc2 gene. *Genesis* 45:101-106.

- Hevner RF, Shi L, Justice N, Hsueh Y, Sheng M, Smiga S, Bulfone A, Goffinet AM, Campagnoni AT, Rubenstein JL (2001) Tbr1 regulates differentiation of the preplate and layer 6. *Neuron* 29:353-366.
- Hino O, Klein-Szanto AJ, Freed JJ, Testa JR, Brown DQ, Vilensky M, Yeung RS, Tartof KD, Knudson AG (1993) Spontaneous and radiation-induced renal tumors in the Eker rat model of dominantly inherited cancer. *Proc Natl Acad Sci U S A* 90:327-331.
- Hsu PP, Kang SA, Rameseder J, Zhang Y, Ottina KA, Lim D, Peterson TR, Choi Y, Gray NS, Yaffe MB, Marto JA, Sabatini DM (2011) The mTOR-regulated phosphoproteome reveals a mechanism of mTORC1-mediated inhibition of growth factor signaling. *Science* 332:1317-1322.
- Huang J, Manning BD (2008) The TSC1-TSC2 complex: a molecular switchboard controlling cell growth. *Biochem J* 412:179-190.
- Huang J, Dibble CC, Matsuzaki M, Manning BD (2008) The TSC1-TSC2 complex is required for proper activation of mTOR complex 2. *Mol Cell Biol* 28:4104-4115.
- Huang J, Wu S, Wu CL, Manning BD (2009) Signaling events downstream of mammalian target of rapamycin complex 2 are attenuated in cells and tumors deficient for the tuberous sclerosis complex tumor suppressors. *Cancer Res* 69:6107-6114.
- Ito N, Rubin GM (1999) gigas, a Drosophila homolog of tuberous sclerosis gene product-2, regulates the cell cycle. *Cell* 96:529-539.
- Jacinto E, Loewith R, Schmidt A, Lin S, Ruegg MA, Hall A, Hall MN (2004) Mammalian TOR complex 2 controls the actin cytoskeleton and is rapamycin insensitive. *Nat Cell Biol* 6:1122-1128.

- Jambaque I, Cusmai R, Curatolo P, Cortesi F, Perrot C, Dulac O (1991) Neuropsychological aspects of tuberous sclerosis in relation to epilepsy and MRI findings. *Dev Med Child Neurol* 33:698-705.
- Jones AC, Daniells CE, Snell RG, Tachataki M, Idziaszczyk SA, Krawczak M, Sampson JR, Cheadle JP (1997) Molecular genetic and phenotypic analysis reveals differences between TSC1 and TSC2 associated familial and sporadic tuberous sclerosis. *Hum Mol Genet* 6:2155-2161.
- Jones AC, Shyamsundar MM, Thomas MW, Maynard J, Idziaszczyk S, Tomkins S, Sampson JR, Cheadle JP (1999) Comprehensive mutation analysis of TSC1 and TSC2-and phenotypic correlations in 150 families with tuberous sclerosis. *Am J Hum Genet* 64:1305-1315.
- Karbowniczek M, Astrinidis A, Balsara BR, Testa JR, Lium JH, Colby TV, McCormack FX, Henske EP (2003) Recurrent lymphangiomyomatosis after transplantation: genetic analyses reveal a metastatic mechanism. *Am J Respir Crit Care Med* 167:976-982.
- Kenerson H, Dundon TA, Yeung RS (2005) Effects of rapamycin in the Eker rat model of tuberous sclerosis complex. *Pediatr Res* 57:67-75.
- Knowles MA, Habuchi T, Kennedy W, Cuthbert-Heavens D (2003) Mutation spectrum of the 9q34 tuberous sclerosis gene TSC1 in transitional cell carcinoma of the bladder. *Cancer Res* 63:7652-7656.
- Kobayashi T, Minowa O, Kuno J, Mitani H, Hino O, Noda T (1999) Renal carcinogenesis, hepatic hemangiomas, and embryonic lethality caused by a germ-line Tsc2 mutation in mice. *Cancer Res* 59:1206-1211.
- Kobayashi T, Minowa O, Sugitani Y, Takai S, Mitani H, Kobayashi E, Noda T, Hino O (2001) A germ-line Tsc1 mutation causes tumor development and embryonic

lethality that are similar, but not identical to, those caused by Tsc2 mutation in mice. *Proc Natl Acad Sci U S A* 98:8762-8767.

Krueger DA, Care MM, Holland K, Agricola K, Tudor C, Mangeshkar P, Wilson KA, Byars A, Sahmoud T, Franz DN (2010) Everolimus for subependymal giant-cell astrocytomas in tuberous sclerosis. *N Engl J Med* 363:1801-1811.

Kwiatkowski DJ (2010) Animal models of lymphangioleiomyomatosis (LAM) and tuberous sclerosis complex (TSC). *Lymphat Res Biol* 8:51-57.

Kwiatkowski DJ, Zhang H, Bandura JL, Heiberger KM, Glogauer M, el-Hashemite N, Onda H (2002) A mouse model of TSC1 reveals sex-dependent lethality from liver hemangiomas, and up-regulation of p70S6 kinase activity in Tsc1 null cells. *Hum Mol Genet* 11:525-534.

Kwon CH, Zhu X, Zhang J, Baker SJ (2003) mTor is required for hypertrophy of Pten-deficient neuronal soma in vivo. *Proc Natl Acad Sci U S A* 100:12923-12928.

Kyin R, Hua Y, Baybis M, Scheithauer B, Kolson D, Uhlmann E, Gutmann D, Crino PB (2001) Differential cellular expression of neurotrophins in cortical tubers of the tuberous sclerosis complex. *Am J Pathol* 159:1541-1554.

Lamb RF, Roy C, Diefenbach TJ, Vinters HV, Johnson MW, Jay DG, Hall A (2000) The TSC1 tumour suppressor hamartin regulates cell adhesion through ERM proteins and the GTPase Rho. *Nat Cell Biol* 2:281-287.

Larson AM, Hedgire SS, Deshpande V, Stemmer-Rachamimov AO, Harisinghani MG, Ferrone CR, Shah U, Thiele EA (2011) Pancreatic neuroendocrine tumors in patients with tuberous sclerosis complex. *Clin Genet*.

Larson Y, Liu J, Stevens PD, Li X, Li J, Evers BM, Gao T (2010) Tuberous sclerosis complex 2 (TSC2) regulates cell migration and polarity through activation of CDC42 and RAC1. *J Biol Chem* 285:24987-24998.

- Lathia JD, Mattson MP, Cheng A (2008) Notch: from neural development to neurological disorders. *J Neurochem* 107:1471-1481.
- Lee L, Sudentas P, Donohue B, Asrican K, Worku A, Walker V, Sun Y, Schmidt K, Albert MS, El-Hashemite N, Lader AS, Onda H, Zhang H, Kwiatkowski DJ, Dabora SL (2005) Efficacy of a rapamycin analog (CCI-779) and IFN-gamma in tuberous sclerosis mouse models. *Genes Chromosomes Cancer* 42:213-227.
- Levine D, Barnes PD, Madsen JR, Abbott J, Mehta T, Edelman RR (1999) Central nervous system abnormalities assessed with prenatal magnetic resonance imaging. *Obstet Gynecol* 94:1011-1019.
- Ma J et al. (2010) Mammalian target of rapamycin regulates murine and human cell differentiation through STAT3/p63/Jagged/Notch cascade. *J Clin Invest* 120:103-114.
- Magnitsky S, Walton RM, Wolfe JH, Poptani H (2008) Magnetic resonance imaging detects differences in migration between primary and immortalized neural stem cells. *Acad Radiol* 15:1269-1281.
- Marcotte L, Crino PB (2006) The neurobiology of the tuberous sclerosis complex. *Neuromolecular Med* 8:531-546.
- Marcotte L, Aronica E, Baybis M, Crino PB (2012) Cytoarchitectural alterations are widespread in cerebral cortex in tuberous sclerosis complex. *Acta Neuropathol* 123:685-693.
- Masri J, Bernath A, Martin J, Jo OD, Vartanian R, Funk A, Gera J (2007) mTORC2 activity is elevated in gliomas and promotes growth and cell motility via overexpression of rictor. *Cancer Res* 67:11712-11720.
- Meikle L, Pollizzi K, Egnor A, Kramvis I, Lane H, Sahin M, Kwiatkowski DJ (2008) Response of a neuronal model of tuberous sclerosis to mammalian target of

rapamycin (mTOR) inhibitors: effects on mTORC1 and Akt signaling lead to improved survival and function. *J Neurosci* 28:5422-5432.

Meikle L, Talos DM, Onda H, Pollizzi K, Rotenberg A, Sahin M, Jensen FE, Kwiatkowski DJ (2007) A mouse model of tuberous sclerosis: neuronal loss of Tsc1 causes dysplastic and ectopic neurons, reduced myelination, seizure activity, and limited survival. *J Neurosci* 27:5546-5558.

Mhaweck-Fauceglia P, Alvarez V, Fischer G, Beck A, Herrmann FR (2008) Association of TSC1/hamartin, 14-3-3sigma, and p27 expression with tumor outcomes in patients with pTa/pT1 urothelial bladder carcinoma. *Am J Clin Pathol* 129:918-923.

Miloloza A, Rosner M, Nellist M, Halley D, Bernaschek G, Hengstschlager M (2000) The TSC1 gene product, hamartin, negatively regulates cell proliferation. *Hum Mol Genet* 9:1721-1727.

Milunsky A, Ito M, Maher TA, Flynn M, Milunsky JM (2009) Prenatal molecular diagnosis of tuberous sclerosis complex. *Am J Obstet Gynecol* 200:321 e321-326.

Mizuguchi M, Takashima S, Yamanouchi H, Nakazato Y, Mitani H, Hino O (2000) Novel cerebral lesions in the Eker rat model of tuberous sclerosis: cortical tuber and anaplastic ganglioglioma. *J Neuropathol Exp Neurol* 59:188-196.

Molyneaux BJ, Arlotta P, Hirata T, Hibi M, Macklis JD (2005) Fez1 is required for the birth and specification of corticospinal motor neurons. *Neuron* 47:817-831.

Napolioni V, Moavero R, Curatolo P (2009) Recent advances in neurobiology of Tuberous Sclerosis Complex. *Brain Dev* 31:104-113.

Nguyen L, Besson A, Heng JI, Schuurmans C, Teboul L, Parras C, Philpott A, Roberts JM, Guillemot F (2006) p27kip1 independently promotes neuronal differentiation and migration in the cerebral cortex. *Genes Dev* 20:1511-1524.

- Nie D, Di Nardo A, Han JM, Baharanyi H, Kramvis I, Huynh T, Dabora S, Codeluppi S, Pandolfi PP, Pasquale EB, Sahin M (2010) Tsc2-Rheb signaling regulates EphA-mediated axon guidance. *Nat Neurosci* 13:163-172.
- Nieto M, Monuki ES, Tang H, Imitola J, Haubst N, Khoury SJ, Cunningham J, Gotz M, Walsh CA (2004) Expression of Cux-1 and Cux-2 in the subventricular zone and upper layers II-IV of the cerebral cortex. *J Comp Neurol* 479:168-180.
- Niida Y, Lawrence-Smith N, Banwell A, Hammer E, Lewis J, Beauchamp RL, Sims K, Ramesh V, Ozelius L (1999) Analysis of both TSC1 and TSC2 for germline mutations in 126 unrelated patients with tuberous sclerosis. *Hum Mutat* 14:412-422.
- Niida Y, Stemmer-Rachamimov AO, Logrip M, Tapon D, Perez R, Kwiatkowski DJ, Sims K, MacCollin M, Louis DN, Ramesh V (2001) Survey of somatic mutations in tuberous sclerosis complex (TSC) hamartomas suggests different genetic mechanisms for pathogenesis of TSC lesions. *Am J Hum Genet* 69:493-503.
- Onda H, Lueck A, Marks PW, Warren HB, Kwiatkowski DJ (1999) Tsc2(+/-) mice develop tumors in multiple sites that express gelsolin and are influenced by genetic background. *J Clin Invest* 104:687-695.
- Orlova KA, Parker WE, Heuer GG, Tsai V, Yoon J, Baybis M, Fenning RS, Strauss K, Crino PB (2010a) STRADalpha deficiency results in aberrant mTORC1 signaling during corticogenesis in humans and mice. *J Clin Invest* 120:1591-1602.
- Orlova KA, Tsai V, Baybis M, Heuer GG, Sisodiya S, Thom M, Strauss K, Aronica E, Storm PB, Crino PB (2010b) Early Progenitor Cell Marker Expression Distinguishes Type II From Type I Focal Cortical Dysplasias. *J Neuropathol Exp Neurol*.
- Osborne JP, Fryer A, Webb D (1991) Epidemiology of tuberous sclerosis. *Ann N Y Acad Sci* 615:125-127.

- Park SH, Pepkowitz SH, Kerfoot C, De Rosa MJ, Poukens V, Wienecke R, DeClue JE, Vinters HV (1997) Tuberous sclerosis in a 20-week gestation fetus: immunohistochemical study. *Acta Neuropathol* 94:180-186.
- Parker WE, Orlova KA, Heuer GG, Baybis M, Aronica E, Frost M, Wong M, Crino PB (2011) Enhanced epidermal growth factor, hepatocyte growth factor, and vascular endothelial growth factor expression in tuberous sclerosis complex. *Am J Pathol* 178:296-305.
- Peterson TR, Laplante M, Thoreen CC, Sancak Y, Kang SA, Kuehl WM, Gray NS, Sabatini DM (2009) DEPTOR is an mTOR inhibitor frequently overexpressed in multiple myeloma cells and required for their survival. *Cell* 137:873-886.
- Pollizzi K, Malinowska-Kolodziej I, Stumm M, Lane H, Kwiatkowski D (2009a) Equivalent benefit of mTORC1 blockade and combined PI3K-mTOR blockade in a mouse model of tuberous sclerosis. *Mol Cancer* 8:38.
- Pollizzi K, Malinowska-Kolodziej I, Doughty C, Betz C, Ma J, Goto J, Kwiatkowski DJ (2009b) A hypomorphic allele of Tsc2 highlights the role of TSC1/TSC2 in signaling to AKT and models mild human TSC2 alleles. *Hum Mol Genet* 18:2378-2387.
- Potter CJ, Huang H, Xu T (2001) Drosophila Tsc1 functions with Tsc2 to antagonize insulin signaling in regulating cell growth, cell proliferation, and organ size. *Cell* 105:357-368.
- Pymar LS, Platt FM, Askham JM, Morrison EE, Knowles MA (2008) Bladder tumour-derived somatic TSC1 missense mutations cause loss of function via distinct mechanisms. *Hum Mol Genet* 17:2006-2017.
- Qin W, Chan JA, Vinters HV, Mathern GW, Franz DN, Taillon BE, Bouffard P, Kwiatkowski DJ (2010a) Analysis of TSC cortical tubers by deep sequencing of

- TSC1, TSC2 and KRAS demonstrates that small second-hit mutations in these genes are rare events. *Brain Pathol* 20:1096-1105.
- Qin W, Kozlowski P, Taillon BE, Bouffard P, Holmes AJ, Janne P, Camposano S, Thiele E, Franz D, Kwiatkowski DJ (2010b) Ultra deep sequencing detects a low rate of mosaic mutations in tuberous sclerosis complex. *Hum Genet* 127:573-582.
- Richardson EP, Jr. (1991) Pathology of tuberous sclerosis. Neuropathologic aspects. *Ann N Y Acad Sci* 615:128-139.
- Ridler K, Bullmore ET, De Vries PJ, Suckling J, Barker GJ, Meara SJ, Williams SC, Bolton PF (2001) Widespread anatomical abnormalities of grey and white matter structure in tuberous sclerosis. *Psychol Med* 31:1437-1446.
- Roach ES, Gomez MR, Northrup H (1998) Tuberous sclerosis complex consensus conference: revised clinical diagnostic criteria. *J Child Neurol* 13:624-628.
- Roach ES, Smith M, Huttenlocher P, Bhat M, Alcorn D, Hawley L (1992) Diagnostic criteria: tuberous sclerosis complex. Report of the Diagnostic Criteria Committee of the National Tuberous Sclerosis Association. *J Child Neurol* 7:221-224.
- Rosner M, Hengstschlager M (2004) Tuberin binds p27 and negatively regulates its interaction with the SCF component Skp2. *J Biol Chem* 279:48707-48715.
- Rosner M, Hengstschlager M (2011) Nucleocytoplasmic localization of p70 S6K1, but not of its isoforms p85 and p31, is regulated by TSC2/mTOR. *Oncogene*.
- Rosner M, Freilinger A, Hengstschlager M (2007) Akt regulates nuclear/cytoplasmic localization of tuberin. *Oncogene* 26:521-531.
- Rosner M, Hofer K, Kubista M, Hengstschlager M (2003) Cell size regulation by the human TSC tumor suppressor proteins depends on PI3K and FKBP38. *Oncogene* 22:4786-4798.

- Ruegg S, Baybis M, Juul H, Dichter M, Crino PB (2007) Effects of rapamycin on gene expression, morphology, and electrophysiological properties of rat hippocampal neurons. *Epilepsy Res* 77:85-92.
- Sabers CJ, Martin MM, Brunn GJ, Williams JM, Dumont FJ, Wiederrecht G, Abraham RT (1995) Isolation of a protein target of the FKBP12-rapamycin complex in mammalian cells. *J Biol Chem* 270:815-822.
- Saito T (2006) In vivo electroporation in the embryonic mouse central nervous system. *Nat Protoc* 1:1552-1558.
- Samuel-Abraham S, Leonard JN (2010) Staying on message: design principles for controlling nonspecific responses to siRNA. *FEBS J* 277:4828-4836.
- Sancak O, Nellist M, Goedbloed M, Elfferich P, Wouters C, Maat-Kievit A, Zonnenberg B, Verhoef S, Halley D, van den Ouweland A (2005) Mutational analysis of the TSC1 and TSC2 genes in a diagnostic setting: genotype--phenotype correlations and comparison of diagnostic DNA techniques in Tuberous Sclerosis Complex. *Eur J Hum Genet* 13:731-741.
- Sarbassov DD, Ali SM, Sabatini DM (2005) Growing roles for the mTOR pathway. *Curr Opin Cell Biol* 17:596-603.
- Sarbassov DD, Ali SM, Sengupta S, Sheen JH, Hsu PP, Bagley AF, Markhard AL, Sabatini DM (2006) Prolonged rapamycin treatment inhibits mTORC2 assembly and Akt/PKB. *Mol Cell* 22:159-168.
- Sato N, Koinuma J, Ito T, Tsuchiya E, Kondo S, Nakamura Y, Daigo Y (2010) Activation of an oncogenic TBC1D7 (TBC1 domain family, member 7) protein in pulmonary carcinogenesis. *Genes Chromosomes Cancer* 49:353-367.
- Scheithauer BW, Reagan TJ (1999) *Neuropathology*, 3rd Edition. New York: Oxford University Press.

- Shigeyama Y, Kobayashi T, Kido Y, Hashimoto N, Asahara S, Matsuda T, Takeda A, Inoue T, Shibutani Y, Koyanagi M, Uchida T, Inoue M, Hino O, Kasuga M, Noda T (2008) Biphasic response of pancreatic beta-cell mass to ablation of tuberous sclerosis complex 2 in mice. *Mol Cell Biol* 28:2971-2979.
- Sjodahl G, Lauss M, Gudjonsson S, Liedberg F, Hallden C, Chebil G, Mansson W, Hoglund M, Lindgren D (2011) A systematic study of gene mutations in urothelial carcinoma; inactivating mutations in TSC2 and PIK3R1. *PLoS One* 6:e18583.
- Soucek T, Yeung RS, Hengstschlager M (1998) Inactivation of the cyclin-dependent kinase inhibitor p27 upon loss of the tuberous sclerosis complex gene-2. *Proc Natl Acad Sci U S A* 95:15653-15658.
- Soucek T, Pusch O, Wienecke R, DeClue JE, Hengstschlager M (1997) Role of the tuberous sclerosis gene-2 product in cell cycle control. Loss of the tuberous sclerosis gene-2 induces quiescent cells to enter S phase. *J Biol Chem* 272:29301-29308.
- Sparagana SP, Roach ES (2000) Tuberous sclerosis complex. *Curr Opin Neurol* 13:115-119.
- Tanaka K et al. (2011) Oncogenic EGFR signaling activates an mTORC2-NF-kappaB pathway that promotes chemotherapy resistance. *Cancer Discov* 1:524-538.
- Tapon N, Ito N, Dickson BJ, Treisman JE, Hariharan IK (2001) The Drosophila tuberous sclerosis complex gene homologs restrict cell growth and cell proliferation. *Cell* 105:345-355.
- Tavazoie SF, Alvarez VA, Ridenour DA, Kwiatkowski DJ, Sabatini BL (2005) Regulation of neuronal morphology and function by the tumor suppressors Tsc1 and Tsc2. *Nat Neurosci* 8:1727-1734.

- Tee AR, Manning BD, Roux PP, Cantley LC, Blenis J (2003) Tuberous sclerosis complex gene products, Tuberin and Hamartin, control mTOR signaling by acting as a GTPase-activating protein complex toward Rheb. *Curr Biol* 13:1259-1268.
- Tiberio D, Franz DN, Phillips JR (2011) Regression of a cardiac rhabdomyoma in a patient receiving everolimus. *Pediatrics* 127:e1335-1337.
- Tillema JM, Leach JL, Krueger DA, Franz DN (2012) Everolimus alters white matter diffusion in tuberous sclerosis complex. *Neurology* 78:526-531.
- Tsai V, Parker WE, Orlova KA, Baybis M, Chi AW, Berg BD, Birnbaum JF, Estevez J, Okochi K, Sarnat HB, Flores-Sarnat L, Aronica E, Crino PB (2012) Fetal Brain mTOR Signaling Activation in Tuberous Sclerosis Complex. *Cereb Cortex*.
- Uhlmann EJ, Apicelli AJ, Baldwin RL, Burke SP, Bajenaru ML, Onda H, Kwiatkowski D, Gutmann DH (2002a) Heterozygosity for the tuberous sclerosis complex (TSC) gene products results in increased astrocyte numbers and decreased p27-Kip1 expression in TSC2+/- cells. *Oncogene* 21:4050-4059.
- Uhlmann EJ, Wong M, Baldwin RL, Bajenaru ML, Onda H, Kwiatkowski DJ, Yamada K, Gutmann DH (2002b) Astrocyte-specific TSC1 conditional knockout mice exhibit abnormal neuronal organization and seizures. *Ann Neurol* 52:285-296.
- van Slegtenhorst M, Verhoef S, Tempelaars A, Bakker L, Wang Q, Wessels M, Bakker R, Nellist M, Lindhout D, Halley D, van den Ouweland A (1999) Mutational spectrum of the TSC1 gene in a cohort of 225 tuberous sclerosis complex patients: no evidence for genotype-phenotype correlation. *J Med Genet* 36:285-289.
- van Slegtenhorst M et al. (1997) Identification of the tuberous sclerosis gene TSC1 on chromosome 9q34. *Science* 277:805-808.
- van Tilborg AA, de Vries A, Zwarthoff EC (2001) The chromosome 9q genes TGFBR1, TSC1, and ZNF189 are rarely mutated in bladder cancer. *J Pathol* 194:76-80.

- Wang Y, Greenwood JS, Calcagnotto ME, Kirsch HE, Barbaro NM, Baraban SC (2007) Neocortical hyperexcitability in a human case of tuberous sclerosis complex and mice lacking neuronal expression of TSC1. *Ann Neurol* 61:139-152.
- Way SW, McKenna J, 3rd, Mietzsch U, Reith RM, Wu HC, Gambello MJ (2009) Loss of Tsc2 in radial glia models the brain pathology of tuberous sclerosis complex in the mouse. *Hum Mol Genet* 18:1252-1265.
- Way SW, Rozas NS, Wu HC, McKenna J, 3rd, Reith RM, Hashmi SS, Dash PK, Gambello MJ (2012) The differential effects of prenatal and/or postnatal rapamycin on neurodevelopmental defects and cognition in a neuroglial mouse model of tuberous sclerosis complex. *Hum Mol Genet* 21:3226-3236.
- Wiederrecht GJ, Sabers CJ, Brunn GJ, Martin MM, Dumont FJ, Abraham RT (1995) Mechanism of action of rapamycin: new insights into the regulation of G1-phase progression in eukaryotic cells. *Prog Cell Cycle Res* 1:53-71.
- Wilcox KS, Buchhalter J, Dichter MA (1994) Properties of inhibitory and excitatory synapses between hippocampal neurons in very low density cultures. *Synapse* 18:128-151.
- Wilson C, Idziaszczyk S, Parry L, Guy C, Griffiths DF, Lazda E, Bayne RA, Smith AJ, Sampson JR, Cheadle JP (2005) A mouse model of tuberous sclerosis 1 showing background specific early post-natal mortality and metastatic renal cell carcinoma. *Hum Mol Genet* 14:1839-1850.
- Wolf HK, Normann S, Green AJ, von Bakel I, Blumcke I, Pietsch T, Wiestler OD, von Deimling A (1997) Tuberous sclerosis-like lesions in epileptogenic human neocortex lack allelic loss at the TSC1 and TSC2 regions. *Acta Neuropathol* 93:93-96.
- Wullschlegel S, Loewith R, Hall MN (2006) TOR signaling in growth and metabolism. *Cell* 124:471-484.

- Yang Q, Inoki K, Kim E, Guan KL (2006) TSC1/TSC2 and Rheb have different effects on TORC1 and TORC2 activity. *Proc Natl Acad Sci U S A* 103:6811-6816.
- Yates JR, Maclean C, Higgins JN, Humphrey A, le Marechal K, Clifford M, Carcanti-Rathwell I, Sampson JR, Bolton PF (2011) The Tuberous Sclerosis 2000 Study: presentation, initial assessments and implications for diagnosis and management. *Arch Dis Child*.
- Yeung RS, Katsetos CD, Klein-Szanto A (1997) Subependymal astrocytic hamartomas in the Eker rat model of tuberous sclerosis. *Am J Pathol* 151:1477-1486.
- Yeung RS, Xiao GH, Jin F, Lee WC, Testa JR, Knudson AG (1994) Predisposition to renal carcinoma in the Eker rat is determined by germ-line mutation of the tuberous sclerosis 2 (TSC2) gene. *Proc Natl Acad Sci U S A* 91:11413-11416.
- Yu J, Parkhitko AA, Henske EP (2010) Mammalian target of rapamycin signaling and autophagy: roles in lymphangioleiomyomatosis therapy. *Proc Am Thorac Soc* 7:48-53.
- Yu Y, Yoon SO, Poulogiannis G, Yang Q, Ma XM, Villen J, Kubica N, Hoffman GR, Cantley LC, Gygi SP, Blenis J (2011) Phosphoproteomic analysis identifies Grb10 as an mTORC1 substrate that negatively regulates insulin signaling. *Science* 332:1322-1326.
- Zaroff CM, Barr WB, Carlson C, LaJoie J, Madhavan D, Miles DK, Nass R, Devinsky O (2006) Mental retardation and relation to seizure and tuber burden in tuberous sclerosis complex. *Seizure* 15:558-562.
- Zeng LH, Xu L, Gutmann DH, Wong M (2008) Rapamycin prevents epilepsy in a mouse model of tuberous sclerosis complex. *Ann Neurol* 63:444-453.
- Zeng LH, McDaniel S, Rensing NR, Wong M (2010) Regulation of cell death and epileptogenesis by the mammalian target of rapamycin (mTOR): A double-edged sword? *Cell Cycle* 9.

- Zeng LH, Rensing NR, Zhang B, Gutmann DH, Gambello MJ, Wong M (2011) Tsc2 gene inactivation causes a more severe epilepsy phenotype than Tsc1 inactivation in a mouse model of tuberous sclerosis complex. *Hum Mol Genet* 20:445-454.
- Zhao CT, Li K, Li JT, Zheng W, Liang XJ, Geng AQ, Li N, Yuan XB (2009) PKCdelta regulates cortical radial migration by stabilizing the Cdk5 activator p35. *Proc Natl Acad Sci U S A* 106:21353-21358.
- Zhou J, Shrikhande G, Xu J, McKay RM, Burns DK, Johnson JE, Parada LF (2011) Tsc1 mutant neural stem/progenitor cells exhibit migration deficits and give rise to subependymal lesions in the lateral ventricle. *Genes Dev* 25:1595-1600.
- Zhu G, Chow LM, Bayazitov IT, Tong Y, Gilbertson RJ, Zakharenko SS, Solecki DJ, Baker SJ (2012) Pten deletion causes mTorc1-dependent ectopic neuroblast differentiation without causing uniform migration defects. *Development* 139:3422-3431.